



Cite this: *Mater. Adv.*, 2025,  
6, 7685

## Additively manufactured metal-matrix composites and their assessment as orthopedic implants

Eisha Khalid, <sup>a</sup> Ahmed Bahgat Radwan, <sup>\*a</sup> Md Mizanur Rehman, <sup>b</sup> Niko Eka Putra, <sup>c</sup> Lidy E. Fratila-Apachitei, <sup>c</sup> Jie Zhou, <sup>c</sup> Amir A. Zadpoor <sup>c</sup> and Noora Al-Qahtani <sup>\*a</sup>

Additive manufacturing (AM), also known as 3D printing, is gaining the attention of various industries as a viable alternative to conventional manufacturing, empowering design freedom, novel architectures, composition control, and sustainability. Meanwhile, metal matrix composites (MMCs) are being investigated for orthopedic implant applications due to their flexibility to achieve excellent strength, corrosion resistance, and bioactivity. Combining these two research fronts by utilizing AM for manufacturing multi-functional MMC bone scaffolds, having specific structures and compositions, has led to the recent development of a new generation of biomaterials with enhanced material properties not achievable with monolithic counterparts. Aimed at understanding the status of the research on the topic and identifying the remaining challenges, this review article discusses the utilization of AM for realizing the design vision of different MMC scaffolds, focusing on the synergistic combination of mechanical and biological characteristics, such as enhanced biodegradability, strength, and osteogenic properties. It starts by discussing the requirements for orthopedic implants and different AM techniques utilized thus far for manufacturing them, especially MMC orthopedic implants. Then, it delves into different MMCs, including Ti-, Mg-, and Fe-matrix composites that have been 3D printed into bone-substituting scaffolds and discusses their recent progress and specific characteristics. Finally, we identify the knowledge gaps and potential directions for developing MMCs further toward clinically viable, advanced orthopedic implants.

Received 25th May 2025,  
Accepted 18th September 2025  
DOI: 10.1039/d5ma00537  
[rsc.li/materials-advances](http://rsc.li/materials-advances)

### 1. Introduction

Trauma, tumors, aging, and genetic disorders can result in significant bone deformity, defects, or loss, which may require assistive implants to treat and restore complete functionality of the damaged bone(s). Osteoporosis, for example, is a serious health condition affecting 200 million people worldwide.<sup>1</sup> It is characterized by decreased bone mass, leading to fragile bone and eventual fracture.<sup>1,2</sup> Bone tumors or metastases in bone are another health complication that can cause pathological fractures and decreased mobility.<sup>3</sup> While being rare, giant tumors of bones account for 15–20% of all benign tumors, which are locally aggressive bone tumors commonly occurring in young adults.<sup>4</sup> Surgery is the most common treatment option for tumor removal, and the residual cavity formed during surgery

is then filled up with bone grafts to preserve the bone.<sup>4</sup> In addition, congenital bone disorders affect children from an early age, such as osteogenesis imperfecta (OI), which causes brittle bones and frequent fractures, and fibrous dysplasia, which causes fibrous (scar) tissues to replace healthy and normal bone tissues.<sup>5,6</sup> Depending on the fracture specifics, the broken bones are treated with telescopic rods that grow with the bone, thereby reducing surgical re-interventions, especially for children.<sup>5</sup>

The orthopedic and biomedical implant research communities seek to improve patient care and provide safer implants by understanding the intricate interplay between biology, mechanics, and biomaterials and optimizing material design and manufacturing routes. Amongst the metallic group of biomaterials, stainless steel, CoCr-, and Ti-based materials are sought after for long-term or permanent implants, while Mg- and Fe-based implants are designed for short-term or temporary bone substitution. Most of these alloys were initially developed and manufactured for applications other than implants.<sup>7</sup> This called for the efforts to design better materials tailored specifically for biomedical applications, considering the specific requirements of the biomaterials implanted into

<sup>a</sup> Center for Advanced Materials, Qatar University, Doha 2713, Qatar.  
E-mail: [ahmedbahgat@qu.edu.qa](mailto:ahmedbahgat@qu.edu.qa), [noora.alqahtani@qu.edu.qa](mailto:noora.alqahtani@qu.edu.qa)

<sup>b</sup> Biological program, Department of Biological and Environmental Sciences, College of Arts and Sciences, Qatar University, Doha 2713, Qatar

<sup>c</sup> Department of Biomechanical Engineering, Faculty of Mechanical Engineering, Delft University of Technology, Mekelweg 2, 2628 CD Delft, The Netherlands



the human body, particularly younger and more active patients, and the trend towards less invasive surgeries, requiring materials to withstand higher stresses and complex biological environments.<sup>7,8</sup>

Biodegradable metals can, at least in theory, bring back the native bone tissue while disappearing through gradual biodegradation. However, multiple challenges must be addressed before realizing this ideal scenario. Two major challenges stand out. First, the rate of metallic corrosion should be adjusted in accordance with the rate of bone tissue regeneration so that the biodegradable metal neither loses its structural integrity too soon nor impedes bone regeneration due to its too slow biodegradation. Second, most biodegradable metals and alloys exhibit some levels of cytotoxicity, which may hinder complete bone regeneration. Two technologies have emerged in recent years that address the abovementioned challenges. First, additive manufacturing (AM), also known as 3D printing, has been used to tailor the micro-architecture of biodegradable porous metals, adjusting their biodegradation rate. This is particularly useful for biodegradable metals, such as Fe, generally with a lower biodegradation rate. Second, combining biodegradable metals with some other materials to form metal matrix composites (MMCs) has been used to address the cytotoxicity of metals and induce bioactivity, such as an osteogenic response. This review is positioned at the interface of these two technologies and concerns the biomaterials that can simultaneously address both major challenges hampering the translation of biodegradable metals into routine clinical practice.

MMCs are an excellent choice for customized implant applications, where the control over reinforcing and matrix phases makes one capable of configuring properties at the material design stage. Conventional manufacturing techniques suitable for MMCs, such as powder metallurgy, have limitations in realizing material design ideas, especially in architecture, to mimic the interconnected porous structures and topography of the native bone matrix. On the other hand, AM has revolutionized the manufacturing industries to form complex and customizable products and has been employed to produce biomedical implants.<sup>9</sup> Recently, AM has been applied to manufacture MMCs for orthopedic implants. It has received much attention, mainly in the scientific community, due to its capability of achieving the performance and architecture of implants that better mimic the natural bone. The integration of AM into the implant manufacturing route to produce MMC-based orthopedic implants offers unparalleled advantages, allowing for precise control over the architecture and composition of the implants. The continuing demand for advanced and customized solutions in orthopedic surgery drives the exploration of AM for MMCs as a promising frontier for innovation.

In recent years, numerous articles on AM for MMCs have been published across a wide range of journals. A thorough literature search has identified the review articles that fall under one of the following categories: (i) focusing solely on AM techniques without referring to specific applications,<sup>10-18</sup> (ii) focusing on AM of metals and alloys for specific

applications including implant applications with no mention of MMCs;<sup>11,18-20</sup> (iii) focusing on selective AM techniques for MMCs<sup>21,22</sup> potentially for a broad range of applications; (iv) focusing on AM of specific MMCs such as Mg-based or Ti-based composites;<sup>23-25</sup> or (v) detailing bone implant requirements without connecting them to AM or relevant biomaterials.<sup>26-28</sup> Moreover, although the mechanical characteristics of AM MMCs have been frequently reported,<sup>9,21,22,29,30</sup> their biological effects, either *in vitro* or *in vivo*, are often not included. Rarely has a literature study been performed at an intersection of implant requirements, AM methods for MMCs, MMC materials, and their mechanical and biological assessments for orthopedic applications. Therefore, this review aims to address this gap by analyzing the basic requirements for bone implants, exploring the AM methods suitable for producing MMC bone implants – their capabilities and challenges, providing an overview of the achieved performance of Ti-, Mg-, and Fe-based composites fabricated by AM, and finally indicating the directions of this research domain. It places its focus specifically on Ti-, Mg-, and Fe-based MMCs within the AM landscape, based on the following considerations. Ti-based MMCs are considered the benchmark for permanent load-bearing implants due to their excellent strength, fatigue resistance and biocompatibility, while Mg-based MMCs possess higher degradability, being suitable for short-term bone repair or replacement and Fe-based MMCs have slower corrosion kinetics, endowing them with the capability of medium-term biomechanical support. In other words, these three material systems complement each other and span the whole spectrum from permanent implants, *i.e.*, Ti, to slowly and fast degrading alternatives, *i.e.*, Mg, and Fe respectively. It is important to note that the issues to address in the case of zinc-based MMCs are very different, primarily concerning the poor mechanical properties of zinc, including low fatigue strength and creep resistance, and thus the type of materials added to Zn-based alloys, such as graphene and its derivatives or carbon nanotube<sup>31,32</sup> are meant to enhance their mechanical properties, instead of bioactive ceramics added to Ti-, Mg- and Fe-based materials. In other words, this review takes an application-specific approach to connect the dots between AM processes, MMCs based on the three material systems, and their potential in orthopedic applications.

## 2. Requirements of materials used as orthopedic implants

Biomaterials are natural or synthetic materials used to repair, replace, or augment the body's damaged tissues (nerves, bones, *etc.*).<sup>33</sup> Natural biomaterials are derived from natural renewable resources, including plants, microorganisms, *etc.*, while synthetic biomaterials are artificial materials and/or the materials that may have been derived from non-renewable materials. Biomaterials have been used for centuries to treat different human conditions. One of their earliest uses dates back to ancient Egyptians when naturally derived sutures from animal



tissues were used to stitch wounds.<sup>7</sup> Metals were among the first materials used to treat arthritis and bone defects.<sup>7</sup> Some metals spontaneously oxidize and form a stable oxide layer on their surfaces when in contact with air or a corrosive environment, which protects the inner material from corroding further. However, this layer can be damaged, leading to further corrosion. Due to this property of metals, ceramics, being ionic compounds, were then explored for biomedical implants, as they were considered better than metals in terms of chemical stability. In the 1970s, a new concept was proposed: biomaterials should be engineered to initiate a positive tissue response once implanted, thus helping healing. This concept triggered the emergence of bioactive ceramics.<sup>7</sup> Bioactive ceramics have been an active area of research ever since, especially for hard tissue repair. In the meantime, soft materials, such as synthetic

polymers and biological materials have also been used as biomaterials, depending on the functional requirements. Synthetic polymers may have better mechanical properties, while biological materials tend to have better immunogenic properties.<sup>34</sup> Soon afterward, tissue regeneration emerged as another important strategy, which is the recovery of tissue loss through the growth and proliferation of special cells that generate the required tissue matrix to restore impaired function.<sup>35</sup> The regenerative capabilities of biomaterials were investigated and engineered to introduce healing factors into the biomaterials to be implanted, including the incorporation of bioactive molecules that are osteoinductive in the porous scaffolds.<sup>35</sup> Fig. 1a shows the progressive evolution of biomaterials of each generation and the corresponding targeted properties.

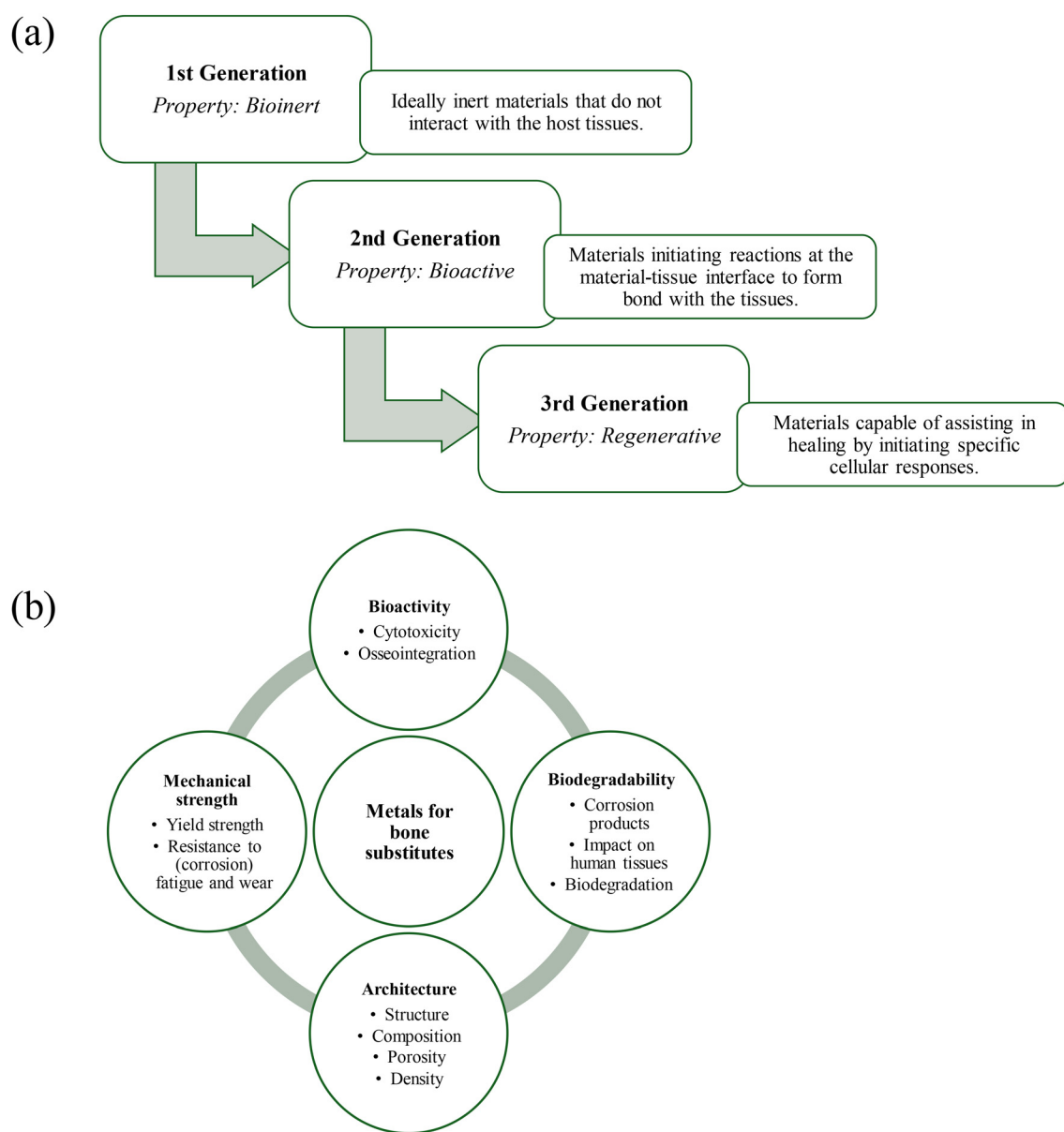


Fig. 1 (a) Chronological classification of biomaterials concerning targeted properties and (b) requirements for metal-based orthopedic implants.



Irrespective of the class of biomaterials, tremendous growth has been seen in the active exploration and design of new materials for biomedical applications, with every material having its own advantages, limitations, and specific uses.<sup>36</sup> Some of the recently explored avenues include smart materials,<sup>37,38</sup> meaning that the implanted materials assist in healing through geometrical features or embedded molecules, and/or react to changes in external environment. This includes designing materials' bulk composition, surface properties, architecture, or microstructure to interact with biological surroundings. This review article focuses explicitly on the AM of MMCs recently engineered for their use in orthopedic applications. The key features required in biomaterial design for orthopedic implants are illustrated in Fig. 1b and are described in detail in the following subsections.

## 2.1. Biocompatibility

Biocompatibility refers to the capability of biomaterial to be safe and functional for a specific application.<sup>39</sup> Introducing an implant into the human body initiates a natural defense mechanism called foreign body reaction, which includes inflammation and fibrotic processes. Furthermore, the implantation of a biomaterial damages the tissues around the implant, which triggers inflammatory reactions<sup>40</sup> with cells from the immune system attacking the foreign object to either digest or encapsulate it to protect our bodies. These interactions happen in three phases: phase 1 is the water–surface interactions within nanoseconds after implantation, followed by phase 2 of protein interactions within the next few seconds. Stages 3 and 4 occur within hours and days after implantation, respectively, when the implant is interacting with cells. The biomaterials properties can influence these interactions with impact on subsequent cellular functions.<sup>41,42</sup>

Biomaterial safety implies that it should not generate toxic effects locally, remotely or systemically. For example, metallic implants may release ions or corrosion products that can become toxic above a certain concentration.<sup>43</sup> The severity of the toxic response depends heavily on the extent to which metal ions and debris are released.<sup>43</sup> Excessive release of metal ions or metallic particles due to implant biodegradation may overwhelm the antioxidant systems,<sup>44</sup> producing more potential free radicals, which results in adverse reactions (*i.e.*, cytotoxicity), leading to cell death and eventual organ dysfunction. In addition, the associated inflammation can cause damage to proteins, mitochondria, and even DNA, thus causing genotoxicity.<sup>28</sup> If the ion concentration increases further, ions can enter the lymphatic and systemic circulation, reaching vital organs, causing systemic toxicity.<sup>28,45,46</sup>

Osseointegration is an important requirement for the long-term stability of cementless bone implants<sup>47</sup> and for tissue regeneration that can be achieved through primary fixation and tissue ingrowth involving cell migration, adhesion, proliferation and differentiation on the implant surface.<sup>48</sup> It is a time-dependent process leading to structural and functional connection between the implant and the living bone.<sup>48</sup> Osseointegration can be facilitated by providing (bio)chemical and

physical surface cues, (*e.g.*, by introducing growth factors, designing the biomaterial's surface topography, *etc.*) to support beneficial tissue-implant interactions.<sup>47</sup>

Biological evaluation of medical devices is guided by the ISO 10993 standards that outline risk-based strategies for assessment.<sup>49</sup> Based on the end-use application, biocompatibility can be evaluated through *in vitro* or *in vivo* testing and related strategies can be selected, including irritation tests, hemocompatibility, local implantation toxicity, systemic toxicity, *etc.*<sup>49</sup> The most common *in vitro* testing methods are immersion and electrochemical analysis in a physiological environment to understand materials' biodegradation processes and the leading corresponding byproducts, which helps in cytotoxicity evaluation. Moreover, animal, or human cell cultures are used to understand cell attachment, proliferation, and differentiation, thereby providing a picture of potential osseointegration. On the other hand, *in vivo* testing of implants in animal subjects allows the evaluation of toxicity and osseointegration, paving the way for further optimizing the implant's biomaterial composition and structural design.

## 2.2. Biodegradability

Biodegradation is the gradual breakdown of a material mediated by biological environments, which may be associated with biological activity.<sup>39</sup> As described earlier, once in contact with the biological system, metals may corrode or form a passivation layer; both release metallic ions to different extents into the system, possibly triggering immune responses or adverse tissue reactions.<sup>50</sup> This not only causes discomfort to the patient but also has the potential to cause sepsis and severe health risks. Secondary surgical interventions may be needed to remove implants due to such immune response complications.<sup>51</sup> A second surgery is often associated with additional health risks, financial burdens, and time expenditures for the patient and the healthcare system. Improving biomaterials' properties, including composition, architecture, surface modifications,<sup>52</sup> and manufacturing methods, are suggested to minimize or avoid implant-related complications.<sup>53</sup>

Biodegradable implants present a remarkable solution to these problems by eliminating long-term biocompatibility issues by offering the possibility to finely tune the rate of implant biodegradation within the required timeframe for bone regeneration without producing any harmful byproducts. They structurally support the bone during the healing phase while gradually shifting the weight-carrying task to the regenerating bone, further stimulating bone tissue regeneration.<sup>8</sup> Moreover, the risk of inflammation at the implant site can be significantly reduced in the case of biodegradable implants.<sup>42,54</sup> The suitable range of biodegradation rates for bone-substituting materials is  $0.2\text{--}0.5\text{ mm year}^{-1}$ .<sup>55</sup> New materials are being designed as alternatives to metal implants in order to have lower cytotoxicity and better biodegradability, biocompatibility, wear resistance, and strength.<sup>56–58</sup> In addition, MMCs are being actively researched as potential alternatives to biodegradable metals by engineering their structures and exploring different manufacturing routes, but significant



research still needs to be conducted before their clinical adoption.

### 2.3. Microarchitecture

Biomaterials are generally engineered based on composition design (*i.e.*, a combination of two or more elements/materials), microarchitecture design (*i.e.*, distribution of materials in 3D space), or an integration of both design approaches. Tuning the material allotment in space expands the design space and serves as a new variable for creating advanced materials to exhibit specific property profiles.<sup>59–61</sup> Bone-substituting materials are often designed to resemble the bone structurally and functionally. The bone itself has a porous structure, with an outer layer comprising of a compact solid-like structure with a porosity of 5–30%, known as the cortical bone, and an inner highly porous interconnected structure with a porosity ranging between 30% and 95%, known as the trabecular, cancellous, or spongy bone.<sup>36,62</sup> Therefore, the scaffolds produced for orthopedic implants should be porous to provide proper nutrient supply within the scaffold, ensuring the viability and proliferation of bone cells.<sup>36</sup> Moreover, to better mimic the original bone, functionally graded scaffolds have been developed,<sup>27,63</sup> whose porosity gradient is aimed to be close to the bone structure, along with their structure and morphology. From a material's composition perspective, alloy design is a frequently adopted approach well developed for biomedical implants to optimize mechanical integrity and induce bioactivity. Conversely, the combination of two different materials along with a preselected microarchitecture is a developing arena, promising new insights into property-specific material designs. Within this context, the concept of *meta*-biomaterials is emerging, where the microarchitecture and surface of bone-substituting

materials are rationally designed to equip them with unusual yet favorable mechanical,<sup>64,65</sup> mass transport,<sup>66</sup> and biological<sup>67</sup> properties. Moreover, the overall strength of the implants is determined by the combination of its composition and structural features.<sup>68</sup> Therefore, the perspective of material design is very much aligned with the orthopedic requirements.

Fig. 2 shows various microarchitectural configurations for biomaterial design. Generally, MMCs can be classified as continuously reinforced composites (long wires, filaments, fibers, *etc.*) and discontinuously reinforced composites (short whiskers, small particles, short fibers, *etc.*).<sup>69</sup> Compared with discontinuous reinforcements, continuous dispersion gives better strength and stiffness; however, it is costly, anisotropic, and challenging to produce.<sup>69</sup> Reinforcing the metal matrix with particles or fibers having different configurations (unidirectional, laminates, or short fiber) strengthens the metal and can also induce bioactivity, depending on the reinforcing agent(s).<sup>70,71</sup> Stranded structures can be engineered for added strength, and thermal<sup>72</sup> and electrical<sup>73</sup> conductivity in one direction. Cellular materials (foams or lattices) are made by designing pore connectivity or specific material allotment in space. This gives rise to a porous structure especially suitable for bone implants since the bone is cellular.<sup>74</sup> Sandwich structures are great for strength and flexural stiffness, where the core material is light with stiff outer faces.<sup>75</sup> Lastly, multi-layer structures are significant for combining strength and controlled permeability for light, gases, moisture, *etc.*<sup>59</sup> Since MMCs' properties depend on the size and volume of reinforcement phases, along with the nature of the matrix-reinforcement interface, optimal mechanical and biological properties can be attained when fine, thermally, and chemically stable reinforcement particles are dispersed in the metal matrix.

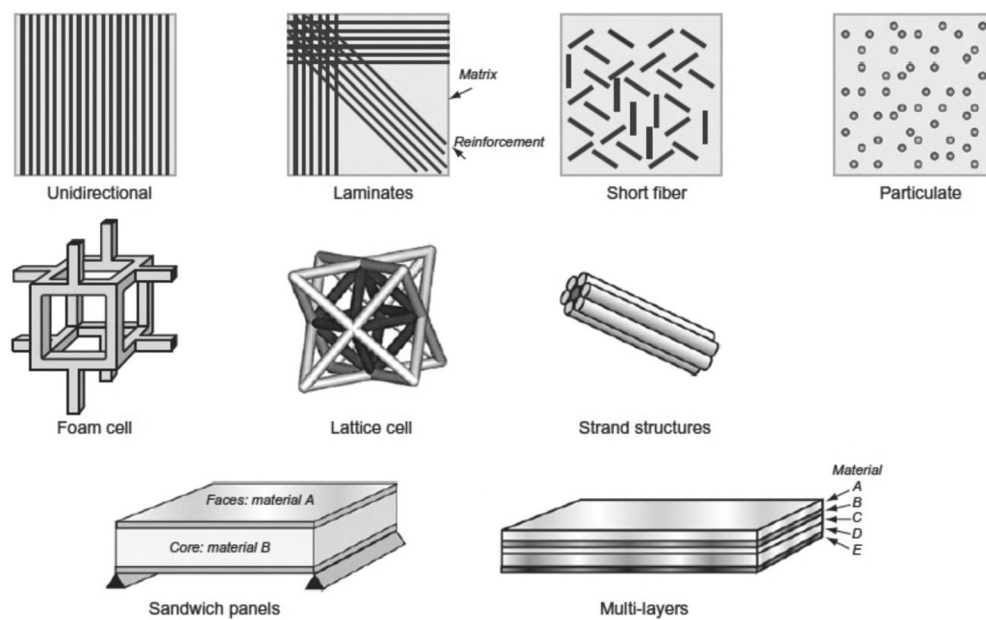


Fig. 2 Schematic drawings of different configurations of (composite) material architectures.<sup>59</sup> The figure is reproduced with permission from Elsevier, copyright 2013.



Biomaterials with architecture-guided cell response can enhance their biocompatibility for bone applications. Architectural features and surface irregularities may allow bone ingrowth.<sup>36,76</sup> Moreover, due to environmental interactions, (multi-scale) surface roughness potentially alters the surface's chemical composition and energy with impact on cellular responses.<sup>77</sup>

The feature size in implant design is important, too. Nano-scale surface features may allow calcium phosphate (CaP) deposition on the surface oxide layer but may not accommodate collagen fibrils.<sup>68</sup> Features ranging from a few to tens of micrometers offer optimum accommodation for the smallest capillaries and whole cells, while features larger than this enables lamellar or cortical bone formation.<sup>68</sup> Porous implants provide a larger surface area to facilitate tissue adhesion, growth, and, thus, better osseointegration, even deep into the porous structure.<sup>27,76,78</sup> Pore dimensions have a similar trend to feature size, where pore sizes of 100  $\mu\text{m}$  and above favor lamellar bone formation, while pore sizes of 200–350  $\mu\text{m}$  favors bone ingrowth.<sup>78</sup> Moreover, the pore sizes of cancellous or trabecular bone range between 200 and 1000  $\mu\text{m}$ ; therefore, achieving bone scaffolds within this pore size range would produce bone-mimicking implants and allow for adequate bone growth and fluid circulation.<sup>78</sup> A previous study investigated the biological behavior of porous Ti scaffolds with different pore size ranges.<sup>79</sup> Scaffolds with smaller pores (45–106  $\mu\text{m}$ ) provided more surface area for cell attachment and had an excellent cell growth rate within the first 3 days. However, the rate became slower after that. On the contrary, the larger pore-size scaffolds (300–500  $\mu\text{m}$ ) initially showed a slower cell growth rate, but the rate tremendously increased towards the end of the 12-day culture time. Moreover, for bone scaffolds, having a combination of macro- (larger than 50  $\mu\text{m}$ ) and micro- (smaller than 20  $\mu\text{m}$ ) pores may be more favorable as compared with only macro-porous structure since micro-pores may induce and increase protein adsorption and cell attachment, which promotes bone regeneration.<sup>78</sup> In a nutshell, a combination of large and small features can influence the stability of implants within the human body and should be considered in the geometrical design of implants.

A biomechanical mismatch between the bone implant and adjacent bone can give rise to the stress-shielding effect,<sup>54,62</sup> which causes surrounding bone to be relieved from the load, reducing bone density. In association with the stress-shielding effect, periprosthetic osteolysis may occur, possibly resulting in the loosening of the inserted implant, subsidence, and eventual failure, typically in joint arthroplasty.<sup>80,81</sup> This issue can be addressed by intelligent selection of implant biomaterials and microarchitecture to minimize the mismatch in the elastic

modulus with the adjacent bone, which reduces the stress-shielding effect, improving the overall function of bone implants.<sup>82</sup> Thus, the porous architecture of implants can improve osseointegration<sup>83</sup> while minimizing the stress shielding effect.<sup>76,84</sup>

Microarchitecture and its effects have been widely studied for metallic implants,<sup>59,76</sup> mainly focusing on the impact of porosity in biodegradable metals. However, it is a growing area of research for MMCs.<sup>21,85</sup> A significant challenge for biodegradable porous implants remains, as to the finding of a balance between biodegradation and cytotoxicity. Combining appropriate microarchitecture with careful design of biomaterial composition may offer novel solutions for this challenge, where reinforcing materials can be chosen for required features to modulate biodegradation, initiate specific cell functions, and/or reduce toxicity.

#### 2.4. Mechanical properties – quasi-static and dynamic

Sustaining mechanical loads, either quasi-static (tensile, compressive, or bending) or multiaxial cyclic loading, is one of the significant challenges that orthopedic implants face within the body. Static and dynamic stresses paired with the complex and aggressive body environment comprising electrolytes, proteins, enzymes, etc., make the working condition exceedingly intricate, requiring implants to be structurally strong but not excessively stiff and have positive host-response upon implantation. As the implant degrades within the bodily fluids, it becomes important that the changes in its mechanical properties are tailored well to match the bone tissue regeneration rate.<sup>86</sup> The mechanical properties of materials depend on their composition and processing/fabrication history, as well as their microarchitectural design, including porosity.<sup>7</sup> The requirement of interconnected porosity may be limitedly met due to the mechanical strength requirements for load-bearing applications.<sup>62</sup> A bone substitute should be capable of providing mechanical support from *in vitro* trials to *in vivo* implantation. Microstructural designing, such as adding reinforcing agents, alloying elements, and/or grain size alterations, significantly affects the mechanical properties of the resulting material.

Conventional quasi-static mechanical testing of materials usually comprises uniaxial loading to understand the mechanical behavior, where load/stress is applied, and the resulting deformation is recorded. The typical data extracted from the load-displacement curves of these tests are ultimate tensile or compressive strength, yield strength, ductility (or elongation), and elasticity modulus. Quasi-static loading conditions include tensile, compression, shear, and torsion. Compression testing is often conducted for biomedical scaffolds, considering that

**Table 1** Mechanical properties of different bone tissues as adopted from ref. 90 and 91–93. The values can vary depending on species, age, anatomical position, and testing conditions

Bone	Porosity (%)	Compressive strength (MPa)	Tensile strength (MPa)	Elastic modulus – tensile (GPa)	Elongation at break	Mass density (g $\text{cm}^{-3}$ )
Cortical	5–30	130–240	25–283	5–23 (GPa)	1.07–2.10	1.8–2.0
Cancellous	30–95	0.12–1.1	15–38	10–1570 (MPa)	—	1.0–1.4



compression is the dominant form of loading experienced *in vivo* by most bone implants and hard tissues. The implant's overall compressive strength describes its ability to withstand compressive loads before failure. The mechanical properties of cancellous and cortical bone are listed in Table 1. Repetitive loading on implants can initiate crack formation, followed by crack growth and failure due to overload, even if the stress levels are far below the yield strength of the biomaterial.<sup>7</sup> Fatigue is associated with crack initiation and growth, resulting in degradation of mechanical properties and leading to the failure of a component under cyclic loading.<sup>7,87</sup> Superimposing fatigue with a corrosive biological environment makes the situation more challenging, significantly decreasing the material's durability. Many implants endure millions of loading cycles throughout their lifetimes. Therefore, they may fail due to fatigue. Even for metallic mechanically stable implants and interfaces, fatigue failure is an area of concern<sup>88,89</sup> due to time-dependent dynamic loading and micromotion, which can eventually lead to structural changes in the bones and/or implant. To test biomedical implants' endurance or fatigue limit, fatigue tests usually run for  $1 \times 10^7$ – $10^8$  loading cycles to establish the endurance limit.<sup>7</sup> If the maximum stress on the implant is lower than the endurance limit, the given material is expected to perform its function indefinitely without failure.

Crack initiation in implants is a combined result of chemical and mechanical attacks. The crack initiation can occur through the stress concentrations between the different phases of the implant material<sup>94</sup> or through the formation of slip planes that consequently break down the protective oxide (passivation) layer due to cyclic loading, thus exposing the unprotected regions through which the crack propagates further.<sup>89</sup> Moreover, the material's surface under loading is most susceptible to crack initiation since stresses are the highest at the surfaces, meaning that surface finish and residual stresses are vital in determining the overall testing results.<sup>7</sup> Careful monitoring of corrosion current density during *in vitro* corrosion fatigue testing can give indications of crack initiation.<sup>89</sup> On the other hand, crack propagation can be accelerated due to hydrogen embrittlement at the crack's tip in aqueous media, thereby reducing the implant's durability. Therefore, the spontaneous re-passivation ability of the material becomes an advantageous property to protect the surface layer from crack propagation.<sup>95</sup> The corrosion potential also changes during fatigue tests in corrosive media, which depends on one or both processes: the exposure of new surface due to the formation of slip bands and crack initiation and propagation, which shift the corrosion potential towards negative value.<sup>95</sup> As re-passivation occurs, the corrosion potential returns to positive values. Therefore, the final corrosion potential is determined by the relative velocities of new surface layer formation and its re-passivation.<sup>95</sup> The morphology of wear debris due to fatigue wear must also be considered during corrosion testing to better understand the host-tissue reaction to the debris *in vivo*.

Developing orthopedic implants resistant to fatigue, fracture, and wear is crucial. Gearing biomaterials research toward

composite materials for bone-substituting implants is an effective strategy for developing interconnected networks of different materials or phases of different materials that can endure cycles of stresses and trap wear debris once it is formed due to surface fatigue.

### 3. Additive manufacturing

Porous metals were historically fabricated by using conventional techniques for various industrial applications. However, with the introduction of porous metals for orthopedic applications, the requirements for controlled porosity and improved properties emerged. The conventional techniques appeared incapable of precisely controlling porosity and producing a predefined internal architecture and contoured external structure.<sup>9,62</sup> To overcome these challenges, AM has become the most promising alternative. AM is an advanced manufacturing technique that builds near-*net*-shape objects with complex geometries, layer-by-layer, in a controlled manner, using the data from digital models or computer-aided design (CAD).<sup>9,36,62,82</sup> The digital design gives AM a significant advantage in exercising precise control over the intricate geometrical design required for the manufactured part.<sup>9,62,82,96</sup> In recent years, AM has evolved tremendously and has been applied across many industries, from nanotechnology to space exploration. For the biomedical sector, AM has great potential for implant design as it enables rapid prototyping and manufacturing with high resolution, precise control over macro and micro architecture, light-weight (due to the architected nature of materials), and short lead times, as compared with the traditional fabrication routes.<sup>9,36,82,97</sup> In addition, conventional manufacturing methods produce a considerable amount of waste material. In contrast, AM techniques are environmentally friendly and sustainable and support circular economy<sup>98</sup> since they produce less material waste and CO<sub>2</sub> emissions. Implementing AM ensures reductions in energy consumption and production costs.<sup>98</sup>

Depending on manufacturing needs, different AM techniques have been crafted for smart manufacturing through layer-by-layer deposition, which allows for exploring different material and design concepts. Various factors contribute to the selection of the AM process, including the material to be processed, lead time, post-processing requirements, the accuracy of the part, the final properties required, and the surface quality of the final product. According to the ASTM's AM technology standards, AM processes are grouped into seven categories (Table 2).

Table 2 Seven categories of AM techniques and their respective processes according to ASTM<sup>21,99</sup>

Category	VAT	BJ	MJ	SL	ME	PBF	DED
Process	SLA DLP	3D printing Ink-jetting	Polyjet Ink-jetting Thermojet	UC LOM	FDM	SLS SLM EBM	DMD LC EBDM



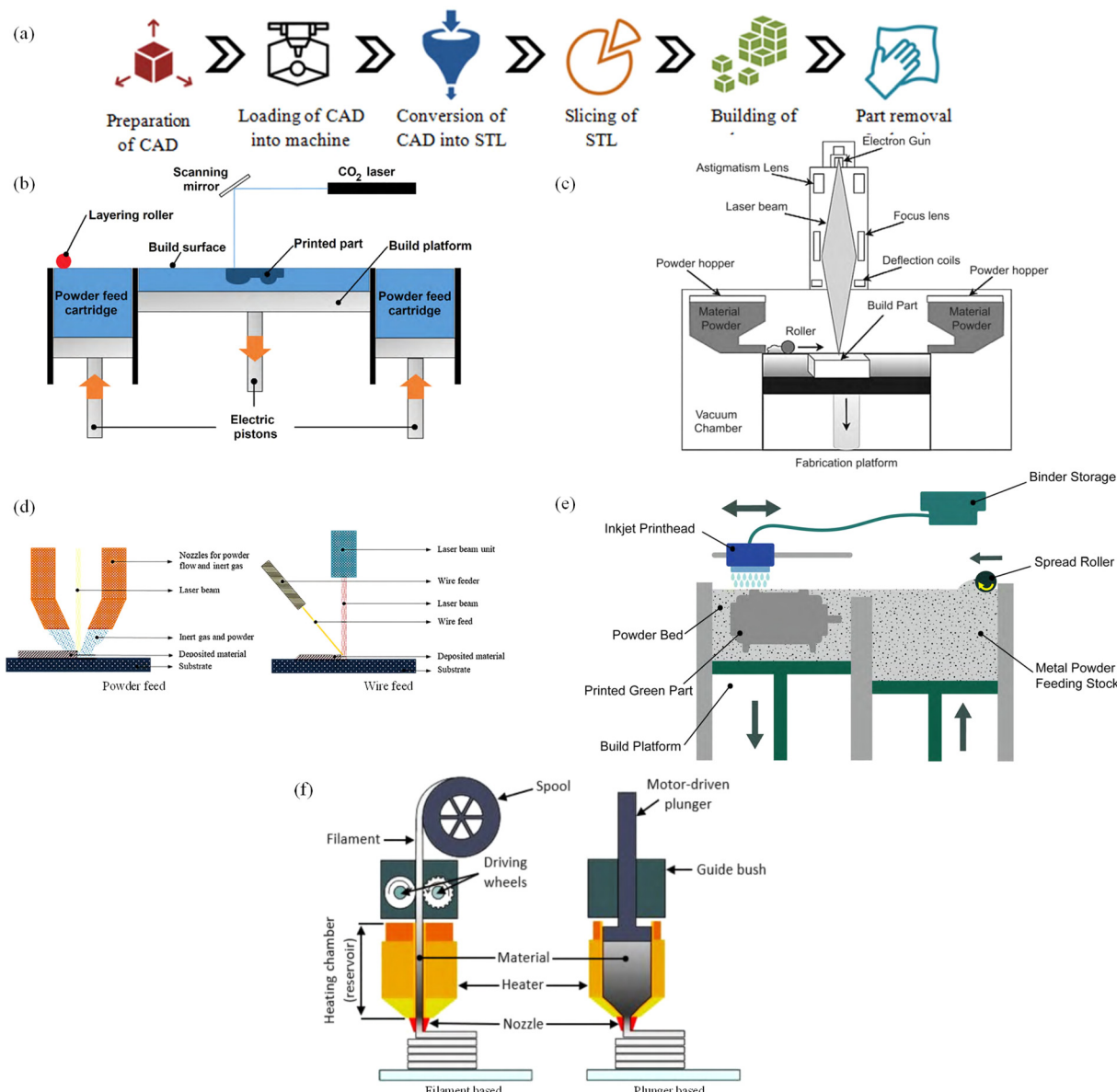


**Fig. 3** (a) Typical steps in AM processes,<sup>104</sup> and schematic drawings of various AM techniques suitable for MMC orthopedic implants: (b) selective laser sintering and melting,<sup>105</sup> (c) electron beam melting,<sup>106</sup> (d) direct melt deposition,<sup>104</sup> (e) binder jetting,<sup>107</sup> and (f) material extrusion.<sup>108</sup> (a, d) are reproduced from University Malaysia Pahang Publishing, copyright 2022, licensed under CC BY 4.0; (b) is reproduced from IET, copyright 2024, licensed under CC BY 4.0; (c) is reproduced with permission from Elsevier, copyright 2024; (e) is reproduced from MDPI, copyright 2025, licensed under CC BY 4.0; and (f) is reproduced from Elsevier, copyright 2022, licensed under CC BY 4.0.

The general steps of AM and its main variants currently used in manufacturing bone substitutes are presented in Fig. 3a and b-f, respectively. The general workflow of AM involves three

stages. The initial stage is scheduling and designing the desired part, typically done by 3D scanning or with CAD software. This is followed by the actual printing stage, where the desired

**Table 3** Comparisons between various AM technologies

AM technologies	Heat source	Initial material	Environment	Residual stresses	Surface finish
SLM, SLS	Laser	Powder	Inert	High	Low
EBM	Electron beam	Powder	Vacuum	Low	Low
DED	Laser, electron beam, plasma arc	Powder, wire	Inert	High	Low
BJ	—	Powder	Room temperature	Low	Low
ME	Heated printhead	Filament, wire or granule	Room temperature or inert	Low	Low



design is printed with the selected material fed into the system. Finally, the last stage is the post-processing of the AM part, which includes cleaning, heat treatments, or decorative enhancements.<sup>9</sup> Table 3 shows the fundamental differences between AM technologies regarding heat sources, materials utilized, environment required for printing, residual stresses, and surface finish of the built parts, while Table 4 outlines the broad advantages and disadvantages of each technology. The main features of these AM techniques are analyzed well in the literature<sup>62,100–103</sup> and are briefly overviewed in the following subsections within the context of AM for MMCs.

### 3.1. Selective laser sintering

Selective laser sintering (SLS, described in the current subsection) and selective laser melting (SLM, described in the following subsection) are both laser powder bed fusion (LPBF) 3D printing technologies working with a laser beam as their energy source. While the SLS is primarily used for polymers, SLM's main application is for metals. That said, SLS can be used in some cases for metals, too.

SLS works by sintering fine powder, either directly or indirectly, layer by layer by using a laser beam. The coherent and directional laser beam heats the powder to a temperature below its melting point, causing powder particles to fuse through solid-state diffusion. However, in practice, the process often involves partial melting, where the surface of the particles may be slightly melted to enhance the bonding. Still, complete melting and solidification do not occur.<sup>109</sup> The amount of the liquid phase resulting from partial melting controls densification and can lead to better particle bonding and reduce the porosity by changing temperature-dependent properties such as viscosity, wettability, *etc.*<sup>110</sup> Partial melting often results in incomplete densification and residual porosity tends to compromise the stress transfer between the reinforcement and metal matrix once the composite is subjected to mechanical

loading. SLS is predominantly used for polymers and ceramics but is also applied to metals for which a high-power laser is required to selectively scan and fuse metal particles on the powder bed.

As the laser moves away, the partially molten material is solidified due to heat transfer by conduction, convection, and radiation.<sup>15</sup> A single layer of powder is sintered and fused according to the first 2D cross-section of the given 3D model.<sup>71</sup> This process is repeated layer by layer, by subsequent lowering of the build platform at a predefined layer thickness. One of the applications of SLS to metals is when a powder mixture of two metals is used, one with a low sintering temperature and another main metal. The laser beam then melts the low-sintering temperature metal that binds to the main metal particles.

In indirect SLS, a preprocessing step involves coating the powder with a binding polymer that needs to be debonded from the green part later.<sup>62</sup> Subsequent debonding and post-processing steps could lead to low density and weak metal-reinforcement interfacial bonding. SLS is a lengthy manufacturing process since it involves preprocessing the powder and a sintering process, which consumes significant time. Laser-beam-based AM processes including SLS generate high residual stresses in the built material due to rapid heating and cooling of the powder bed and printed part, which in turn causes local plastic deformation and compressive residual stress under the top surface.<sup>111</sup> Therefore, post-AM heat treatments are required to minimize residual stress and improve surface quality, which adds to the total time needed for a finished product.<sup>62,112</sup>

To produce MMCs, reinforcement addition usually requires pre-mixing of required reinforcement with the matrix powder before the SLS process, which ensures uniform particle distribution and enhanced mechanical properties. During the SLS process, the interaction between the matrix and reinforcing particles may occur and the phases in the matrix alloy may become dissolved or transformed to other phases, which is

Table 4 Advantages and disadvantages of different AM technologies

AM technique	Advantages	Disadvantages
SLS	<ul style="list-style-type: none"> <li>– No support structures</li> <li>– Complex geometries</li> </ul>	<ul style="list-style-type: none"> <li>– Limited material compatibility</li> <li>– Rough surface</li> <li>– High residual stresses</li> <li>– Post processing</li> <li>– Lengthy processing</li> </ul>
SLM	<ul style="list-style-type: none"> <li>– Wider material compatibility</li> <li>– No support structures</li> <li>– Complex geometries</li> </ul>	<ul style="list-style-type: none"> <li>– Rough surface</li> <li>– High residual stresses</li> <li>– Lengthy processing</li> </ul>
EBM	<ul style="list-style-type: none"> <li>– Low residual stresses</li> <li>– No oxidation due to inert environment</li> <li>– No additives required for melting</li> </ul>	<ul style="list-style-type: none"> <li>– Rough surface</li> <li>– Low dimensional accuracy</li> <li>– Retention time within vacuum chamber after fabrication</li> <li>– High residual stresses</li> <li>– Lengthy post processing</li> </ul>
DED	<ul style="list-style-type: none"> <li>– Wide range of materials</li> <li>– Multi-material AM</li> <li>– Powder and wire feedstocks</li> </ul>	<ul style="list-style-type: none"> <li>– Lengthy post processing</li> <li>– Interlayer porosity</li> </ul>
BJ	<ul style="list-style-type: none"> <li>– Low energy consumption</li> <li>– Less oxidation</li> <li>– Low residual stresses</li> </ul>	<ul style="list-style-type: none"> <li>– Interlayer porosity</li> <li>– Filament breakage</li> </ul>
ME	<ul style="list-style-type: none"> <li>– Less energy consumption</li> <li>– Filament, granules, ink feedstocks</li> <li>– Low residual stresses</li> <li>– Multi-material AM</li> </ul>	



highly dependent on the parameters used for printing the part, such as laser power, scanning speed, hatching distance, and layer thickness, each of which affects the thermal history. Powder bed-based AM processes may allow for better dispersion of reinforcing particles and retention of non-equilibrium phases due to rapid cooling rates, which usually enhances the mechanical strengths of the prepared parts.<sup>29</sup>

### 3.2. Selective laser melting

Selective laser melting (SLM) is one of the most widely used and versatile AM processes and is very similar to SLS. The laser beam melts the powdered material in SLM and fuses powder particles, which require higher laser power than SLS. The choice of process parameters and laser used to achieve consolidation determines whether SLS or SLM would be obtained for the given material system since laser-material interaction controls the extent of consolidation.<sup>110,113</sup> A combination of a low scanning rate and high laser power would feed in more heat, resulting in SLM, while a higher scanning rate and low laser power would result in SLS.<sup>110</sup> SLM commonly uses ytterbium fiber laser, such as a 200 W model, with an inert gas such as Ar or N in the building chamber, which ensures minimum oxygen contamination during the process.<sup>114</sup> A thin layer of powder is melted, the next layer is deposited on the previous layer, and the process is repeated layer-by-layer by following the design features from the CAD model. The substrate temperature can also be controlled, allowing for the control of the cooling rate and, thus, post-solidification defect minimization. SLM is compatible with various materials, including aluminum, titanium, nickel alloys, MMCs, and amorphous materials.<sup>114</sup> Amongst important parameters for SLM are laser power, scan speed, hatch spacing, overlaps, *etc.*, which can be controlled, and the desired microstructure can be engineered. Micro-porous or dense structures can be made by controlling these process parameters, such as laser power.<sup>62</sup> Some of the drawbacks of the SLM process include lengthy fabrication time, high costs, surface roughness of the finished products (roughness being dependent on powder characteristics and process parameters),<sup>114</sup> internal stresses due to high cooling rates, occurrence of balling due to surface oxide films and Marangoni convection,<sup>115</sup> and vaporization phenomena that occur due to the high temperatures of the melt pool, enabling some of the elements to evaporate out of the melt pool.<sup>62</sup>

Generally, a powder with very fine particle sizes has poor flowability. In contrast, a powder with a mixture of coarse and fine particles has good flowability and is beneficial for uniform powder particle distribution within the SLM system to improve the density of the resulting products.<sup>116</sup> Powder particle shape and size are crucial parameters, although they are regarded as external parameters that cannot be controlled since powder manufacturers mainly supply powders. Regular and spherical powders are preferred for SLM since particles do not cling to each other and ensure better flowability and packing density.<sup>116,117</sup> Similar to SLS applied to MMCs, reinforcing particles are often added to the metal powder before the melting process,<sup>118</sup> which allows for good dispersion.

Moreover, due to complete melting, interfacial bonding between the matrix and the reinforcement is stronger due to complete melting than that resulting from SLS.

Reinforcing particles can be added through an *ex situ* or an *in situ* approach to manufacture MMCs using SLM, both of which have merits and demerits. In the *ex situ* approach, particles are added to the metal powder before manufacturing begins. These particles remain in their original form throughout the process, leading to their presence in the final composite product.<sup>119</sup> This approach gives more control over the morphology and distribution of the reinforcements, along with more material choice options. Yet, the interfacial bonding is weaker, and the risk of reinforcement contamination exists, leading to potentially weaker mechanical properties. On the other hand, the *in situ* approach refers to the formation of reinforcement particles through chemical reactions with the metal matrix during manufacturing.<sup>119</sup> The laser's thermal energy initiated and supplied facilitates overcoming the reactants' activation energy barrier, thus forming new compounds.<sup>115</sup> This *in situ* reaction is exothermic, and the additional thermal energy facilitates melting, improving the constituents' bonding.<sup>119</sup> In contrast to the *ex situ* approach, the *in situ* one provides better reinforcement distribution and stronger interfacial bonding.<sup>119</sup> However, the choices of reinforcements are narrow, with potential reaction complexity and unwanted phase production during the process.<sup>29,119,120</sup>

*In situ* reinforcing during SLM has been attempted, leading to the formation of, for example, TiB/TiN/TiC/Ti<sub>5</sub>S<sub>3</sub> in a Ti matrix.<sup>119</sup> A study reported improved hardness and compressive strength through the *in situ* formation of fine, needle-like TiB from TiB<sub>2</sub> during SLM from a ball-milled Ti-TiB<sub>2</sub> powder mixture.<sup>119,121</sup> Ti-TiB composites are specifically beneficial as biomedical composites because B is also biocompatible. In addition, TiB provides mechanical and chemical stability. However, an excessive addition of reinforcement leads to detrimental effects on strength and especially on ductility.<sup>122</sup> In another study using SLM, the *ex situ* approach was utilized to incorporate mesoporous silica into the ZK60 matrix to enhance its resistance to biodegradation.<sup>123</sup> Mesoporous silica was considered favorable for Mg surfaces owing to its high corrosion resistance. Moreover, silica particles were homogeneously dispersed in the Mg matrix, leading to strong interface binding. Controlling and optimizing the SLM parameters, including laser type, laser power, wavelength, *etc.*, can improve the quality and performance of SLM-prepared products.<sup>10</sup> For instance, excessive power used in SLM may lead to severe defects, such as keyhole pores, interfacial cracking and agglomeration. In addition, the inherent nature of the SLM process involving full melting can create large thermal gradients within the product and rapid solidification can lead to high residual stresses and the coalescence of the clusters in the printed composites.<sup>122</sup>

### 3.3. Electron beam melting

Electron beam melting (EBM) works very similarly to SLM. Instead of a laser, it uses an electron beam generated by a tungsten filament, accelerated, and directed by magnetic fields



in a vacuum chamber. As compared with an inert atmosphere, the vacuum chamber ensures that oxidation does not occur during fabrication, which is an important consideration for reactive metals, such as titanium, magnesium, iron, *etc.*, assuring high-quality products.<sup>13</sup> The optimization of the EBM process is more challenging due to the numerous controllable parameters, including the electron beam's power, focus, scanning velocity, line spacing, diameter, substrate plate temperature, contour, and scanning strategies.<sup>13</sup> Since the electron beam is powerful enough to raise the temperature and eventually melt the materials and bind them layer by layer, additives are not required to aid in the melting process.<sup>62</sup> In contrast to SLM, brittle materials can be manufactured by EBM by avoiding solidification defects that arise from internal stresses due to rapid cooling from their melting or solidifying points that usually occur in the SLM process. Increasing the powder bed temperatures can significantly reduce the cooling rate,<sup>114</sup> allowing defect-free brittle materials to be produced. In addition, the formation of brittle phases in the material can be avoided, leading to a more ductile material with a somewhat lower strength.<sup>114</sup> EBM is an excellent tool for manufacturing porous structures for biomedical implants since the temperature supply is relatively uniform, making it possible to create stronger connections between the layers.<sup>54,62</sup> Some limitations of this technique include low surface quality and dimensional accuracy,<sup>62</sup> due to the wider electron beam compared to lasers and the increased time required for cooling the part before removing it from the substrate due to high temperatures in the vacuum chamber.<sup>114</sup>

The dispersion of reinforcing particles is significant in the case of MMCs, and uniform dispersion is required for better structural and mechanical properties. A study has shown that during EBM, the behavior of reinforcing particles is influenced by dynamic wetting and Laplace pressure, where the wetting drives the particles into the melt pool.<sup>124</sup> In contrast, the curvature forces due to Laplace pressure hinder their submergence.<sup>124</sup> Poor wettability of reinforcing materials can produce an energy barrier at the particle-matrix interface, leading to particle agglomeration. However, subsequent layering with an optimum thickness can mitigate this challenge, which can be achieved by rapid solidification during the EBM process, ensuring a homogenous reinforcement distribution.<sup>124</sup> Though the pre-heated bed is beneficial for reducing cooling rate, elevated temperatures and longer dwell times can promote elemental vaporization from metal matrix and reinforcements, along with grain coarsening and unwanted reactions between the matrix and reinforcements.<sup>125</sup> EBM produces low surface finish, which could be beneficial for some bone implants to enhance cell attachment, while other products might require surface treatments as post-processing.<sup>126</sup> For instance, for Ti alloys, different surface modification methods are employed to enhance the mechanical and tribological properties of Ti implants at the surface.

### 3.4. Directed energy deposition

Directed energy deposition (DED) involves using thermal energy in the form of a laser, electron beam, plasma arc, *etc.*,

to melt the material directly discharged from a nozzle. Direct melt deposition (DMD) or laser metal deposition (LMD) are two subsets of DED that specifically use a CO<sub>2</sub> laser beam to melt the material that gets seamlessly fused with the material deposited in the previously printed layers.<sup>62,104</sup> The material feedstock can be either powder or wire, depending on which the DMD process is called powder-fed or wire-fed. In a powder-fed system, metal powder is sprayed toward the substrate's melt pool, the laser beam (partially) melts the powder on the fly, and the (semi) melted powder deposits on a substrate. This process is iterated according to the given design until the finished product is achieved. If the powder is made of a metal with a high melting point, another metal with a low melting point acts as a binder, and some additives acting as fluxing or deoxidizing agents are often added to the main metal powder.<sup>104</sup> The wire feeding system comprises wire feedstock delivered from the side at a certain angle, enabling the production of near-net-shape parts. The process parameters to be controlled in DMD include laser power, beam spot diameter, feedstock rate, gas flow rate, and scanning speed. Due to the low complexity of this method, DED is usually used to manufacture and repair larger parts.<sup>21</sup>

For the AM of MMC products, two powder or wire feedstocks can simultaneously be fed to the DED system using separate hoppers, which skips the requirement of mixing powders before 3D printing and avoids the possibility of segregation between different metal powders or reinforcements due to the differences in their densities.<sup>127</sup> The utilization of varying material feedstocks within one print cycle with precise control over the location of deposition of those materials within the component allows the production of MMCs and functionally graded materials (FGMs).<sup>104,128</sup> Moreover, manufacturing FGMS through multi-material AM is achievable compared to conventional manufacturing methods.<sup>129</sup> To improve the wear- and corrosion-resistance properties, in a study, the authors manufactured functionally graded multilayers using DED, with layers having different compositions fed by a twin feeder system.<sup>129</sup> A gradient shift in composition resulted in a micro-hardness gradient at the interface. Sharp material transitions can be substituted by gradual interfaces, thereby avoiding the stress concentrations at the sharp transition regions.<sup>129</sup> In another study, laser cladding (LD) was used to deposit MMC coating composed of Inconel 718 and tungsten carbide (WC). The authors studied the resulting thermal history of the molten pool as a function of different parameters involved in LD.<sup>130</sup> The study showed that the low scanning speed caused the precipitation of carbides due to a relatively long melt pool lifetime. In contrast, a high scanning speed caused improper wetting of WC particles with the matrix. The optimum molten pool lifetime was determined to be 0.68 s.<sup>130</sup> Moreover, the compatibility between the matrix and reinforcing ceramic was considered crucial; materials with higher chemical affinity would promote the decomposition of the ceramic, which would eventually be detrimental to the performance of the composite part.<sup>129</sup>

It is crucial to achieve uniform dispersion of reinforcing particles and avoid agglomeration for MMC production using



DED. Partial dissolution of phases within the metal matrix occurs in laser DED processes, which promotes interfacial reactions between the metal and the ceramic particles of the reinforcement.<sup>129</sup> DED can lead to uneven melting and distribution if factors like laser power, scanning speed, layer thickness, *etc.*, are not carefully controlled.<sup>29,124</sup> Moreover, thermal history management is crucial during DED to retain different phases. Controlled cooling, post-processing, and process optimization are required to ensure proper thermal management during and after the DED process since the thermal history can create defects and unwanted phase distributions.<sup>124</sup> Cracks can be induced within the material due to large thermal gradients during the process, which can lead to catastrophic failure of produced MMC parts.<sup>131</sup> A higher content of ceramics also leads to crack formation. For instance, in a study on DED for Ti–TiC, it was found that an addition of TiC greater than 5 wt% led to crack formation due to higher dendritic TiC occurrence.<sup>132</sup> When mechanical load is applied to a MMC part with a high TiC content, densely populated particles hinder plastic deformation and cause stress to be localized. Micro-cracks are prone to generate, extend and merge in the vicinities, leading to premature failure.<sup>132</sup> Therefore, even though, theoretically, a higher content tends to increase the strength, structural differences and microcracks often lead to a high brittleness and even a low strength. It has been shown that differences in lattice structure, mechanical properties, and thermal expansion between the matrix and reinforcement can lead to cracking at the materials' interface.<sup>131,133,134</sup> Moreover, mechanical properties depend heavily on the interface and adhesion between the matrix and reinforcement. To address the interface issue, a study explored the encapsulation of ceramic particles with metallic coating to enhance the adhesion and reduce crack formation due to material mismatch.<sup>131</sup> In short, sensible material choice and DED process optimization along with appropriate post-processing could lead to MMCs with desired properties.

### 3.5. Binder jetting

Binder jetting (BJ), first developed and patented at the Massachusetts Institute of Technology (MIT) in 1993, is a non-beam-based multistep AM process in which a binder, typically a polymeric liquid, is dispersed through a print jet on layers of powder, one layer at a time.<sup>62,97,135–137</sup> Two types of materials are used in BJ: a powdered material of which the part is to be made (*e.g.*, metal or ceramic) and a binder material that glues the powdered material with each other and between the layers.<sup>114</sup> The binder material is deposited by a print head over the powder layer, binding the loose powder particle. The stage moves down with increments equal to the thickness of the deposited layer. The process is repeated for building the entire structure,<sup>62</sup> called the 'green' part, which is not yet ready to be used and requires post-processing to achieve desired properties.<sup>97</sup> BJ can process many types of powdered materials and is a relatively fast process. Still, the post-processing steps of the green part are time-consuming, including curing, de-powdering, debinding, sintering, and finishing.<sup>114,135</sup> Since BJ

predominantly depends on the bonding between the powder and binder, almost any material can be printed using this process.<sup>135</sup> Moreover, this method has relatively low energy consumption, reduced oxidation, and low thermal and residual stresses in the resulting parts.<sup>111</sup>

In a study on the bonding at the metal–ceramic interface, the authors used BJ to produce a cellular structure of cordierite ( $2\text{MgO}\cdot 2\text{Al}_2\text{O}_3\cdot 5\text{SiO}_2$ ), followed by sintering, pouring a zinc alloy (Zn–4Al–0.4Mg) melt into the cellular structure and then allowing solidification to take place.<sup>138</sup> Bonding was expected due to mechanical interlocking and/or chemical reactions. Mechanical interlocking indeed occurred when the molten zinc alloy was drawn to rough ceramic surfaces due to capillary action, where solidification occurred, creating mechanical bonding at the interface. However, a chemical reaction was not observed due to the stability of the ceramic. While a strong interface was preferred, the authors considered that chemical reactions could have an adverse effect, causing degradation of the constituent materials.

The metal matrix and reinforcing agents should have compatible properties for adequate bonding, including comparable particle sizes and shapes, thermal expansion coefficients, binder compatibility, chemical stability, *etc.*<sup>138</sup> Smaller particles have higher surface area-to-volume ratios than larger powder particles, leading to better sinterability and smoother surfaces with higher sintered densities.<sup>12</sup> On the other hand, finer particles agglomerate more than coarser particles, owing to higher friction between particles.<sup>12,14</sup> BJ is followed by a debinding step that involves removing the binder material prior to sintering. Debinding usually occurs chemically, or thermally ( $\sim 600\text{--}700\text{ }^\circ\text{C}$ ), or as a combination of both in an inert, reducing, or vacuum environment that reduces the carbon content from the retained binder residing inside the green body, reducing the formation of carbides during post-processing stages.<sup>12</sup>

Apart from BJ process parameters, the overall density of the prepared part is also dependent on temperature, pressure, time, and environment of the post-processing steps. Sintering causes bond formation between contacting particles, which reduces the porosity and causes the formation of equiaxed grains and grain growth, along with the possibility of forming secondary phases, which can impact the mechanical properties. The absence of a heat source in BJ prevents the formation of *in situ* compounds. Therefore, reinforcements are required to be incorporated within the feedstock.<sup>29</sup> However, researchers have developed *in situ* processes during the post-processing steps for producing MMC parts.<sup>139,140</sup> For instance, researchers formed Inconel 625-based MMCs using BJ and a carbon-containing binder.<sup>140</sup> During the sintering step after BJ, carbides were formed due to the reactions between the Inconel elements (Cr, Mo, Nb) and carbon from the binder, which was distributed across the grain boundaries, forming an interconnected network across the matrix.<sup>139,141</sup>

Compared with laser powder bed fusion (LPBF) processes, BJ leads to interlayer porosity, facilitating cracks to coalesce, which is detrimental to the structural integrity of the final

part.<sup>12</sup> The pores cause anisotropic mechanical properties and can act as stress concentrators, leading to premature failure.<sup>12</sup> Even though sintering helps in particle bonding, dimensional accuracy, and mechanical properties, often, it does not eliminate porosity completely. Studies have shown that given the same pore sizes and porosities, BJ results in weaker parts as compared with LPBF.<sup>12,142–144</sup> This was attributed to BJ finally giving rise to equiaxed grains and frequent twinning during post-processing of cubic close-packed austenitic metals, such as the Inconel 625 alloy, leading to a lack of grain orientation and weaker material, as compared with LPBF processes that generate complex microstructures with grains oriented along a particular direction, producing a much stronger and continuous structure.<sup>12</sup> Moreover, the sintering environment significantly determines the prepared part's final density and mechanical properties. Regardless of sintering temperature, the Ar environment was found to lead to a lower density, while vacuum resulted in a higher density and improved mechanical properties.<sup>12</sup>

### 3.6. Material extrusion

Extrusion-based 3D printing is a comparatively simpler and cheaper AM process that utilizes feedstock materials in the form of filaments, granules, or inks (liquid state) to print materials following the design from a CAD model.<sup>11,20,108</sup> When this technology appeared in the late 1980s, it was primarily used for polymeric materials. Since the last decade, the technology has been developed to contain advanced features, including high building speed and compatibility with a range of materials, including ceramics, glass, metals, food, and constructional materials.<sup>20,108,145,146</sup> The feedstock material, usually filament, is heated until its viscosity decreases. The liquified feedstock is collected in a reservoir, from which it is pushed out of a nozzle to bond and settle over the previous layer.<sup>108</sup> The control of the temperature for softening the material and initiating chemical changes through curing between the depositing layer and pre-deposited layer are the key elements to ensure bonding between subsequent layers of the printed part.<sup>108,146</sup> The main parameters involved in the printing process are hatch spacing, layer thickness, orientation, nozzle diameter, extruder temperature, and velocity.<sup>146–148</sup> For example, when printing a material containing metal or ceramic particles to produce MMC scaffolds, the solid metal powder and ceramic powder are blended with a binder. After the part is printed, debinding and sintering are required, which are expensive and time-consuming steps.<sup>147</sup> Multi-material extrusion-based 3D printing has recently been explored, which involves multiple filaments and print heads, and it is challenging due to the differences in melting point between different materials involved.<sup>108</sup> Extrusion-based AM does not require a high-power source, compared with SLM, EBM, *etc.*, and thus, costs less and is safer to use.<sup>148</sup> It also gives more control over material composition since filaments with different combinations can be used. Moreover, if the temperature during the printing phase is carefully controlled, the residual stresses are lower than in high-power AM methods. In the case of the

feedstock containing metal particles, surface roughness can also be improved by utilizing finer particles in addition to reduced layer thickness.<sup>148</sup>

However, extrusion-based AM is prone to porosity due to the layer-by-layer deposition of the material. The existence of porosity will interfere with interlayer thermal transmission, may weaken the interfacial bonding and lead to the formation of more voids.<sup>149</sup> The size, morphology, and quantity of the pores are determined by nozzle diameter, infill percentage, printing speed, layer height, *etc.*<sup>149,150</sup> In a study, the impacts of two printing parameters (*i.e.*, infill percentage and layer height) were analyzed to determine their effects on the resulting porosity and strength of the material.<sup>150</sup> Variations in these two parameters resulted in porosity values ranging between 9 and 22%. It was found that the infill percentage was the dominant factor influencing the resulting structure by consistently reducing porosity and increasing ultimate tensile strength, as evidenced by the acquired data when the infill percentage increased from 85 and 90% to 95 and 100%. Other challenges concern filament breakage and nozzle coggage, causing geometrical misalignment and even manufacturing failure. An accelerometer is often employed to monitor the condition of the nozzle by measuring the vibration of the mounting bar that supports the liquefier assembly.<sup>149</sup>

## 4. Metal matrix composites for bone implants

One of the methods to achieve desired material properties is by engineering materials' composition. This can be done by either forming a homogenous mixture of two or more metals to form alloys or by combining two or more distinct materials with different physical, chemical, and mechanical properties, forming composites. Both material design approaches have been actively adopted to form advanced (biodegradable) implants, and these approaches can even be implemented simultaneously using AM methods. Moreover, porous structures can be manufactured using AM,<sup>82,83</sup> which are known to enhance osteogenesis<sup>84,151</sup> and reduce the volume of MRI image artifacts in the cases of metal implants made of titanium alloys or tantalum.

One prominent composite material class is MMCs, which are multiphase or hybrid materials formed by continuous or discontinuous dispersion of a reinforcing material into a metal matrix,<sup>152</sup> contributing toward meeting host-specific implant biocompatibility requirements, including, biodegradation, and/or mechanical properties. The constituents in MMCs must remain distinct throughout the processing history of the material, which is distinctly different from alloys formed during melting and/or heat treatment. The scale of the reinforcing constituent should be smaller than the scale of the component being manufactured,<sup>69</sup> which excludes laminated or coated structures. MMCs are tailored to combine the best properties of individual materials, such as the ductility of metals and the toughness of a ceramic reinforcement.<sup>153</sup> The capacity of



reinforcing phases to enhance the properties of MMCs is dependent on their composition, morphology, distribution, and volume fraction.<sup>141</sup> Typically, MMCs have higher strength than the corresponding metal matrix owing to different strengthening mechanisms, including Hall-Petch strengthening, load transfer strengthening, Orowan strengthening, and dislocation strengthening.<sup>29</sup> The uniform distribution of reinforcements into the matrix through AM promotes these strengthening mechanisms, thus allowing MMCs to reach their full potential.<sup>29</sup>

Agglomeration is often observed in various conventional fabrication processes for MMCs, which is the clustering of particles when solid particles encounter a non-wetting medium during a liquid-state fabrication process.<sup>153,154</sup> This significantly reduces the strain at failure owing to the preferential nucleation of cracks in the clustered regions, followed by crack propagation and fracture.<sup>153</sup> One of the benefits of using AM over conventional fabrication methods for designing and fabricating MMCs is the controlled dispersion of the reinforcing component to achieve complete benefits of MMCs<sup>152</sup> and avoid agglomeration.<sup>153</sup>

Generally, different AM techniques can be used to manufacture MMCs for structural applications, specifically for the automotive and aerospace industries. By contrast, limited work has been conducted to investigate the AM of MMCs for biomedical applications through intensive *in vitro* and *in vivo* studies. This review article focuses on understanding tailored AM MMC scaffolds and their corresponding biological assessment for orthopedic applications.

An ideal bone substitute should possess bone-mimicking properties and architectural features, including an intricate interconnected porous structure with mechanical properties close to those of the bone. Moreover, the biodegradation rate must be precisely controlled to ensure complete bone regeneration in an optimum time frame and prevent the implant from persisting beyond the bone's healing period. This strategy eliminates the requirement for secondary surgery to remove the implant. Another issue that must be dealt with in developing metallic implants concerns post-implantation diagnostic imaging since most metals are not MRI-friendly. The presence of implants hinders accurate diagnostics by causing image artifacts and poses a significant risk to patients' safety during MRI procedures. AM MMCs may address these challenges and requirements by controlling the geometry and the composition of the built implant. A summary of the current literature on the AM of MMCs and their mechanical and corrosion assessments for orthopedic applications is presented in Table 5. It is worth noting that the studies differ significantly in terms of material composition, AM process and testing conditions. Therefore, often, the mechanical properties and degradation rates cannot be directly compared with each other across different studies. Nevertheless, the overview reveals a general range within each of the MMC material systems to understand the achieved results and identify the gaps. Similarly, while it is difficult to directly compare the cytotoxicity of implants due to different methods used in different studies, Table 6 is formulated to give

an overall view of the interpretation of the testing results so far reported in the literature. It is worth noting that only three of the studies conducted *in vivo* trials, in addition to customary *in vitro* testing.

#### 4.1. Ti-based MMCs

Ti-based alloys such as TiAlV have been widely used for permanent orthopedic implants due to their fatigue strength, high strength-to-weight ratio,<sup>88</sup> and minimal corrosion *in vivo*.<sup>165</sup> The high reactivity of Ti causes the rapid formation of a passive oxide layer ( $TiO_2$ ), promoting corrosion resistance and cytocompatibility.<sup>96</sup> This high reactivity also calls for precise control over fabrication parameters to avoid contamination during AM and the ensuing alteration of mechanical properties.<sup>7</sup> The key challenges with Ti-based biomaterials lie in optimizing their mechanical properties to meet the requirements of bone replacement and avoiding the stress shielding effect, which has been widely reported for Ti-based load-bearing implants.<sup>7,165</sup> In addition, although Ti-based implants are cytocompatible and can support osseointegration,<sup>7,175</sup> meaning that bone directly integrates with the Ti-based implant without rejecting it,<sup>88</sup> they are not bioactive and, thus, do not induce bone healing or osteoinduction. Changing the composition of such implants by alloying Ti with other elements is proven to help with osteoinduction. Examples include Ti alloys containing Nb.<sup>175</sup>

Although Ti is resistant to corrosion and is capable of forming a  $TiO_2$  oxide layer, there is still a possibility of corrosion through prolonged exposure to bodily fluids and mechanical stresses.<sup>46,176,177</sup> Moreover, the toxicity of Ti-based implants is highly dependent on their material composition, *e.g.*, TiAlV *vs.* TiNb.<sup>175</sup> In certain studies, particles originating from implants were observed in *peri-implant* tissues, serum, and bone marrow, which then traveled to the lungs, spleen, liver, and kidney, suggesting the corrosion of Ti-based implants.<sup>175,176,178</sup> The particles resulting from corrosion may elicit biological responses, the extent of which is dependent on the size, quantity, and composition of these particles. Cells can interact with these particles and metallic ions within non-toxic ranges, but ion concentrations can affect their behavior since they are sensitive to ions.<sup>177</sup> The corrosion causes the release of Ti ions along with other metallic ions from the Ti alloy implant, which can potentially reduce the implant's lifetime and cause cellular and systemic toxicity.<sup>179</sup> Even the noble metals intentionally added to Ti to increase the antibacterial properties of implants are getting attention due to the possible toxicological effects of the ions of these elements (like  $Ag^+$  and  $Au^+$ ).<sup>175,180</sup> Moreover, although the exact mechanism of antibacterial action is not fully understood, genotoxicity due to Ti-based implants has been reported, with physicochemical characteristics of metallic ions enabling them to reach even DNA, producing genotoxicity by breaking DNA strands, mitotic spindles and/or leading to the loss of chromosomes during cell division.<sup>175,177</sup> Similarly, the exact mechanism of ion release and transport is not clear. Different hypotheses have been put forward to explain the causes of Ti-based implant toxicities.





Table 5 A summary of the existing literature on the mechanical and corrosion assessments of additively manufactured MMCs for biomedical applications, alongside conventionally prepared Ti, Fe, and Mg

Materials and AM technique	Test condition	Ultimate Strength (MPa)	Elastic Modulus (GPa)	Yield Strength (MPa)	Microhardness (HV)	Biodegradation rates (mm year <sup>-1</sup> )	Key findings	Ref.
Conventional Ti	- Compression	8.9-630	3.5-200	21-1117				155-158
Conventional Mg	- Compression	97-325	41-45	65-100			<i>In vitro</i> : 0.01-2.5*	159-162
Conventional Fe	- Compression	597-580	210	48.2-500			<i>In vivo</i> : 0.39-2.3**	155,163,164
Ti6Al4V-5 TCP (wt%)	3DF	324.6 ± 12	6.18 ± 0.79				- The effect of TCP particle content on the porosity is minimum.	165
Ti6Al4V-10 TCP (wt%)		358 ± 24	5.74 ± 0.95				- Increase in porosity (48% to 70%) caused decrease in compressive strength.	
Ti-silica 1 g Silica in 2 g Ti	SLS	- Compression	142				- Sintering increased compressive strength as compared with non-sintered parts, from ~20 MPa to 142 MPa, and contributed towards more cell growth.	166
Ti6Al4V-10 HA (wt%)	Extrusion- based AM	- Compression	60				- Compressive strength decreased with increase in HA content.	
Ti6Al4V-0.05 EB (vol%)	SLM	- Three-point bending	1131 ± 36.3	55.6 ± 0.09			- Scaffolds sintered in air had a higher compressive strength (60.4 MPa) than those sintered in an argon atmosphere (~10 MPa).	167
Ti6Al4V-0.5 EB (vol%)	ZK30-5BG SLM	- Microhardness	745.93 ± 113.51	45.56 ± 2.92			- Increase in EB caused a decrease in flexural strength and an increase in roughness.	168
ZK30-10BG (wt%)							- BG enhanced corrosion resistance and increased microhardness.	169
ZK30-15BG (wt%)								
ZK30-10BG (wt%)							- ZK30/10BG showed higher hardness due to a thicker precipitate layer acting as a barrier for degradation.	
ZK60-5MBG LPBF (wt%)	Extrusion- based AM	- Hydrogen evolution (10-d) and electrochemical tests (SBF, 37 °C)	145.1 ± 9.2	36.7 ± 5.3	121.7 ± 8.5	96.8 ± 10.2	- MBG in Mg led to improved mechanical performance and corrosion resistance due to the formation of a protective apatite layer.	170
MgZn-5 β TCP (wt%)	Extrusion- based AM compression	- Microhardness, tensile Immersion (7-d) and electrochemical tests (SBF, 37 °C)	Non-degraded: 40.9 ± 17.5	Degraded: 0.32 ± 0.2	Degraded: 21.86 ± 14	0.31	- Addition of TCP improved degradation and strength.	171
MgZn-10 β TCP (wt%)		- Immersion (14-d) and electrochemical tests (r-SBF 37 °C)	39.1 ± 22.7	0.1218 ± 0.097	5.7 ± 3.3	0.7	- Mg-Zn 5 wt% TCP showed most uniform particle dispersion and a decreased <i>in vitro</i> biodegradation rate.	
							- The fluctuations of mechanical strength remained within the required range for cancellous bones after 14 days of immersion.	



Table 5 (continued)

Materials and AM technique	Test condition	Ultimate Strength (MPa)	Elastic Modulus (GPa)	Yield Strength (MPa)	Microhardness (HV)	Biodegradation rates (mm year <sup>-1</sup> )	Key findings	Ref.
Fe-5Al (vol%) AM	Extrusion - Compression	Degraded: 0.23 ± 0.05	Degraded: 3.4 ± 0.2	0.08 ± 0.01	- The mechanical integrity remained within the range of the cancellous bone after 28 days of biodegradation.	86		
Fe-10Al (vol%)	- Immersion (28-d) and electrochemical tests (r-SBF, 37 °C)	0.30 ± 0.02	2.25 ± 0.02	0.09 ± 0.01				
Fe-15Al (vol%)		0.17 ± 0.07	1.5 ± 0.3	0.11 ± 0.02				
Fe-20Al (vol%)		0.13 ± 0.05	0.8 ± 0.2					
FeMn-20Al (vol%)	Extrusion - Compression based AM	3.9 ± 0.9	Degraded: 0.09 ± 0.01	Degraded: 1.8 ± 0.6	0.24	- Biodegradation rates for both Al concentrations (20 and 30 vol%) were within the ideal biodegradation range.	55	
FeMn-30Al (vol%)	- Immersion (28-d) and electrochemical tests (r-SBF, 37 °C),	0.009	2.26 ± 0.89	0.01	0.27			
Fe-30 CaSiO <sub>3</sub> (wt%)	Extrusion - Compression based AM	126						
	- Immersion (35-d) (Tris-HCl)							
Fe-2.5BR (wt%)	SLM	- Compression	Non-degraded: 267 ± 12	Non-degraded: 152.77 ± 8.84	17.37 ± 1.64% weight-loss	- Macropore morphology did not significantly impact the overall compressive strength.	172	
Fe-5BR (wt%)		- Immersion (28-d) and electrochemical tests (SBF, 37 °C)	315.5 ± 14.8	200.4 ± 11.1	146.5 ± 12.7	- Increasing the sintering temperature (1150–1350 °C) notably increased the compressive strength to 126 MPa owing to higher densification.		
Fe-7.5BR (wt%)	SLM	- Compression	286.3 ± 16.2	61.4 ± 13.9	131.44 ± 15.34	- Higher weight loss observed for the composite scaffolds, as compared with the Fe scaffolds.		
Fe-2BR-2.5Pd (wt%)			131.35 ± 9.15	0.07 ± 0.01	-79.8% increase in compressive yield strength due to an addition of 5 wt% BR.	-79.8% increase in compressive yield strength due to an addition of 5 wt% BR.	173	
Fe-2BR-5Pd (wt%)		- Immersion (21-d) and electrochemical tests (SBF, 37 °C)	14.8	200.4 ± 11.1	146.5 ± 12.7	- Enhanced corrosion rates of the composite scaffolds due to local pitting facilitated by BR.		
Fe-2BR-10Pd (wt%)			137.65 ± 10	124.65 ± 7.04	0.16 ± 0.02	- Compressive strength of Fe-2Pd-2.5BR decreased by increasing BR content to 10 wt%.		
Fe-4BR-2.5Pd (wt%)		- Immersion (21-d) and electrochemical tests (SBF, 37 °C)	147 ± 7	130.3 ± 9.9	0.31 ± 0.02	- Scaffolds showed 6x faster corrosion than Fe due to Pd-rich intermetallic phases inducing uniform micro-galvanic corrosion.		
Fe-4BR-5Pd (wt%)			175.3 ± 7.64	131.69 ± 8.45	0.41			
Fe-4BR-10Pd (wt%)			164 ± 8.8	140.29 ± 9	0.6			
			163 ± 17.7	119.7 ± 12	0.76			

The values were expressed in \* mg cm<sup>-2</sup> h<sup>-1</sup>, \*\* mg mm<sup>-2</sup> y<sup>-1</sup> and \*\*\* mL cm<sup>-2</sup>.



Table 6 Literature on the biological assessments of MMC implants prepared using AM

Materials, AM	technique	Testing conditions	Observations	Ref.
Ti6Al4V-TCP	<i>In vitro</i> : – Ion exchange dynamics with SBS and alpha-MEM supplemented with 10% fetal bovine serum (FBS). 3DF – $t = 1\text{--}7$ d SBS, 3-9 w FBS	<i>In vitro</i> : – Dorsal muscles in dogs. $t = 12$ w <i>In vitro</i> : – MG63 (MTT assay) – Direct contact method. – $t = 7$ d	– Ti6Al4V with 10 wt% TCP showed maximum bioactivity confirmed by Ca and P content analysis over 9 weeks, with Ca increasing from 16 to 35 ppm and P increasing from 4 to 13 ppm. – <i>In vivo</i> testing confirmed osteoinductive property of the 10 wt% TCP scaffolds due to ectopic bone formation in 3 out of 4 dogs. – Bone formation observed in close association with TCP particles in the strut, with total bone area percentage of ~19.5% as compared to ~2.2% in the pores. – Optical density of cells increased from 0.017 to 2.3 from 4 h to 7 d, confirming viable cell growth. 166	165
Ti6Al4V-HA	<i>In vitro</i> : – rBMSCs (live/dead viability assay, F-actin and DAPI staining)		– Rough surface of Ti6Al4V-HA scaffolds provided better attachment of rBMSCs as compared with 167 comparatively smooth surface of Ti6Al4V scaffolds. – A higher HA content led to reduced cell death and better biocompatibility.	167
Extrusion AM	– Direct contact method – $t = 7$ d	<i>In vitro</i> : – MC3T3-E1 cells (WST-1 assay, ALP activity, ARS staining, western blotting for OPN, OCN, RUNX2) – Direct contact method	– Increase in EB (0–0.5 vol%) content increased the hydrophilicity, suggesting better protein adsorption. – Excessive $\text{CaTiO}_3$ formation in Ti – 0.5 vol% EB was identified as a potential cytotoxic agent, while Ti – 0.05 vol% EB showed better cell attachment, viability and differentiation. – Ti – 0.05 vol% EB demonstrated highest bone volume percentage (33%), along with reduced inflammatory response and bone regeneration of the defected bone.	168
Ti6Al4V-EB		<i>In vitro</i> : – MC3T3-E1 cells (WST-1 assay, ALP activity, ARS staining, western blotting for OPN, OCN, RUNX2) – Direct contact method	– The addition of BG decreased $\text{Mg}^{2+}$ release, thus increasing cytocompatibility. – Higher BG addition caused higher relative growth rate (~70% to 93%). – BG addition increased the relative growth rate of cells, thus reducing toxicity.	169
SLM		<i>In vitro</i> : – Mouse L929 fibroblasts (MTT assay) – Indirect contact method – $t = 4$ w	– MBG consistently showed better cell viability (94% in 100% extract) than BG due to the availability of a high surface area for cell adsorption.	170
ZK30-BG		<i>In vitro</i> : – Human MG-63 cells (CCK-8 assay, live/dead viability assay) – Indirect contact method – $t = 1, 2, 3$ d	– Cell proliferation was enhanced with MBG addition due to reduced ion release, thus providing a mild environment for cell survival.	171
ZK60-MBG		<i>In vitro</i> : – MC3T3-E1 cells (live/dead viability assay, ALP activity, trypan blue assay, alizarin red S staining) – Direct contact method – $t = 1, 3, 5$ d	– $\text{MgZn-5}$ and 10 wt% $\beta$ -TCP showed high metabolic activity.	171
LPBF		<i>In vitro</i> : – MC3T3-E1 cells (live/dead viability assay, ALP activity, trypan blue assay, alizarin red S staining) – Direct contact method – $t = 7, 14$ d	– MgZn-15% $\beta$ -TCP showed cytotoxicity with metabolic activity below 20%. – Improved cytocompatibility reported for composites with 5 and 10 wt% $\beta$ -TCP.	172
MgZn- $\beta$ -TCP		<i>In vitro</i> : – MC3T3-E1 cells (live/dead viability assay, ALP activity, trypan blue assay, prestoBlue assay, collagen type-1 staining, staining)	– Stretched preosteoblasts observed for composites with 5 and 10 wt% $\beta$ -TCP confirmed spreading morphology. – 10–20 vol% Al showed better cytocompatibility, as reflected in increased cell count ( $3.97\text{--}15 \times 10^4$ ).	173
Extrusion 3D-printing	Direct and indirect contact method – $t = 1\text{--}28$ d	<i>In vitro</i> : – MC3T3-E1 cells (MTT assay, live/dead viability assay, immunostaining for RUNX2, OPN)	– Ca <sup>2+</sup> , Mg <sup>2+</sup> , and Si <sup>4+</sup> release in the culture medium enhanced biocompatibility as compared with Fe-control scaffolds. – For 100% extracts <sup>b</sup> , the cellular activities were generally suppressed, while 50% extract <sup>a</sup> showed good metabolic activity. – Mineralization process indicated through osteopontin detection in the extracellular matrix of cells.	55
Fe-Ak		<i>In vitro</i> : – MC3T3-E1 cells (MTT assay, live/dead viability assay, DCFH-DA assay, F-actin staining, PTI).	– Preosteoblasts showed good metabolic activity in 50% of extracts <sup>a</sup> (~88%). – 50% extracts <sup>a</sup> from FeMn– were better than 50% extracts from Fe-Ak from previous study. <sup>86</sup> – A higher concentration of Fe ions during scaffold degradation from the composite scaffolds as compared with Fe scaffolds (3.82 ppm vs. 1.14 ppm), which is beneficial for achieving a tumor therapeutic effect. – 30CS scaffolds had excellent photothermal effect due to their rapid temperature increase to 50 °C in PBS under a laser power density of 0.6 W cm <sup>-2</sup> . – Long term rBMSC proliferation was not negatively affected by short term thermal therapy, indicated by the recovery of cell viability within 3 days.	172
Extrusion AM	– Direct and indirect contact method. – $t = 2$ d			



Table 6 (continued)

Materials, AM technique	Testing conditions	Observations	Ref.
Fe-BR SLM	<i>In vivo</i> : – Tumor-bearing mice and defected femur of rabbits. (H&E staining, PTT) – $t = 15$ d mice, 8 w rabbits	<ul style="list-style-type: none"> <li>– Live/dead and CCK-8 assays showed a mortality rate of 92.4% of the cultured Sa2 tumor cells after irradiation for 15 min followed by incubation with the composite scaffolds for 4 h.</li> <li>– <i>In vivo</i> implantation of the scaffolds in mice showed the 30CS treated with 15 min laser had most effective tumor killing capabilities.</li> <li>– Relative tumor reduction of 97% as compared with pure <math>\text{CaSiO}_3</math> scaffold.</li> <li>– 8-week scaffold implantation in rabbits showed significant bone growth for the 30CS scaffolds as compared with the Fe-scaffolds.</li> <li>– Fe-5 wt% BR showed higher cell growth and viability as compared with the Fe scaffolds. <sup>173</sup></li> <li>– Increased ALP expression indicated enhanced osteoblast differentiation and Ca, Mg and Si ion release contributed towards osteogenesis and cell proliferation.</li> <li>– Increase in Pd and BR content had a mild inhibitory effect on cell growth, although cell viability of 174 over 80% for all the extracts after 5 days indicated favorable biocompatibility.</li> <li>– Pd was hypothesized to cause cytotoxicity at higher concentrations, although it showed low solubility and toxicity at tested concentrations (up to 5 wt%).</li> </ul>	173
Fe-BR-Pd	<i>In vitro</i> : – MG-63 cells (CCK-8, ALP activity, live/dead viability assays) – Indirect contact method. – $t = 7$ d		
	<i>In vitro</i> : – MG-63 cells (CCK-8, live/dead viability assay) – Indirect contact method. – $t = 5$ d		

<sup>a</sup> 50% extracts: 1 mL medium for 5  $\text{cm}^2$  of scaffold diluted to 50%. <sup>b</sup> 100% extracts: 1 mL medium for 5  $\text{cm}^2$  of scaffold.

One of the propositions is that there is a limited solubility of metal species released from Ti-based implants in the absence of wear.<sup>46,181</sup> Therefore, they tend to remain in an area close to the implant, leading to local accumulation. Another suggestion is that the passive dissolution of the metal binds to serum proteins, causing lymphocyte reaction and a stronger inflammatory response.<sup>176</sup> On the contrary, it was also suggested that even with the metal–protein complex formation, the transport of Ti is minimal,<sup>176,182</sup> which was supported by low Ti ion concentrations in urine.<sup>182</sup> An additional aspect of responses due to implants includes inflammation around the implants. It has been suggested that the debris from worn TiAlV alloy can release inflammatory mediators, causing osteolysis.<sup>176</sup>

Ti-based composite materials fabricated using AM present a potential solution to these challenges by adding reinforcing materials that can alter the mechanical properties, support bone healing, and reduce toxicities. So far, SLS/SLM and extrusion-based 3D printing have been used to produce Ti-matrix composites (TMCs). All studies<sup>168</sup> have reported enhanced bioactivity of AM TMCs with different reinforcing materials, including tricalcium phosphate (TCP), hydroxyapatite (HA), and silica. Typically, ceramic particles enhance the surface roughness of 3D printed parts, positively influencing cell adhesion and proliferation (Fig. 4a–d). Along with the ceramic content, the manufacturing and sintering environment plays a vital role in controlling the surface features of the scaffolds, which can be observed in Fig. 4a–c, where an increasing HA content corresponds to increased surface roughness, and sintering the scaffold in air, as compared to sintering in argon, appeared to result in micropores on the struts.<sup>165</sup> However, the mechanical integrity of air-sintered scaffolds was found to be higher, which was linked to the oxygen in air promoting interface reaction and bonding between the matrix and ceramics.<sup>167</sup> Post-AM heat treatment applied to Ti-silica composites<sup>166</sup> not only increased the compressive strength of the implant but also improved cell growth, which was evident from higher optical density values obtained from the 3-(4,5-dimethylthiazol-2-yl)-2,5-diphenyltetrazolium bromide (MTT) assay using human osteogenic sarcoma cell lines (Fig. 4f). In addition, the cell attachment and growth were favored by the presence of micropores on the surface of the bone scaffolds, signifying the importance of implant design.

It is commonly seen that an excessive increase in ceramic content in a metal matrix composite scaffold leads to decreased mechanical strength. Therefore, an optimal content must be formulated for different reinforcements.<sup>167,168</sup> A detailed study on the Ti6Al4V-TCP composite scaffolds prepared through 3D fiber deposition (3DF), a type of extrusion-based AM, with different TCP powder particle sizes, revealed that the particle content did not have a substantial effect on the overall porosity of the implant.<sup>165</sup> However, with a higher content of larger particle sizes (125–250  $\mu\text{m}$ ), the distribution of TCP particles was less homogenous with more TCP particles on the surface, as compared with smaller particle sizes (63–125  $\mu\text{m}$ ). Therefore, smaller particle sizes were selected as the powder of choice. Apart from TCP particle sizes, higher porosities (ranging from

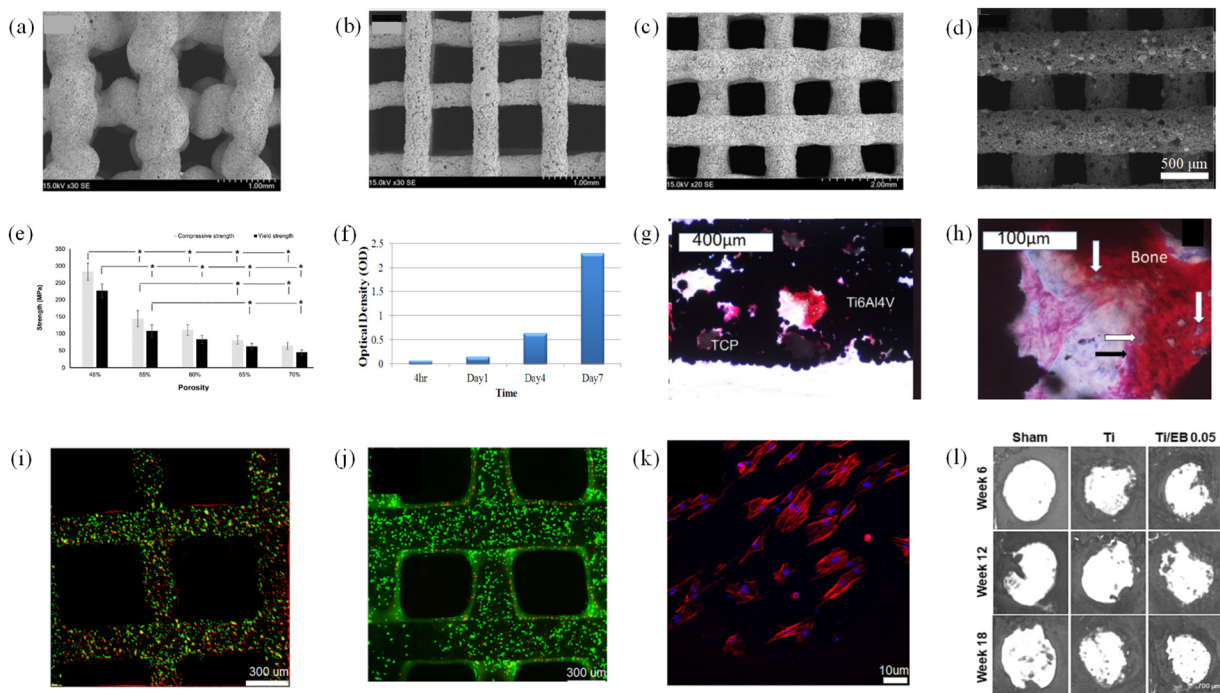


**Fig. 4** (a) SEM images of 3D printed Ti6Al4V-HA scaffolds with 8 wt% HA sintered in argon, (b) 25 wt% HA sintered in argon, (c) 25 wt% HA sintered in air, and (d) Ti-10 wt% TCP manufactured by 3DF. (e) Compressive strength of the Ti6Al4V-10 wt% scaffolds that were 3DF manufactured and sintered, having a range of porosities from 48% to 70%. Significant differences ( $p < 0.05$ ) are indicated with \*.<sup>165</sup> (f) MTT assay resulted in an osteoblast-like cell environment for the Ti-silica composite scaffolds prepared through SLS.<sup>166</sup> (g and h) Minimal bone formation observed in the Ti6Al4V-10 wt% TCP scaffolds in the vicinity of TCP particles with an osteoid layer (black arrow) and osteocytes (white arrow).<sup>165</sup> Fluorescence morphology of rBMSCs cultured for 3 days on the struts of 3D printed (i) Ti6Al4V-8 wt% HA and (j) Ti6Al4V-25 wt% HA sintered in argon, showing a higher content HA providing better cell viability.<sup>167</sup> (k) cytoskeleton fluorescence morphology after 7 day direct culture on Ti6Al4V-25 wt% HA, showing extension state of cells, indicating good biocompatibility<sup>167</sup> and (l) representative micro-CT images of mouse calvarial defect implanted with sham, Ti, and Ti-EB 0.05 vol% EB at weeks 6, 12, and 18.<sup>168</sup> (a–e, g and h) are reproduced from Elsevier, copyright 2021, licensed under CC BY 4.0; (f) is reproduced with permission from Elsevier, copyright 2013; (i–k) is reproduced with permission from John Wiley and Sons, copyright 2020; and (l) is reproduced with permission from Elsevier, copyright 2024.

48–70%) led to decreased compressive strengths (Fig. 4e). Adding more than 10% TCP caused the scaffolds to become brittle after sintering, with increased heterogeneity in micro-structure, which could act as crack initiation sites. Therefore, 10 wt% of ceramic addition was chosen for further analysis. Bioactivity was analyzed *in vitro* for this composition by measuring the Ca and P ions present in a simulated physiological solution (SPS) and in a cell culture medium (CM) after immersing the scaffolds in the solutions for different durations. After 1 week of immersion in CM, CaP was deposited on the scaffold surface. Therefore, decreased Ca and P ion concentrations were observed in the solution. In the case of immersion experiments in SPS, no Ca and P ions were present at first but appeared over time, with gradually increasing concentrations. This behavior is consistent with the observations reported in the literature<sup>183,184</sup> and validates the retained ability of TCP added to Ti-based scaffolds to interact with the surrounding biological medium. *In vivo* experiments were carried out where the scaffolds with 0, 5, and 10 wt% TCP were implanted in the dorsal muscles of mature dogs. All the scaffolds showed the penetration of fibrous tissues and the absence of tissue inflammation and toxicity. Although the exact mechanism with which TCP helps in

osteogenesis is not fully understood, TCP is known to regulate osteogenic processes like the formation of blood vessels, differentiation of mesenchymal stem cells, and release of growth factors, which collectively provide a conducive environment for bone formation.<sup>185</sup> In line with this mechanism, in the study on 10 wt% TCP scaffolds, vascularization and ectopic bone formation were observed after 12 weeks of implantation, as shown in the histological images in Fig. 4g and h, which confirmed their osteoinductive capability.<sup>165</sup> The bone formation was mainly in the proximity of TCP particles inside the composite struts, with bone area percentages being  $2.2 \pm 2\%$  and  $19.5 \pm 12.8\%$  in the total available pore area and in the available pore area inside the struts of the scaffolds, respectively. Another study utilized HA as a reinforcing material in the Ti6Al4V matrix and observed better cell adhesion and proliferation on the scaffolds with a higher HA content along with the appearance of elongated morphologies in the F-actin staining test (Fig. 4i–k).<sup>167</sup> Moreover, a higher HA content caused the formation of more reaction products (such as  $\text{CaTiO}_3$ ,  $\text{TiP}$ , etc) and agglomeration, which in turn impacted the mechanical properties. This could be correlated to brittle phase formation, inducing local stress concentration points and thus increasing

the probability of crack formation and propagation under compression.

Another research explored biological sources of HA (*i.e.*, equine bones (EB)) as a reinforcing material added to the Ti6Al4V matrix, and SLM printing was used to produce orthopedic implants.<sup>108</sup> Composite implants with an optimum volume fraction of EB promised better protein adsorption due to increased hydrophilicity and roughness. Prolonged immersion in SBF caused the reductions in strength and formation of microcracks, which was correlated to the dissolution of the HA phase. Though Ti is stable, reinforcing agents can affect the long-term interfacial stability, which affects the load-bearing capabilities of the implant as well.

*In vivo* testing, using a mouse calvarial defect model, revealed superior bone regeneration compared to the sham and Ti implant group (Fig. 4l). In the 18<sup>th</sup> week, the bone volume to total volume ratios of the sham, Ti, and Ti - 0.05 vol% EB groups were 13%, 27%, and 33%, respectively, which showed the osteogenic ability of the Ti/EB composite.

Since Ti-based materials typically have higher compressive strengths than bone, the same was observed in the studies on AM TMCs. However, the Young's modulus of the Ti6Al4V - 10 wt% TCP scaffolds fell within the bone range,<sup>142</sup> which could eliminate the concerns about the stress-shielding effect. Moreover, the *in vivo* tests of the 3DF-printed Ti6Al4V-TCP for 14 weeks and SLM-printed Ti6Al4V-EB for 18 weeks showed comparable results: bone regeneration of approximately 19.5% and 33%, respectively, with minimal inflammation. However, an excess volume fraction of EB was associated with potential cytotoxicity. The addition of ceramic particles increased surface roughness in all the studies, which enhanced cell attachment and growth. Overall, manufacturing TMCs for bone substitutes through AM has been actively explored by creating unique combinations of ceramics (TCP, HA, silica, or EB) and Ti-matrix (Ti or Ti6Al4V) and the *in vitro* and *in vivo* investigations have demonstrated enhanced mechanical properties, cytocompatibility, and osseointegration, paving the way for further optimization toward clinical use.

#### 4.2. Mg-based MMCs

Mg and its alloys have comparable mechanical properties to human bone, making them attractive materials for implants. The density of human cortical bone (1.75 g cm<sup>-3</sup>) is within the range of the densities of Mg and its alloys (1.738–1.85 g cm<sup>-3</sup>).<sup>169</sup> Moreover, their biodegradability allows them to be used as temporary stent and bone implant materials, eliminating the requirement of secondary surgery for implant removal.

Another advantage is that, since Mg is found within the body, it is not inherently toxic and excess Mg<sup>2+</sup> or Mg(OH)<sub>2</sub>, which are corrosion products are excreted out along with urine.<sup>186,187</sup> Moreover, Mg-based alloys have antibacterial properties since releasing Mg<sup>2+</sup> into the microenvironment due to degradation potentially increases local pH and demonstrates inhibitory effect on bacteria.<sup>188</sup> However, as Mg degrades, it releases hydrogen that can accumulate in surrounding tissues and form gas cavities, creating pressure and inducing

mechanical disturbances in bone regeneration.<sup>189,190</sup> Excess of hydrogen can spread within the body and cause wound dehiscence, subcutaneous emphysema, disruption to the balance of blood cell parameters, or blockage of the bloodstream, ultimately decreasing the survival rate.<sup>189–192</sup> Another issue caused by hydrogen evolution is the potential diffusion of hydrogen into the implant and pre-existing crack tips, leading to hydrogen embrittlement of the implants, thus resulting in premature failure.<sup>192,193</sup> In addition, when Mg is alloyed with other elements, the probability of toxicity increases, depending on the element(s) and the corresponding occurrence of galvanic corrosion. For instance, although they are trace elements within the human body, adding excess Zn, Mn, and Sr can induce neurotoxicity, while Sn can be carcinogenic.<sup>25</sup> The challenges associated with Mg-based implants include their non-uniform corrosion behavior along with hydrogen gas evolution, which can lead to the formation of harmful hydrogen gas pockets, eventually causing gas embolism.<sup>94,194,195</sup> Therefore, the corrosion must be controlled to ensure gradual degradation, thus guaranteeing proper bone adhesion and growth before the implant dissolves. Adding non-toxic phases to the Mg matrix is a potential solution to addressing these challenges and has been frequently reported to enhance bone regeneration. Although various calcium- and phosphate-based Mg-matrix composites have been researched and proven to have excellent results for toxicity and immunological reactions, there is limited evidence of their preparation using AM for biomedical applications.<sup>195</sup> Until now, bioactive glass (BG),<sup>169</sup> mesoporous bioactive glass (MBG)<sup>170</sup> and  $\beta$ -TCP<sup>171</sup> have been explored as reinforcing materials in the Mg matrix through AM for orthopedic applications.

In a study,  $\beta$ -TCP was used as a reinforcing agent in the MgZn matrix to produce composite scaffolds using extrusion-based 3D printing.<sup>171</sup> Adding different weight fractions of  $\beta$ -TCP (*i.e.*, 5, 10, and 15 wt%) significantly enhanced the resulting mechanical and biological properties to different extents. Uniform dispersion of  $\beta$ -TCP particles was observed on the struts of the scaffolds with 5 and 10 wt%  $\beta$ -TCP, while clustering was seen in the 15 wt%  $\beta$ -TCP composite scaffolds (Fig. 5a–d). Moreover, due to the interfacial bonding between the MgZn matrix and reinforcements, effective load transfer resulted in the compressive yield strengths of the 5 and 10 wt%  $\beta$ -TCP scaffolds being  $23.4 \pm 13.4$  MPa and  $31.3 \pm 1.9$  MPa, respectively. *In vitro* corrosion reduced the compressive strengths of the scaffold materials, with the strength reducing with the immersion time, which can be attributed to material loss. However, even after 14 days of immersion testing, the mechanical properties remained within the range required for bone-substituting materials. Moreover, the corrosion rates of the composite scaffolds (0.5–2.3 mm year<sup>-1</sup>) were very close to bulk materials with similar compositions despite the porous structure, which established this manufacturing route's effectiveness in converting the design of Mg-based MMCs into scaffolds. *In vitro* cell culture studies on the MgZn-5 wt% and 10 wt%  $\beta$ -TCP scaffolds showed spreading of preosteoblasts, indicating osteogenic differentiation (Fig. 5e–h). After 7 days,



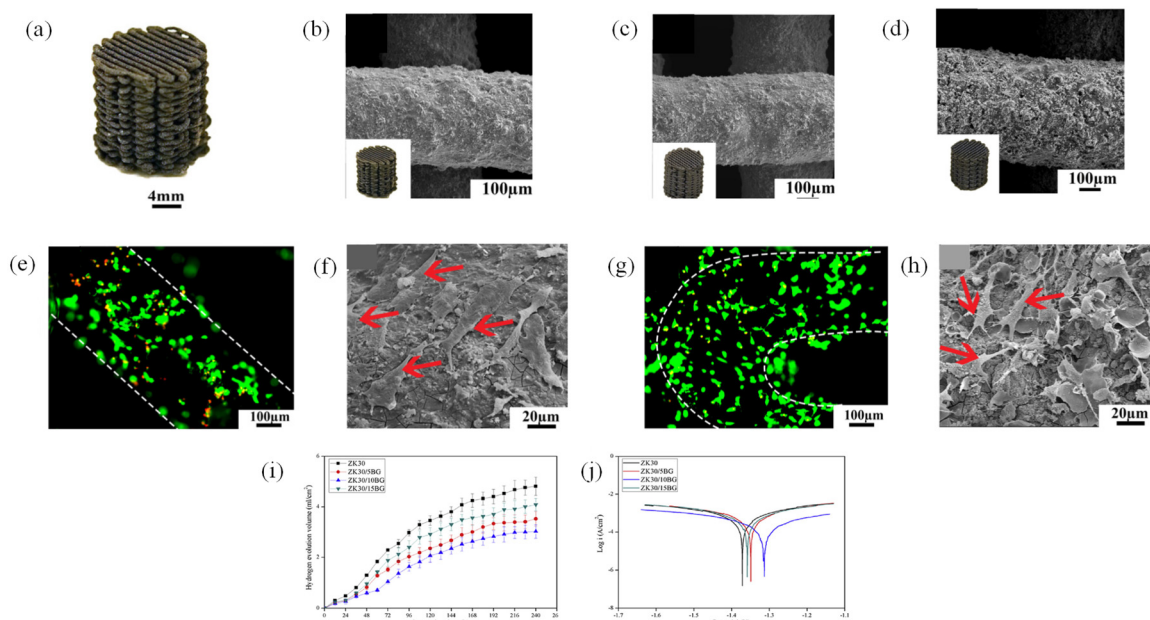


**Fig. 5** (a) Extrusion-based 3D printed MgZn-10 wt% TCP scaffold, magnified SEM images of the struts of 3D printed MgZn- $x$ TCP scaffolds with  $x$  ranging from (b) 5 wt% and (c) 10 wt% to (d) 15 wt%.<sup>171</sup> Fluorescence staining of MC3T3-E1 direct culture on the MgZn- $x$ TCP scaffolds and corresponding morphologies for  $x$ : (e and f) 5 wt% TCP and (g and h) 10 wt% TCP, respectively.<sup>171</sup> (i) Hydrogen evolution (j) Tafel plots of ZK30/xBG,  $x$  being 0, 5, 10, and 15 wt%.<sup>169</sup> (a–h), and (i and j) are reproduced with permission from Elsevier, copyright 2022, and copyright 2019, respectively.

the cell viability stayed the same for the MgZn-5 wt%  $\beta$ -TCP composite, while the cell viability declined for the MgZn 10 wt%  $\beta$ -TCP composite. Additionally, the presence of the calcified matrix in the staining tests confirmed matrix mineralization of the MgZn- $\beta$ -TCP composites with both 5 and 10 wt%  $\beta$ -TCP, confirming extrusion-based 3D printed MgZn- $\beta$ -TCP scaffolds' potential in satisfying most of the bone substitute requirements.

Bioactive glass (BG) reinforcement in the ZK30 magnesium alloy prepared using SLM was reported to enhance the micro-hardness and corrosion resistance (Fig. 5j).<sup>169</sup> The hydrogen evolution rate also decreased during prolonged immersion (Fig. 5i). Moreover, the toxicity levels of the prepared specimen were correlated to the relative growth rate (RGR) of Mouse L929 fibroblasts. As the BG content increased, RGR progressively increased, indicating decreased toxicity. The increase in the RGR was suggested to be caused by the reduction in the release of Mg<sup>2+</sup> ion due to the BG addition and/or by BG itself, promoting the bioactivity through the deposition of Ca-P compounds, which provided favorable sites for osteoblast attachment and growth.

In another study,<sup>170</sup> LPBF was used to prepare the ZK60 alloy reinforced with mesoporous bioactive glass (MBG). While LPBF comprises of a range of laser-based AM processes, the study used SLM. The incorporation of MBG into the Mg matrix provided more adsorption sites, which promoted the deposition of a much more protective apatite layer and gave rise to high corrosion resistance, thus addressing one of the key challenges of Mg-based implants.<sup>170</sup> However, adding MBG and BG led to decreased weight losses at different time points

as compared to ZK60—the composite with MBG showed relatively lower weight losses than that with BG. The reduced weight losses were attributed to the forming of an *in situ* apatite film on the matrix due to the accumulation of Ca<sup>2+</sup> and HPO<sub>4</sub><sup>2-</sup> ions. Similar to the BG added to the composite,<sup>169</sup> MBG also enhanced cell proliferation, which was attributed to reduced ion release and consequently created a mild cell survival environment. MBG addition was favored over BG due to better overall performance, enhanced corrosion resistance, and cell growth.

Another layer-by-layer manufacturing method, friction stir additive manufacturing (FSAM), was used to create Mg-based composite implants. Although FSAM does not involve digital designs and the achievement of near-net-shape products, it remains a valuable tool to provide insights into the potential of upgrading the process toward model-to-print prototyping. Mg-matrix composites were investigated using FSAM, specifically the AZ31B alloy reinforced with hydroxyapatite (HA).<sup>196,197</sup> FSAM is a thermomechanical process that leads to grain refinement due to dynamic recrystallization caused by intense frictional forces between the material and the tool that rotates and disperses HA powder particles into AZ31B sheets to form MMCs. Grain refinement of the Mg matrix was the dominant trait that improved corrosion resistance, even though an increase in HA weight percentage reduced corrosion resistance due to enhanced galvanic corrosion at HA-Mg interfaces.<sup>196</sup> Moreover, *in vitro* testing showed lesser platelet aggregation for Mg-HA samples than the as-received Mg, suggesting a reduced risk of thrombosis formation. The Ca/P ratios in the mineral phase of the resulting samples (1.54–1.60) were close to that of

bone (1.64), favoring biominerization.<sup>197</sup> By understanding the composite formation from layered HA powder through FSAM and resulting properties, advancements can lead to the integration of digital design and precision manufacturing to realize the production of customized implants.

Overall, adding ceramics (BG, MBG, and  $\beta$ -TCP) to the Mg-matrix using SLM, LPBF, and extrusion-based 3D printing led to enhanced mechanical properties due to the reinforcement provided by particle-matrix bonding. The mechanical strengths were within the range of bones; MBG addition to ZK60 led to ultimate tensile strength (UTS) being in the range of cortical bone, while  $\beta$ -TCP addition to the MgZn matrix gave Young's modulus within the trabecular/cancellous bone range. Alongside, post-immersion retainment of the mechanical properties of the MgZn- $\beta$ -TCP scaffolds affirmed their capability to provide support during degradation. Cell viability was also observed through direct and indirect contact methods. Stretched/fusiform-shaped cells were observed in fluorescence imaging for direct and indirect cell cultures with MgZn- $\beta$ -TCP and ZK60-MBG, respectively. Compared to BG, MBG addition to the Mg-matrix enhanced cell viability (~95% at day 5). The hydrogen evolution was also seen to be controlled by the ceramic addition, thus addressing one of the challenges associated with Mg-based implants. However, *in vivo* studies on Mg-based MMCs must be conducted to confirm these promising results.

#### 4.3. Fe-based MMCs

Fe and its alloys are a promising alternative to Mg alloys for biodegradable applications, with the benefits of no hydrogen evolution and enhanced mechanical properties.<sup>55,198,199</sup> Since Fe degrades slowly, the research on Fe-based materials focuses more on increasing their biodegradation rates,<sup>21,151,199</sup> along with the efforts to change their magnetic behavior to achieve MRI compatibility by designing materials having magnetic susceptibility values in hydrated conditions below  $10^{-2}$ .<sup>55,200</sup> Fe is among the essential minerals for the human body and is highly important for oxygen transport and storage, immune function, DNA repair and synthesis, and energy metabolism.<sup>28,199</sup> However, excessive amounts of essential minerals are also toxic.<sup>78</sup> If iron exceeds the safe limits and reaches  $15\text{--}45\text{ }\mu\text{g L}^{-1}$ , it can cause mild to severe toxicity and accumulation in the liver (hepatotoxicity), while  $5\text{--}40\text{ }\mu\text{g L}^{-1}$  can cause neurotoxicity.<sup>28</sup> As mentioned earlier, alloying elements or non-metal components added to the Fe matrix significantly affect toxicity. For instance, Mn is frequently added to the Fe matrix since it is an essential element for body growth and development, accelerates corrosion, and can potentially aid in anti-ferromagnetic behavior for Fe-implants.<sup>201</sup> However, if Mn is present in large amounts ( $120\text{--}360\text{ }\mu\text{g L}^{-1}$ ) within the body, it can cause neurotoxic effects since Mn can cross the blood-brain barrier.<sup>28,199</sup> It is critical to ensure the production of implants with no or minimal toxicity or accumulation of ions correlated to their biodegradation rates.

Building Fe-matrix composites (FMCs) through AM has been explored using extrusion-based 3D printing and SLM to manufacture geometrically complex structures for orthopedic

applications.<sup>55,86</sup> Silicate-based bioceramic particles of akermanite ( $\text{Ca}_2\text{Mg}(\text{Si}_2\text{O}_7)$ ) (Ak) and bredigite ( $\text{Ca}_7\text{Mg}(\text{SiO}_4)_4$ ) (BR) were added to the Fe-alloy system to accelerate the corrosion of these alloys and induce their bioactivity, using extrusion-based 3D printing and SLM, respectively. Representative images of the resulting structures using extrusion 3D printing and SLM are shown in Fig. 6a-c. The major elements composing akermanite (Ak) and bredigite (BR) are known for enhancing osteogenic and angiogenic capabilities, along with the generation of minimal inflammatory responses to macrophages, promising better osseointegration.<sup>86,173</sup>

The chemical interactions between the material components in the composite blend and the binder needed for extrusion-based 3D printing are crucial since they determine the resulting viscoelastic behavior and, eventually, the overall build of the resulting part. Due to the hydrophilic nature of Ak, its addition to the Fe<sup>55</sup> and FeMn<sup>86</sup> matrixes increase the viscosity of the feedstock, necessitating higher extrusion pressure during 3D printing.<sup>86</sup> Therefore, optimizing the printing parameters is highly important, depending on the binder formulation. Limited architecture has been explored for FMC implants, with porous cylindrical samples being the most common. A study reported successfully prototyping a hip stem and acetabular cup<sup>55</sup> with an intricate, interconnected porous structure for accommodating cell adhesion and proliferation to facilitate successful osseointegration. A lay-down pattern design with interlayer switching between  $0^\circ$  and  $90^\circ$  was used for these porous implants.

In terms of biodegradability, a higher volume fraction of Ak in the Fe-Ak composite scaffolds caused more mass losses<sup>86</sup> due to the higher solubility of Ak in the revised simulated body fluid (r-SBF), as compared with pure Fe, which was directly reflected in the corrosion rates of these composites (Fig. 6e). The deposition of CaP during biodegradation due to the interactions between the released ions and the components in the r-SBF led to a non-uniform mass loss pattern over the 28 days of immersion testing. In addition, Fe-based corrosion products accumulated on the scaffolds promoted passivation, lowering the biodegradation rate as time progressed. It was speculated that the dissolution of Ak provided the ions in the r-SBF with increased access to the Fe surfaces through the micro-channels formed, accelerating corrosion compared to the pure Fe scaffolds (Fig. 6e). In addition to the higher degradation rates, higher volume fractions of Ak (10–20 vol%) in the composites corresponded to higher viability, proliferation, and differentiation of preosteoblasts in a non-osteogenic medium throughout the 28-day experimental period. In contrast, the specimens with 5 vol% Ak showed lower cell viability and no indication of proliferation, and higher release of  $\text{Fe}^{2+}$  ions and were, thus, regarded as cytotoxic (Fig. 6h). Moreover, fibrous collagen formation was identified, which supports osteogenic differentiation and precipitation of minerals.<sup>202,203</sup> Similar to Ak addition to the Fe matrix, higher biodegradation rates were reported for BR and BR-Pd addition to the Fe matrix, with higher weight fractions leading to enhanced corrosion in 28-day and 21-day immersion tests, respectively.<sup>173,174</sup> Moreover, Ca, Mg, and Si



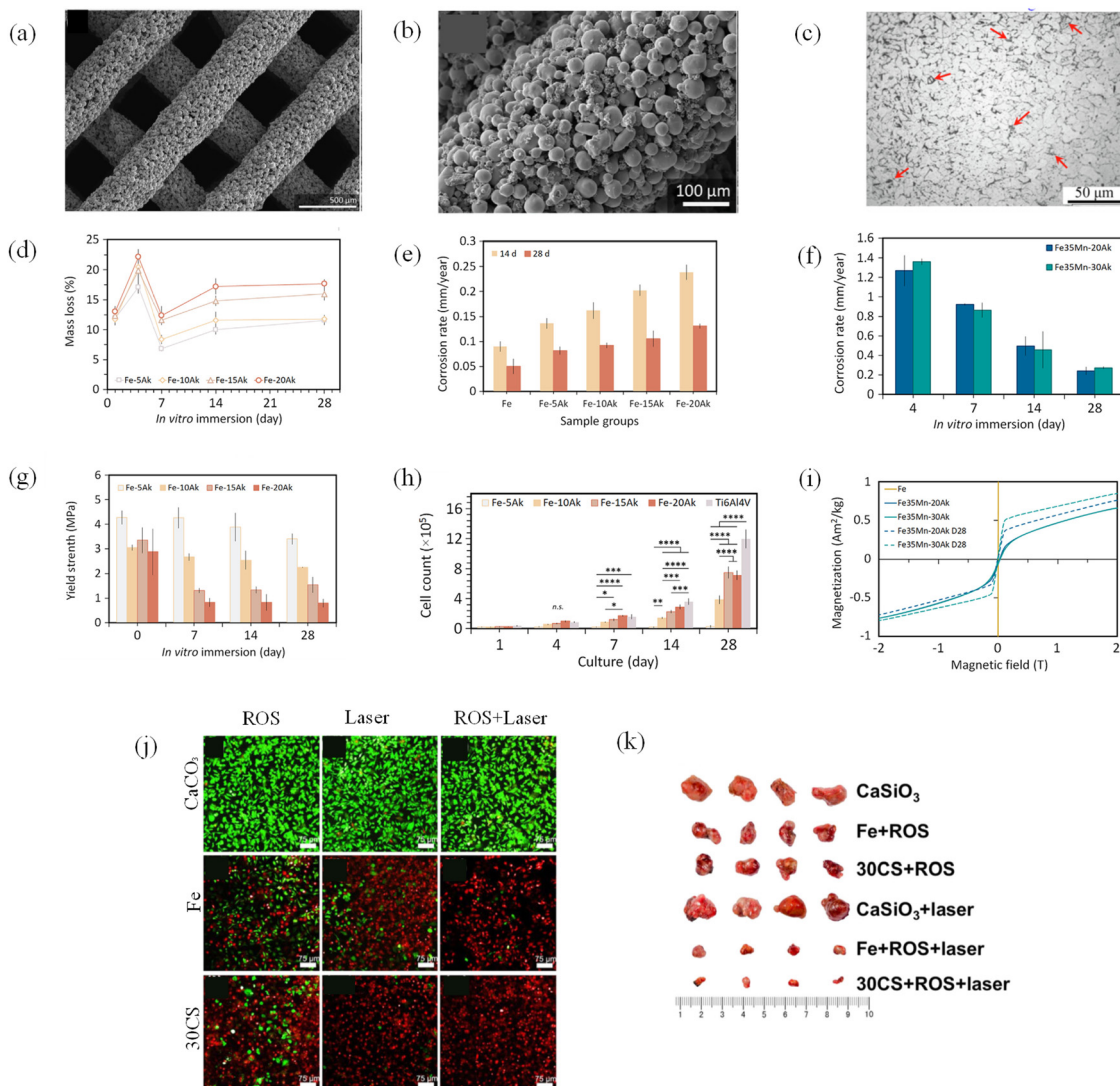


**Fig. 6** Representative images of (a) the struts of the extrusion-based 3D printed Fe–Ak scaffolds<sup>86</sup> and (b) magnified image of the strut of Fe–15 vol% Ak<sup>86</sup> and (c) SLM printed Fe–4Pd–5BR with red arrows pointing at BR. Graphical representation of the extrusion-based 3D printed scaffolds: (d) the mass losses of the Fe–xAk scaffolds through 28-day immersion in the r-SBF,<sup>86</sup> (e) corrosion rates determined from 14- and 28-day immersion testing,<sup>86</sup> (f) corrosion rates of the Fe35Mn–xAk scaffolds,<sup>55</sup> (g) yield strengths of Fe–xAk through 28-day immersion testing,<sup>86</sup> (h) cell count in preosteoblast culture for 28 days<sup>86</sup> and (i) magnetization curves of the FeMn–xAk specimens as-sintered and after *in vitro* degradation for 28 days.<sup>55</sup> (j) Images of the culture of Sa02 tumor cells with CaSiO<sub>3</sub>, Fe, and 30CS scaffolds treated with ROS, laser, and ROS + laser therapies and (k) images of tumors extracted on day 15 for each treatment and material.<sup>172</sup> (a, b, d, e, g and h) are reprinted from Elsevier, copyright 2022, licensed under CC BY 4.0; (c) is reproduced with permission from Elsevier, copyright 2019; (f and i) are reprinted from Elsevier, copyright 2023, licensed under CC BY 4.0; and (j and k) are reprinted from Nature, copyright 2018, licensed under CC BY 4.0.

ion release was reported, which may contribute to bone formation through the observed increase in cytocompatibility of prepared scaffolds with preosteoblasts.<sup>202</sup> This was confirmed through live/dead cell assays that showed high cell viability over time (1–7 days) with higher density of living cells for the Fe–BR composite scaffolds, as compared to the Fe scaffolds.<sup>173</sup> Moreover, this study also showed fusiform-shaped cells after 4 days, which indicated normal cell development.<sup>173</sup> On the other hand, an increase in Pd content (up to 4 wt%) for the sake of increasing biodegradation rate caused a minor decline in cell viability, which suggested its potential cytotoxicity if added in excess quantity.<sup>174</sup>

Regarding mechanical integrity, good interfacial bonding between metal and reinforcing material is essential to ensure higher strength for adequate load transfer from the matrix to the reinforcing phase<sup>29,86</sup> and to minimize the loss in (corrosion) fatigue resistance. Adding Ak to the Fe matrix enabled the composites to maintain their mechanical properties even after 28-day immersion testing<sup>86</sup> (Fig. 6g). The initial values of Young's modulus and yield strength were consistently higher than the post-immersion data. Young's modulus increased from 7-day immersion to 28-day immersion testing due to the good bonding between the biodegradation products and struts of the scaffolds, leading to an apparent strengthening effect.

The progressive deposition of biodegradation products improved Young's modulus. Still, at higher strains, load transfer between the biodegradation products and scaffolds failed, and therefore, yield strength decreased with increasing immersion time.<sup>86</sup>

Post-AM heat treatments, such as sintering, caused the  $\gamma$ -austenite Fe-Mn phase formation, which ensured the anti-ferromagnetic behavior of the scaffolds,<sup>55</sup> having magnetic susceptibility values within the required range (*i.e.*, 3.6 and  $4.5 \times 10^{-3}$  before and after *in vitro* biodegradation, respectively) (Fig. 6i). Moreover, the biodegradation rates of the Fe-Mn-Ak scaffolds were much higher than those of pure Fe,<sup>204</sup> Fe-Mn alloys<sup>205</sup> and Fe-Ak composites<sup>55,86</sup> (Fig. 6d-f). This was a combined result of *in situ* alloying of Fe with Mn, adding Ak particles, and high pore interconnectivity, which provided a larger surface area for biodegradation. In addition, the  $\gamma$ -FeMn phase increased the corrosion tendency by decreasing the standard electrode potential. As described earlier, one of the key challenges of Fe-based implants is to accelerate biodegradability, which was addressed by *in situ* alloying of Fe with Mn along with the addition of Ak and the designing of porous composite structure, ultimately leading to the biodegradation rates of 0.24–0.27 mm year<sup>-1</sup>,<sup>38</sup> which are within the required range.

In another study,<sup>172</sup> Fe-CaSiO<sub>3</sub> composite scaffolds were printed with 70 wt% Fe and 30 wt% CaSiO<sub>3</sub> (30CS), and their potential as a bifunctional material to treat bone cancer was evaluated. In addition to the high compressive strength of the composite scaffolds, as compared with the Fe-scaffolds, an enhanced tumor therapeutic effect was achieved by using a combination of photothermal and ROS therapies, validated *in vitro* and *in vivo*. *In vitro* live/dead and CCK-8 assays revealed that the photothermal treatment of tumor cells for 15 min, followed by incubation with the 30CS scaffolds, resulted in the highest mortality rate of 91.4% (Fig. 6j). Moreover, short-term thermal therapy had no long-term effect on cell proliferation. Similarly, *in vivo* trials on mice confirmed that the 30CS scaffolds showed the best tumor-killing results when irradiated (Fig. 6k). The tumor sizes for the 30CS and Fe scaffolds were much smaller than those of the irradiated CaSiO<sub>3</sub> scaffolds, which showed the potential antitumor efficiency of ROS produced by releasing Fe ions. The antitumor effect of the 30CS scaffolds was attributed to two mechanisms: (i) the high temperature induced by laser irradiation caused the collapse of cell membranes, protein denaturation, mitochondrial dysfunction, and termination of enzyme activity, and (ii) increased ROS production in the tumor cells caused lipid oxidation and damage to protein and DNA.<sup>172</sup> In addition, the osteogenic potential of these scaffolds was confirmed through *in vivo* testing in rabbits, where the scaffolds were implanted and irradiated in rabbits with femoral defects, followed by irradiation for 10 min to confirm no long-term effect of photothermal therapy on osteogenesis. The 30CS scaffolds showed superior bone growth after 8 weeks of implantation owing to the osteogenic properties of Ca and Si ions along with faster biodegradation of CaSiO<sub>3</sub>, leading to better

penetration of bone cells into the scaffolds, supporting bone regeneration.

Building FMCs through AM has been actively pursued using extrusion-based 3D printing and SLM. Extrusion-based 3D printing provides more control over microporosity, which is required for bone scaffolds, while SLM offers better precision and denser structures. Overall, the compressive strengths attained fell within the range necessary for different bone structures by carefully selecting processing routes and ceramic content. The Fe-Ak and FeMn-Ak scaffolds possessed mechanical properties within the trabecular bone range. In contrast, the Fe-BR and Fe-BR-Pd scaffolds had mechanical strengths of dense cortical bone, which is a result of the manufacturing methods used. On the other hand, while the addition of Mn positively influenced cell viability, Pd addition tended to cause toxicity despite the observation that it helped accelerate corrosion. Although an interesting study details the impact of Fe-CaSiO<sub>3</sub> and subsequent treatments for cancer progression through *in vitro* and *in vivo* analysis, further studies must be conducted, especially *in vivo* tests, to provide a detailed analysis of bone regeneration.

## 5. General discussion and future directions

While orthopedic implants have come a long way since their first introduction, research efforts continue to improve their performance and patients' quality of life. Transformative orthopedic interventions have been investigated, including applying hybrid materials, such as MMCs, to achieve the desired strength and regeneration of the damaged bone. While the AM technologies allow for precise control over the architecture of implants with specific placement of materials, as desired, tailoring the mechanical and degradation properties of MMCs according to application requirements is equally important for clinical success. For instance, pediatric patients with ongoing skeletal growth might require materials with high degradability (*e.g.*, Mg-based) to match their metabolic activity, while elderly patients might need implants with reduced degradability and higher stiffness to match their slow recovery (*e.g.*, Fe-based). Moreover, pediatric cortical bone has a stiffness value 30–40% lower and a yield strength value  $\sim 33\%$  lower than those of adult bone.<sup>206</sup> In another metanalysis, the mean elastic modulus for patients  $<40$  years of age was 12.62 GPa, while the value of the patients  $>60$  years was 9.47 MPa.<sup>207</sup> In addition, compressive strength and tensile strength of cortical bone decline by 2% per decade, starting from the third decade of life.<sup>90</sup> Osteoporosis also alters the properties of the bone. For instance, although elastic moduli of femoral cancellous bone show minimum variations between healthy and osteoporosis patients, the maximum strengths vary significantly, *i.e.*,  $14.1 \pm 7.3$  MPa and  $6.1 \pm 3.1$  MPa, respectively.<sup>208</sup> Similarly, anatomical position of implants determines the required properties as well.<sup>209</sup> For example, the scaffolds for supporting the bones of lower extremities, like femur, require higher and cyclic load-



bearing abilities, as compared to humerus or ulna. The elastic moduli vary between 0.008 and 33.7 GPa for different bones within an adult body. For instance, a systematic review and *meta*-analysis of different anatomical positions show that the mean value of elastic modulus of femur is 12.17 GPa while that of cancellous bone is 0.24 GPa.<sup>207</sup> These variations according to age, health and anatomical position call for customized implants to meet patient-specific requirements. Depending on these requirements, a suitable material systems can be chosen and optimized for MMCs, and scaffolds can be manufactured using AM. In addition, AM also enables the use of patient's own medical imaging to create anatomically matched implants.<sup>210-212</sup>

The research carried out so far has concluded that manufacturing bone scaffolds through AM with the addition of reinforcing bioactive materials to the metal matrix can improve mechanical strength, biodegradation rate, and bioactivity. Although significant progress has been made in implant design and AM, some critical challenges still need to be addressed.

Three key challenges for manufacturing next-generation orthopedic implants are (i) to obtain enhanced biocompatibility, (ii) to ensure durability, and in the case of temporary implants, (iii) to form a synergic combination of both these properties to ensure controlled biodegradation and healing simultaneously. Different biomaterials provide different property profiles required for bone substitutes: polymers resemble natural tissues, metals are stronger, while bioceramics are osteoconductive. There is yet no single material solution to meet all the requirements of bone implants. Hybrid materials present an excellent solution to achieving the desired properties. The future lies in an integrative approach where materials science and engineering solutions are combined with regenerative medicine to enable complete bone reconstruction (e.g., through bone regeneration). Moreover, owing to AM, the envelope of possible geometries and microarchitectures has greatly expanded, making it possible to manufacture complex structures with high precision and repeatability.

As for the MMCs for bone implants, despite significant progress in their development, several challenges remain and hinder the exploitation of their full potential and clinical adoption. Future research should aim at overcoming these challenges to enhance the efficacy of implant materials by improving performance, predictability, and overall clinical outcomes. Some of the possible routes that can be explored further are listed below.

One of the most fundamental challenges is understanding the mechanism underlying the interactions between the implants and biological systems. Without this understanding, it is difficult to differentiate between patient- or implant-related factors affecting these implants' safety and overall functionality.<sup>213</sup> Different individuals respond to implants differently with some exhibiting pathological responses to implants.<sup>214-216</sup> Addressing such complications requires a fundamental, scientific understanding of how metallic materials or added reinforcements contribute to immunological events. Specifically, the effects of AM MMC implant's

microarchitecture and composition on the resulting local, systemic and genotoxicities must be assessed. In addition, the mechanism and role of material's chemical composition, structural characteristics (at macro, micro, and nano scales), and physiochemical, mechanical, and biological properties in affecting osteoinduction need to be better understood.<sup>165,217,218</sup> Although osteoinduction, in general, has been studied, it is necessary to study it from the implant material's perspective to understand how altered composition, geometry, and surface impact the induction of bone formation.

While independent studies have been conducted to evaluate the toxicity of metals and their alloys in detail, the toxicity of MMCs is not yet well understood. The addition of reinforcing materials potentially alters the biodegradation process, influencing the type and concentration of the released ions and biodegradation products. This, in turn, alters the cytocompatibility of MMC implants as compared with monolithic metallic implants. Detailed analyses of such hybrid materials are required to understand specific mechanisms that govern any associated type of toxicity.

Another active area of research involves creating dual functionality (e.g., osteogenic and antibacterial) implants along with suitable rates of biodegradation. This might require incorporating elements, antibiotics, or naturally derived anti-bacterial organic molecules into the scaffold design, with potential control over the activation of antibacterial and/or osteogenic capabilities through either controlled biodegradation or stimulus-assisted activation.<sup>188,219,220</sup> Paired with AM and MMCs' capabilities, adding these agents as coatings would revolutionize the orthopedic industry by giving complete control over desired structures, resulting properties, and their dynamics in the biological environment. In addition, multi-material AM allows the creation of gradient architectures with varied compositions, in addition to spatial pore distribution, for mimicking of natural bones. For instance, Ti-based materials are placed in the outer compact layer, resembling the cortical bone, and porous Mg-based materials in the core, resembling the trabecular/cancellous bone.

In terms of biomechanical evaluation, in addition to quasi-static compression testing, (corrosion) fatigue testing should be conducted for bone substitutes. As mentioned earlier, certain bones, including lower limb load-bearing bones, sustain repeated loading cycles, which makes them susceptible to crack formation, growth, and eventual failure.<sup>7</sup> Therefore, materials designed for these implantation sites should be able to sustain cyclic loading, measured by fatigue testing, followed by detailed crack analysis. Biodegradation testing should be paired with the testing under static and dynamic loading conditions in standard physiological media.<sup>221</sup> For instance, a study<sup>222</sup> conducted fatigue tests of FeMn alloy scaffolds with a porous architecture prepared through extrusion-based 3D printing in air and in r-SBF. The results showed that the specimens could withstand 60% of their yield strength for 3 million cycles in the r-SBF compared to 90% of their strength in air. Moreover, *in situ* SEM compression and fatigue testing can be conducted, which, in addition to providing data about mechanical



properties, gives real-time visualization of the biomaterial's response to mechanical stresses, leading to crack initiation and propagation. This way, the failure mechanisms of the implant material can be analyzed.

New bioactive materials that can be added to MMC as the reinforcing agent should be also studied to initiate the healing processes and provide mechanical support at an early stage. There are specific sustainable routes to achieve bioactivity, one of which is introducing eggshell (ES) derived from nature. Eggshells are high in calcium content. So far, disintegrated melt deposition (DMD) without involving CAD files has been used for producing ES-reinforced MMC ingots, followed by machining and forming.<sup>223,224</sup> Using AM as a near-net-shape manufacturing process will give more control over the geometry of such implants and should be explored in future studies.

Despite significant progress made in developing AM MMCs and promising prospect of such biomaterials, there exist a number of barriers that delay their commercialization and clinical translation. Implants are mostly categorized as Class III medical devices due to their high risk and thus they are subjected to the most demanding standards and approval processes.<sup>212</sup> The AM process parameters and the thermal history of MMCs may result in variabilities in microstructure and porosity, thus creating a critical challenge for reproducibility and eventually clinical validation. These variabilities translate into inconsistent mechanical properties, degradation mechanisms, and biological properties, and thus complicate the regulatory approval for clinical use. Therefore, robust quality control needs to be ensured. For instance, powder mixing uniformity, *i.e.*, a mixture having uniform elemental distribution and good flowability, is of profound importance and needs to be maintained over different batches of the same product.<sup>21</sup> Failure to achieve this could lead to local property variations and even premature failure. To address this technological challenge, advanced mixing methods must be utilized, including ball milling, ultrasonic blending, *etc.*, and the compositions of powders must be monitored to ensure homogeneity.<sup>21</sup> In addition, since AM is a layer-by-layer fabrication technology, thermal history or inconsistent recoating can cause lack of fusion within the layers, thus making the product defective. *In-situ* monitoring of the melt pool through thermal imaging could help in gaining valuable insights into the process and even allowing the operator to identify and mitigate defects. For the quality control of AM MMC implants, non-destructive testing (NDT) could be utilized, such as X-ray computed tomography, infrared thermography, and/or ultrasonic inspection to detect internal defects without damaging the implants.<sup>225</sup> Future work could target specifically at defect-mapping frameworks and process parameter optimization, along with *in situ* monitoring for aligning these with international standards (ASTM and ISO) to ensure the consistency and safety of AM MMC implants and faster clinical translation.

Regulatory frameworks play a crucial role in clinical use of any medical device, though the guidelines and procedures differ geographically. For example, in the United States, Food and Drug Administration (FDA) provides a patient-centered

approach for AM medical devices in the design, manufacturing and testing aspects of AM devices and in the evaluation of orthopedic implants.<sup>210,226</sup> Premarket approval (PMA) is very rigorous, requiring long timelines and extensive clinical data. On the other hand, European Union's CE allows for greater performance analysis and post-market surveillance of medical devices, which might lead to devices reaching the European market faster than in the U.S., though they will be obligated to be subjected to risk monitoring.<sup>227,228</sup> In any case, regulatory processes for implants are time-consuming and require extensive clinical trials that typically take years to come to a successful end.<sup>226</sup> Similarly, other regions have their respective regulations and guidelines for adopting medical implants, requiring design optimization and evidence of reliability and repeatability, which also impacts the timelines of approval and market availability. Fabrication process scalability is another bottleneck that might impact large-scale implant production since translation from laboratory settings to industrial production requires intense process and quality control strategies.

From an economic standpoint, while the AM does enable reduced material waste and cost-effective customized implants, their large-scale clinical translation requires larger quantities of high-quality feedstock materials, along with industrial-scale equipment, their maintenance and post-processing, which raises the overall costs. Though the costs would potentially decrease with increased efficiency of AM processes, currently, upscaling remains a serious barrier to translation into clinical practice. The manufacturers need to plan strategically to address these challenges and to be prepared for multi-jurisdictional approvals in order to become suppliers of such devices in the global market. In general, the clinical translation of industrial-scale AM MMCs is dependent on the ongoing research and development with regard to AM materials, AM technology and intensive preclinical and clinical evaluation, along with regulatory compliance for the clinical adoption of such devices.

While it is not possible to put a fixed schedule on the roadmap for moving AM MMCs towards clinical use, a conceptual framework of timelines presents itself as a logical structure across the next phases. For instance, in the near-term (within the next few years), immediate attention is required to fundamental research on the optimization of AM process parameters, the investigation of material composition effects, the standardization of *in vitro* tests, and the building of open repositories of data, which also aligns with the immediate priority categories in standardization roadmaps.<sup>229</sup> Mid-term goals shift to preclinical validation, as the research in a laboratory setting matures during the near-term advancement. This could include systematic *in vivo* studies and the development of predictive models. In the long term, clinical translational steps become crucial, where regulatory pathways, good manufacturing practice (GMP) standards and the initiation of clinical trials take place. Clinical trials usually take 1–5 years for medical implants, depending on the complexity of the implant, along with ~5 years follow ups.<sup>230,231</sup> In addition, once PMA is filed, it takes 180 days for review.<sup>232</sup> If a



breakthrough orthopedic device is designed and proposed, the average decision times is 332 days for PMA and 295 days for *de Novo* – which is a specific pathway for novel implants.<sup>230</sup> This conceptualization of the process provides an incremental framework for advances in scientific research in the near term, translational enablers in the mid-term and subsequently clinical adoption in the long term. It also gives researchers and funding bodies a structured framework to prioritize investments and collaboration. Collaboration amongst materials and biomedical scientists, local and global funding agencies and regulatory bodies will play a crucial role in the successful translation of innovative AM MMCs in the orthopedic devices industry.

## List of abbreviations

3DF	Three-dimensional fiber deposition	LPBF	Laser powder bed fusion
$\alpha$ -MEM	Minimal essential medium Eagle – alpha modification	MBG	Mesoporous bioactive glass
$\beta$ -TCP	Beta tricalcium phosphate	ME	Material extrusion
Ak	Akermanite	MMC	Metal matrix composites
ALP	Alkaline Phosphatase	MRI	Magnetic resonance imaging
AM	Additive manufacturing	MTT	Microculture tetrazolium test
ARS	Alizarin Red S	OCN	Osteocalcin
BG	Bioactive glass	OD	Optical density
BJ	Binder jetting	OI	Osteogenesis imperfecta
BMSCs	Bone marrow-derived mesenchymal stem cells	OPN	Osteopontin
BR	Bredigite	PBF	Powder bed fusion
CAD	Computer aided design	PDMS	Polydimethylsiloxane
CCK-8	Cell counting kit 8	PDP	Potentiodynamic polarization
CM	Cell culture medium	PTT	Partial Thromboplastin Time
DAPI	4',6-diamidino-2-phenylindole staining	rBMSCs	Rat bone marrow mesenchymal stem cells
DCFH-DA	Dichlorodihydrofluorescein Diacetate	RGR	Relative growth rate
DED	Direct energy deposition	RNS	Reactive nitrogen species
DLP	Digital light processing	ROS	Reactive oxygen species
DMD	Direct metal/melt deposition	r-SBF	Revised simulated body fluid
DMD	Direction melt deposition	RUNX <sub>2</sub>	Runt-related transcription factor 2
DMSO	Di methyl sulfoxide	SaO <sub>2</sub>	Arterial Oxygen Saturation
DNA	Deoxyribonucleic acid	SBF	Simulated body fluid
EB	Equine bone	SEM	Scanning electron microscope
EBDM	Electron beam direct melting	SL	Sheet lamination
EBM	Electron beam melting	SLA	Stereolithography
EIS	Electrochemical impedance spectroscopy	SLM	Selective laser melting
ES	Eggshells	SLS	Selective laser sintering
FBS	Fetal bovine serum	SPS	Simulated physiological solution
FDM	Fused deposition modeling	TRIS	Tris (hydroxymethyl) aminomethane
FEM	Finite Element Method	UC	Ultrasonic consolidation
FMC	Fe-metal composites	UC-MSC	Umbilical cord mesenchymal stem cell
FSAM	Friction stir additive manufacturing	UTS	Ultimate tensile strength
HA	Hydroxyapatite	VAT	VAT photopolymerization
HBSS	Hank's balanced salt solution	Vol	Volume
hMSCs	Human mesenchymal stem cell	Wt	Weight
H & E	Hematoxylin and Eosin		
LC	Laser cladding		
LOM	Laminated object manufacturing		

## Conflicts of interest

There are no conflicts to declare.

## Data availability

This review article is based solely on previously published data, as cited throughout the manuscript. No new datasets were generated or analyzed by the authors. Tables 1–6 present summarized information extracted from the literature and are adapted from ref. 1–28, as indicated in the respective table captions. No custom software or code was used in the preparation of this review.

## Acknowledgements

This publication was made possible by the grant ARG No.: ARG01-0518-230219 (QNRF, a member of the Qatar Foundation). The statements made herein are solely the responsibility



of the authors. The authors thank the support of the Center of Advanced Materials, Qatar University.

## References

- R. J. Anish and A. Nair, Osteoporosis Management-Current and Future Perspectives – A Systemic Review, *J. Orthop.*, 2024, **53**, 101–113, DOI: [10.1016/j.jor.2024.03.002](https://doi.org/10.1016/j.jor.2024.03.002).
- A. Qaseem, M. A. Forciea, R. M. McLean and T. D. Denberg, Treatment of Low Bone Density or Osteoporosis to Prevent Fractures in Men and Women: A Clinical Practice Guideline Update from the American College of Physicians, *Ann. Int. Med.*, 2017, **166**(11), 818–839, DOI: [10.7326/m15-1361-suppl\\_file/m15-1361\\_supplement-v1.pdf](https://doi.org/10.7326/m15-1361-suppl_file/m15-1361_supplement-v1.pdf).
- A. B. Christ, A. S. Piple, B. S. Gettleman, A. Duong, M. Chen, J. C. Wang, N. D. Heckmann and L. Menendez, Prevalence of Primary Malignant Tumours, Rates of Pathological Fracture, and Mortality in the Setting of Metastatic Bone Disease, *Bone Jt Open*, 2023, **4**(6), 424–431, DOI: [10.1302/2633-1462.46.bjo-2023-0042.r1/lettertoeditor](https://doi.org/10.1302/2633-1462.46.bjo-2023-0042.r1/lettertoeditor).
- C. Pitsilos, P. Givissis, P. Papadopoulos and B. Chalidis, Treatment of Recurrent Giant Cell Tumor of Bones: A Systematic Review, *Cancers*, 2023, **15**(13), 3287, DOI: [10.3390/cancers15133287](https://doi.org/10.3390/cancers15133287).
- D. Froemel and A. Meurer, Congenital Bone Disorders, *Intramedullary Nailing*, 2015, 565–585, DOI: [10.1007/978-1-4471-6612-2\\_33](https://doi.org/10.1007/978-1-4471-6612-2_33).
- F. Marini, F. Giusti, T. Iantomasi and M. L. Brandi, Congenital Metabolic Bone Disorders as a Cause of Bone Fragility, *Int. J. Mol. Sci.*, 2021, **22**(19), 10281, DOI: [10.3390/ijms221910281](https://doi.org/10.3390/ijms221910281).
- P. Ducheyne, *Comprehensive Biomaterials*, 2011, Vol. 1.
- M. Sandhu, N. Kumar, R. S. Sawhney, S. Kaur and K. Singh, Materials Used in Orthopedic Implants: A Comprehensive Review Study, *Obstet. Gynaecol. Forum*, 2024, **34**(3s), 89–95.
- M. H. Mobarak; M. A. Islam; N. Hossain; M. Z. Al Mahmud; M. T. Rayhan; N. J. Nishi and M. A. Chowdhury, Recent Advances of Additive Manufacturing in Implant Fabrication – A Review, *Applied Surface Science Advances*, Elsevier B. V., 2023, DOI: [10.1016/j.apsadv.2023.100462](https://doi.org/10.1016/j.apsadv.2023.100462).
- B. Gao, H. Zhao, L. Peng and Z. Sun, A Review of Research Progress in Selective Laser Melting (SLM), *Micromachines*, 2023, **14**, 57, DOI: [10.3390/mi14010057](https://doi.org/10.3390/mi14010057).
- A. I. Nurhudan, S. Supriadi, Y. Whulanza and A. S. Saragih, Additive Manufacturing of Metallic Based on Extrusion Process: A Review, *J. Manuf. Process.*, 2021, **66**, 228–237, DOI: [10.1016/j.jmapro.2021.04.018](https://doi.org/10.1016/j.jmapro.2021.04.018).
- N. Huang, O. J. Cook, A. P. Argüelles and A. M. Beese, Review of Process–Structure–Property Relationships in Metals Fabricated Using Binder Jet Additive Manufacturing, *Metallogr., Microstruct., Anal.*, 2023, **12**(6), 883–905, DOI: [10.1007/s13632-023-00998-4](https://doi.org/10.1007/s13632-023-00998-4).
- M. K. Kolamrouri, A. Mohammed, I. Mustafa and K. Naser, Developments on Electron Beam Melting (EBM) of Ti-6Al-4V: A Review, *Trans. Indian Inst. Met.*, 2021, **74**, 783–790, DOI: [10.1007/s12666-021-02230-9](https://doi.org/10.1007/s12666-021-02230-9).
- B. Utela, D. Storti, R. Anderson and M. Ganter, A Review of Process Development Steps for New Material Systems in Three Dimensional Printing (3DP), *J. Manuf. Process*, 2008, **10**(2), 96–104, DOI: [10.1016/j.jmapro.2009.03.002](https://doi.org/10.1016/j.jmapro.2009.03.002).
- E. L. Papazoglou, N. E. Karkalos, P. Karmiris-Obratański and A. P. Markopoulos, On the Modeling and Simulation of SLM and SLS for Metal and Polymer Powders: A Review, *Arch. Comput. Methods Eng.*, 2021, **29**(2), 941–973, DOI: [10.1007/s11831-021-09601-x](https://doi.org/10.1007/s11831-021-09601-x).
- H. Ramazani and A. Kami, Metal FDM, a New Extrusion-Based Additive Manufacturing Technology for Manufacturing of Metallic Parts: A Review, *Prog. Addit. Manuf.*, 2022, **7**(4), 609–626, DOI: [10.1007/s40964-021-00250-x/figures/14](https://doi.org/10.1007/s40964-021-00250-x/figures/14).
- N. Singh, H. Siddiqui, B. S. R. Koyalada, A. Mandal, V. Chauhan, S. Natarajan, S. Kumar, M. Goswami and S. Kumar, Recent Advancements in Additive Manufacturing (AM) Techniques: A Forward-Looking Review, *Met. Mater. Int.*, 2023, **29**(8), 2119–2136, DOI: [10.1007/s12540-022-01380-9/tables/2](https://doi.org/10.1007/s12540-022-01380-9/tables/2).
- P. Badoniya, M. Srivastava, P. K. Jain and S. Rathee, A State-of-the-Art Review on Metal Additive Manufacturing: Milestones, Trends, Challenges and Perspectives, *J. Braz. Soc. Mech. Sci. Eng.*, 2024, **46**(6), 1–34, DOI: [10.1007/s40430-024-04917-8/figures/15](https://doi.org/10.1007/s40430-024-04917-8/figures/15).
- M. Shaikh, F. Kahwash, Z. Lu, M. Alkhreisat, A. Mohammad and I. Shyha, Revolutionising Orthopaedic Implants—a Comprehensive Review on Metal 3D Printing with Materials, Design Strategies, Manufacturing Technologies, and Post-Process Machining Advancements, *Int. J. Adv. Des. Manuf. Technol.*, 2024, **134**(3), 1043–1076, DOI: [10.1007/s00170-024-14218-y](https://doi.org/10.1007/s00170-024-14218-y).
- H. Ramazani and A. Kami, Metal FDM, a New Extrusion-Based Additive Manufacturing Technology for Manufacturing of Metallic Parts: A Review, *Prog. Addit. Manuf.*, 2022, **7**(4), 609–626, DOI: [10.1007/s40964-021-00250-x/figures/14](https://doi.org/10.1007/s40964-021-00250-x/figures/14).
- M. Dadkhah, M. H. Mosallanejad, L. Iuliano and A. Saboori, A Comprehensive Overview on the Latest Progress in the Additive Manufacturing of Metal Matrix Composites: Potential, Challenges, and Feasible Solutions, *Acta Metall. Sin. (Engl. Lett.)*, 2021, **34**(9), 1173–1200, DOI: [10.1007/s40195-021-01249-7](https://doi.org/10.1007/s40195-021-01249-7).
- N. Li, W. Liu, Y. Wang, Z. Zhao, T. Yan, G. Zhang and H. Xiong, Laser Additive Manufacturing on Metal Matrix Composites: A Review, *Chin. J. Mech. Eng. (Engl. Ed.)*, 2021, **34**(1), 1–16, DOI: [10.1186/s10033-021-00554-7/figures/1](https://doi.org/10.1186/s10033-021-00554-7/figures/1).
- H. Attar, S. Ehtemam-Haghghi, D. Kent and M. S. Dargusch, Recent Developments and Opportunities in Additive Manufacturing of Titanium-Based Matrix Composites: A Review, *Int. J. Mach. Tools Manuf.*, 2018, 85–102, DOI: [10.1016/j.ijmachtools.2018.06.003](https://doi.org/10.1016/j.ijmachtools.2018.06.003).
- H. Attar, S. Ehtemam-Haghghi, N. Soro, D. Kent and M. S. Dargusch, Additive Manufacturing of Low-Cost Porous Titanium-Based Composites for Biomedical Applications: Advantages, Challenges and Opinion for Future Development, *J. Alloys Compd.*, 2020, 827, DOI: [10.1016/j.jallcom.2020.154263](https://doi.org/10.1016/j.jallcom.2020.154263).



25 K. V, N. Kumar B, S. Kumar S and V. M, Magnesium Role in Additive Manufacturing of Biomedical Implants – Challenges and Opportunities, *Addit. Manuf.*, 2022, **55**, 102802, DOI: [10.1016/j.addma.2022.102802](https://doi.org/10.1016/j.addma.2022.102802).

26 G. Fernandez de Grado, L. Keller, Y. Idoux-Gillet, Q. Wagner, A. M. Musset, N. Benkirane-Jessel, F. Bornert and D. Offner, Bone Substitutes: A Review of Their Characteristics, Clinical Use, and Perspectives for Large Bone Defects Management, *J. Tissue Eng.*, 2018, **9**, 2041731418776819, DOI: [10.1177/2041731418776819](https://doi.org/10.1177/2041731418776819).

27 T. Wu, S. Yu, D. Chen and Y. Wang, Bionic Design, Materials and Performance of Bone Tissue Scaffolds, *Materials*, 2017, **10**(10), 1187, DOI: [10.3390/ma10101187](https://doi.org/10.3390/ma10101187).

28 R. V. Badhe, O. Akinfose, D. Bijukumar, M. Barba and M. T. Mathew, Systemic Toxicity Eliciting Metal Ion Levels from Metallic Implants and Orthopedic Devices – A Mini Review, *Toxicol. Lett.*, 2021, **350**, 213–224, DOI: [10.1016/j.toxlet.2021.07.004](https://doi.org/10.1016/j.toxlet.2021.07.004).

29 L. Y. Chen, P. Qin, L. Zhang and L. C. Zhang, An Overview of Additively Manufactured Metal Matrix Composites: Preparation, Performance, and Challenge, *Int. J. Extreme Manuf.*, 2024, **6**(5), 052006, DOI: [10.1088/2631-7990/ad54a4](https://doi.org/10.1088/2631-7990/ad54a4).

30 M. P. Behera, T. Dougherty and S. Singamneni, Conventional and Additive Manufacturing with Metal Matrix Composites: A Perspective, *Proc. Manuf.*, 2019, **30**, 159–166, DOI: [10.1016/j.promfg.2019.02.023](https://doi.org/10.1016/j.promfg.2019.02.023).

31 M. Fan, F. Zhao, Y. Liu, S. Yin, S. Peng and Z. Zhang, Zinc Matrix Composites Reinforced with Partially Unzipped Carbon Nanotubes as Biodegradable Implant Materials, *Crystals*, 2022, **12**(8), 1110, DOI: [10.3390/crust12081110](https://doi.org/10.3390/crust12081110).

32 K. Chen, J. Dong, N. E. Putra, L. E. Fratila-Apachitei, J. Zhou and A. A. Zadpoor, Additively Manufactured Function-Tailored Bone Implants Made of Graphene-Containing Biodegradable Metal Matrix Composites, *Prog. Mater. Sci.*, 2026, **155**, 101517, DOI: [10.1016/j.pmatsci.2025.101517](https://doi.org/10.1016/j.pmatsci.2025.101517).

33 S. Downes and A. A. Mishra, Tissue-Biomaterial Interactions, *Adv. Wound Repair Ther.*, 2011, 174–185, DOI: [10.1533/9780857093301.2.174](https://doi.org/10.1533/9780857093301.2.174).

34 C. Kalirajan, A. Dukle, A. J. Nathanael, T. H. Oh and G. Manivasagam, A Critical Review on Polymeric Biomaterials for Biomedical Applications, *Polymers*, 2021, **13**(17), 3015, DOI: [10.3390/polym13173015](https://doi.org/10.3390/polym13173015).

35 M. Vallet-Regí, Evolution of Biomaterials, *Front. Mater.*, 2022, **9**, DOI: [10.3389/fmats.2022.864016/full](https://doi.org/10.3389/fmats.2022.864016).

36 X. Zhou, Y. Feng, J. Zhang, Y. Shi and L. Wang, Recent Advances in Additive Manufacturing Technology for Bone Tissue Engineering Scaffolds, *Int. J. Adv. Des. Manuf. Technol.*, 2020, **108**, 3591–3606, DOI: [10.1007/s00170-020-05444-1/Published](https://doi.org/10.1007/s00170-020-05444-1).

37 J. T. Intravaia, T. Graham, H. S. Kim, H. S. Nanda, S. G. Kumbar and S. P. Nukavarapu, Smart Orthopedic Biomaterials and Implants, *Curr. Opin. Biomed. Eng.*, 2022, **25**, 100439, DOI: [10.1016/j.cobme.2022.100439](https://doi.org/10.1016/j.cobme.2022.100439).

38 P. S. Nerkar; S. J. Tawale; S. M. Saoji and A. D. Doye, Evaluation of Smart Bio-Materials in Orthopedics and Tissue Engineering, *Lecture Notes on Multidisciplinary Industrial Engineering*, 2022, Part F41, pp. 587–600, DOI: [10.1007/978-3-030-73495-4\\_40](https://doi.org/10.1007/978-3-030-73495-4_40).

39 D. W. Grainger, The Williams Dictionary of Biomaterials, *Mater. Today*, 1999, **2**(3), 29, DOI: [10.1016/S1369-7021\(99\)80066-2](https://doi.org/10.1016/S1369-7021(99)80066-2).

40 A. Carnicer-Lombarte, S. T. Chen, G. G. Malliaras and D. G. Barone, Foreign Body Reaction to Implanted Biomaterials and Its Impact in Nerve Neuroprosthetics, *Front. Bioeng. Biotechnol.*, 2021, **9**, 622524, DOI: [10.3389/fbioe.2021.622524/bibtex](https://doi.org/10.3389/fbioe.2021.622524/bibtex).

41 S. Laurén. *Biocompatibility: Biomaterial interaction with the biological surrounding*. <https://www.biolinscientific.com/blog/biocompatibility-biomaterial-interaction-with-the-biological-surrounding> (accessed 2024-05-27).

42 R. Davis, A. Singh, M. J. Jackson, R. T. Coelho, D. Prakash, C. P. Charalambous, W. Ahmed, L. R. R. da Silva and A. A. Lawrence, A Comprehensive Review on Metallic Implant Biomaterials and Their Subtractive Manufacturing, *Int. J. Adv. Des. Manuf. Technol.*, 2022, **120**, 1473–1530, DOI: [10.1007/s00170-022-08770-8](https://doi.org/10.1007/s00170-022-08770-8).

43 R. P. Brown; B. A. Fowler; S. Fustinoni; M. Costa and M. Nordberg, Toxicity of Metals Released from Implanted Medical Devices, *Handbook on the Toxicology of Metals*, 5th edn, 2022, vol. 1, pp. 127–136, DOI: [10.1016/b978-0-12-823292-7.00003-6](https://doi.org/10.1016/b978-0-12-823292-7.00003-6).

44 A. A. Abdal Dayem, M. K. Hossain, S. B. Lee, K. Kim, S. K. Saha, G. M. Yang, H. Y. Choi and S. G. Cho, The Role of Reactive Oxygen Species (ROS) in the Biological Activities of Metallic Nanoparticles, *Int. J. Mol. Sci.*, 2017, **18**(1), 120, DOI: [10.3390/ijms18010120](https://doi.org/10.3390/ijms18010120).

45 J. C. Rubio, M. C. García-Alonso, C. Alonso, M. A. Alobera, C. Clemente, L. Munuera and M. L. Escudero, Determination of Metallic Traces in Kidneys, Livers, Lungs and Spleens of Rats with Metallic Implants after a Long Implantation Time, *J. Mater. Sci. Mater. Med.*, 2008, **19**(1), 369–375, DOI: [10.1007/s10856-007-3002-0/schemes/1](https://doi.org/10.1007/s10856-007-3002-0/schemes/1).

46 H. Matusiewicz and M. Richter, Metals and Metal Ions Release from Metallic Implants in the Animal Body Models: A Review of Experimental Investigations, *World J. Adv. Res. Rev.*, 2022, **2022**(01), 653–676, DOI: [10.30574/wjarr.2022.16.1.1024](https://doi.org/10.30574/wjarr.2022.16.1.1024).

47 A. Hudecki, G. Kiryczynski and M. J. Łos, Biomaterials, Definition, Overview, *Stem Cells Biomater. Regener. Med.*, 2018, 85–98, DOI: [10.1016/b978-0-12-812258-7.00007-1](https://doi.org/10.1016/b978-0-12-812258-7.00007-1).

48 S. Parithimarkalaignan and T. V. Padmanabhan, Osseointegration: An Update, *J. Indian Prosthodont. Soc.*, 2013, **13**(1), 2, DOI: [10.1007/s13191-013-0252-z](https://doi.org/10.1007/s13191-013-0252-z).

49 ISO 10993-12:2021 - *Biological Evaluation of Medical Devices—Part 12: Sample Preparation and Reference Materials*; 2021. <https://www.iso.org/standard/75769.html> (accessed 2025-08-21).

50 W. M. Mihalko, H. Haider, S. Kurtz, M. Marcolongo and K. Urish, New Materials for Hip and Knee Joint Replacement: What's Hip and What's in Kneed?, *J. Orthop. Res.*, 2020, **38**(7), 1436–1444, DOI: [10.1002/jor.24750](https://doi.org/10.1002/jor.24750).



51 J. Pajarin, T. H. Lin, T. Sato, Z. Yao and S. B. Goodman, Interaction of Materials and Biology in Total Joint Replacement - Successes, Challenges and Future Directions, *J. Mater. Chem. B*, 2014, **2**(41), 7094–7108, DOI: [10.1039/c4tb01005a](https://doi.org/10.1039/c4tb01005a).

52 D. A. Florea, D. Albulet, A. M. Grumezescu and E. Andronescu, Surface Modification - A Step Forward to Overcome the Current Challenges in Orthopedic Industry and to Obtain an Improved Osseointegration and Antimicrobial Properties, *Mater. Chem. Phys.*, 2020, **243**, 122579, DOI: [10.1016/j.matchemphys.2019.122579](https://doi.org/10.1016/j.matchemphys.2019.122579).

53 S. Bandopadhyay, N. Bandyopadhyay, S. Ahmed, V. Yadav and R. K. Tekade, Current Research Perspectives of Orthopedic Implant Materials, *Biomater. Bionanotechnol.*, 2019, 337–374, DOI: [10.1016/b978-0-12-814427-5.00010-x](https://doi.org/10.1016/b978-0-12-814427-5.00010-x).

54 K. Ishfaq, M. Rehman, A. R. Khan and Y. Wang, A Review on the Performance Characteristics, Applications, Challenges and Possible Solutions in Electron Beam Melted Ti-Based Orthopaedic and Orthodontic Implants, *Rapid Prototyp. J.*, 2022, **28**, 525–545, DOI: [10.1108/rpj-03-2021-0060](https://doi.org/10.1108/rpj-03-2021-0060).

55 N. E. Putra, M. A. Leeflang, M. Klimopoulou, J. Dong, P. Taheri, Z. Huan, L. E. Fratila-Apachitei, J. M. C. Mol, J. Chang, J. Zhou and A. A. Zadpoor, Extrusion-Based 3D Printing of Biodegradable, Osteogenic, Paramagnetic, and Porous FeMn-Akermanite Bone Substitutes, *Acta Biomater.*, 2023, **162**, 182–198, DOI: [10.1016/j.actbio.2023.03.033](https://doi.org/10.1016/j.actbio.2023.03.033).

56 M. Z. A. Mahmud, M. H. Mobarak, N. Hossain, M. A. Islam and M. T. Rayhan, Emerging Breakthroughs in Biomaterials for Orthopedic Applications: A Comprehensive Review, *Bioprinting*, 2023, **36**, e00323, DOI: [10.1016/j.bioprint.2023.e00323](https://doi.org/10.1016/j.bioprint.2023.e00323).

57 R. Sajjad, S. T. Chauhdary, M. T. Anwar, A. Zahid, A. A. Khosa, M. Imran and M. H. Sajjad, A Review of 4D Printing - Technologies, Shape Shifting, Smart Polymer Based Materials, and Biomedical Applications, *Adv. Ind. Eng. Polym. Res.*, 2024, **7**(1), 20–36, DOI: [10.1016/j.aiepr.2023.08.002](https://doi.org/10.1016/j.aiepr.2023.08.002).

58 Y. Liu, L. Yu, J. Chen, S. Li, Z. Wei and W. Guo, Exploring the Osteogenic Potential of Zinc-Doped Magnesium Phosphate Cement (ZMPC): A Novel Material for Orthopedic Bone Defect Repair, *Biomedicines*, 2024, **12**(2), 344, DOI: [10.3390/biomedicines12020344/s1](https://doi.org/10.3390/biomedicines12020344/s1).

59 M. Ashby, Designing Architectured Materials, *Sci. Mater.*, 2013, **68**(1), 4–7, DOI: [10.1016/j.scriptamat.2012.04.033](https://doi.org/10.1016/j.scriptamat.2012.04.033).

60 C. Wang, Z. Vangelatos, C. P. Grigoropoulos and Z. Ma, Micro-Engineered Architected Metamaterials for Cell and Tissue Engineering, *Mater. Today Adv.*, 2022, **13**, 100206, DOI: [10.1016/j.mtadv.2022.100206](https://doi.org/10.1016/j.mtadv.2022.100206).

61 A. A. Zadpoor, Meta-Biomaterials, *Biomater. Sci.*, 2019, **8**(1), 18–38, DOI: [10.1039/c9bm01247h](https://doi.org/10.1039/c9bm01247h).

62 Z. L. Grace; J. P. Fisher and K. W. Leong, *3D Bioprinting and Nanotechnology in Tissue Engineering and Regenerative Medicine*, Academic Press, 2015.

63 O. L. A. Harrysson, O. Cansizoglu, D. J. Marcellin-Little, D. R. Cormier and H. A. West, Direct Metal Fabrication of Titanium Implants with Tailored Materials and Mechanical Properties Using Electron Beam Melting Technology, *Mater. Sci. Eng. C*, 2008, **28**(3), 366–373, DOI: [10.1016/j.msec.2007.04.022](https://doi.org/10.1016/j.msec.2007.04.022).

64 H. M. A. Kolken, A. F. Garcia, A. Du Plessis, C. Rans, M. J. Mirzaali and A. A. Zadpoor, Fatigue Performance of Auxetic Meta-Biomaterials, *Acta Biomater.*, 2021, **126**, 511–523, DOI: [10.1016/j.actbio.2021.03.015](https://doi.org/10.1016/j.actbio.2021.03.015).

65 A. A. Zadpoor, Mechanical Performance of Additively Manufactured Meta-Biomaterials, *Acta Biomater.*, 2019, **85**, 41–59, DOI: [10.1016/j.actbio.2018.12.038](https://doi.org/10.1016/j.actbio.2018.12.038).

66 S. J. P. Callens, C. H. Arns, A. Kuliesh and A. A. Zadpoor, Decoupling Minimal Surface Metamaterial Properties Through Multi-Material Hyperbolic Tilings, *Adv. Funct. Mater.*, 2021, **31**(30), 2101373, DOI: [10.1002/adfm.202101373](https://doi.org/10.1002/adfm.202101373).

67 S. Amin Yavari, M. Croes, B. Akhavan, F. Jahanmard, C. C. Eigenhuis, S. Dadbakhsh, H. C. Vogely, M. M. Bilek, A. C. Fluit, C. H. E. Boel, B. C. H. van der Waals, T. Vermonden, H. Weinans and A. A. Zadpoor, Layer by Layer Coating for Bio-Functionalization of Additively Manufactured Meta-Biomaterials, *Addit. Manuf.*, 2020, **32**, 100991, DOI: [10.1016/j.addma.2019.100991](https://doi.org/10.1016/j.addma.2019.100991).

68 F. A. Shah, P. Thomsen and A. Palmquist, Osseointegration and Current Interpretations of the Bone-Implant Interface, *Acta Biomater.*, 2019, **84**, 1–15, DOI: [10.1016/j.actbio.2018.11.018](https://doi.org/10.1016/j.actbio.2018.11.018).

69 A. Evans, C. San Marchi and A. Mortensen, *Metal Matrix Composites in Industry*, 2003, DOI: [10.1007/978-1-4615-0405-4](https://doi.org/10.1007/978-1-4615-0405-4).

70 S. Sambasivam, S. Shirbhate, A. S. Abed, P. P. Patil, I. Khan, R. Singh, L. Kansal and A. Awasthi, Significance of Reinforcement in Mg-Based MMCs for Various Applications: A Review, *Mater. Today Proc.*, 2023, DOI: [10.1016/j.matpr.2023.02.161](https://doi.org/10.1016/j.matpr.2023.02.161).

71 S. K. Sharma, K. K. Saxena, A. K. Dixit, R. Singh and K. A. Mohammed, Role of Additive Manufacturing and Various Reinforcements in MMCs Related to Biomedical Applications. *Advances in Materials and Processing Technologies*, Taylor and Francis Ltd. 2024, pp. 231–248, DOI: [10.1080/2374068x.2022.2122005](https://doi.org/10.1080/2374068x.2022.2122005).

72 J. Koráb, P. Štefánik, Š. Kavecký, P. Šebo and G. Korb, Thermal Conductivity of Unidirectional Copper Matrix Carbon Fibre Composites, *Composites, Part A*, 2002, **33**(4), 577–581, DOI: [10.1016/s1359-835x\(02\)00003-9](https://doi.org/10.1016/s1359-835x(02)00003-9).

73 S. Y. Chang, C. F. Chen, S. J. Lin and T. Z. Kattamis, Electrical Resistivity of Metal Matrix Composites, *Acta Mater.*, 2003, **51**(20), 6291–6302, DOI: [10.1016/S1359-6454\(03\)00462-2](https://doi.org/10.1016/S1359-6454(03)00462-2).

74 B. M. Thomson, *BONE. Encyclopedia of Human Nutrition*, 1998, pp. 220–225, DOI: [10.1016/b0-12-226694-3/00029-6](https://doi.org/10.1016/b0-12-226694-3/00029-6).

75 M. Ashby, Designing architectured materials, *Scr. Mater.*, 2013, **68**(1), 4–7, DOI: [10.1016/j.scriptamat.2012.04.033](https://doi.org/10.1016/j.scriptamat.2012.04.033).

76 F. A. Shah, A. Snis, A. Matic, P. Thomsen and A. Palmquist, 3D Printed Ti6Al4V Implant Surface Promotes Bone Maturation and Retains a Higher Density of Less Aged Osteocytes at the Bone-Implant Interface, *Acta Biomater.*, 2016, **30**, 357–367, DOI: [10.1016/j.actbio.2015.11.013](https://doi.org/10.1016/j.actbio.2015.11.013).



77 V. Goriainov, R. Cook, J. M. Latham, D. G. Dunlop and R. O. C. Oreffo, Bone and Metal: An Orthopaedic Perspective on Osseointegration of Metals, *Acta Biomater.*, 2014, **10**(10), 4043–4057, DOI: [10.1016/j.actbio.2014.06.004](https://doi.org/10.1016/j.actbio.2014.06.004).

78 L. Yuan, S. Ding and C. Wen, Additive Manufacturing Technology for Porous Metal Implant Applications and Triple Minimal Surface Structures: A Review, *Bioact. Mater.*, 2019, **4**(1), 56–70, DOI: [10.1016/j.bioactmat.2018.12.003](https://doi.org/10.1016/j.bioactmat.2018.12.003).

79 C. Torres-Sanchez, F. R. A. Al Mushref, M. Norrito, K. Yendall, Y. Liu and P. P. Conway, The Effect of Pore Size and Porosity on Mechanical Properties and Biological Response of Porous Titanium Scaffolds, *Mater. Sci. Eng. C*, 2017, **77**, 219–228, DOI: [10.1016/j.msec.2017.03.249](https://doi.org/10.1016/j.msec.2017.03.249).

80 S. Dhar, D. Sunderamoorthy and H. Majeed, Cysts: Osteolysis and Stress Shielding: More Than Just Filling A Void. In Total Ankle Arthroplasty, ed. Haddad, S. L., *American Academy of Orthopaedic Surgeon*, 2015.

81 D. Savio and A. Bagno, When the Total Hip Replacement Fails: A Review on the Stress-Shielding Effect, *Processes*, 2022, **10**(3), 612, DOI: [10.3390/pr10030612](https://doi.org/10.3390/pr10030612).

82 C. Li, D. Pisignano, Y. Zhao and J. Xue, Advances in Medical Applications of Additive Manufacturing, *Engineering*, 2020, **6**(11), 1222–1231, DOI: [10.1016/j.eng.2020.02.018](https://doi.org/10.1016/j.eng.2020.02.018).

83 C. Song, L. Liu, Z. Deng, H. Lei, F. Yuan, Y. Yang, Y. Li and Y. Jiakuo, Research Progress on the Design and Performance of Porous Titanium Alloy Bone Implants, *J. Mater. Res. Technol.*, 2023, **23**, 2626–2641, DOI: [10.1016/j.jmrt.2023.01.155](https://doi.org/10.1016/j.jmrt.2023.01.155).

84 H. E. Koschwanec and W. M. Reichert, *Textured and Porous Materials. Biomaterials Science: An Introduction to Materials*, 3rd edn, 2013, pp. 321–331, DOI: [10.1016/b978-0-08-087780-8.00030-9](https://doi.org/10.1016/b978-0-08-087780-8.00030-9).

85 P. Sarmah and K. Gupta, Recent Advancements in Fabrication of Metal Matrix Composites: A Systematic Review, *Materials*, 2024, **17**, 4635, DOI: [10.3390/ma17184635](https://doi.org/10.3390/ma17184635).

86 N. E. Putra, K. G. N. Borg, P. J. Diaz-Payne, M. A. Leeflang, M. Klimopoulou, P. Taheri, J. M. C. Mol, L. E. Fratila-Apachitei, Z. Huan, J. Chang, J. Zhou and A. A. Zadpoor, Additive Manufacturing of Bioactive and Biodegradable Porous Iron-Akermanite Composites for Bone Regeneration, *Acta Biomater.*, 2022, **148**, 355–373, DOI: [10.1016/j.actbio.2022.06.009](https://doi.org/10.1016/j.actbio.2022.06.009).

87 M. A. Meyers and K. K. Chawla, *Mechanical Behavior of Materials*, 2008, DOI: [10.1017/cbo9780511810947](https://doi.org/10.1017/cbo9780511810947).

88 T. Karachalios, *Bone-Implant Interface in Orthopedic Surgery: Basic Science to Clinical Applications*, 2013, 9781447154099, pp. 1–342, DOI: [10.1007/978-1-4471-5409-9/COVER](https://doi.org/10.1007/978-1-4471-5409-9/COVER).

89 S. H. Teoh, Fatigue of Biomaterials: A Review, *Int. J. Fatigue*, 2000, **22**(10), 825–837, DOI: [10.1016/S0142-1123\(00\)00052-9](https://doi.org/10.1016/S0142-1123(00)00052-9).

90 E. F. Morgan, G. U. Unnikrisnan and A. I. Hussein, Bone Mechanical Properties in Healthy and Diseased States, *Annu. Rev. Biomed. Eng.*, 2018, **20**, 119, DOI: [10.1146/annurev-bioeng-062117-121139](https://doi.org/10.1146/annurev-bioeng-062117-121139).

91 F. Witte, N. Hort, C. Vogt, S. Cohen, K. U. Kainer, R. Willumeit and F. Feyerabend, Degradable Biomaterials Based on Magnesium Corrosion, *Curr. Opin. Solid State Mater. Sci.*, 2008, **12**(5–6), 63–72, DOI: [10.1016/j.coress.2009.04.001](https://doi.org/10.1016/j.coress.2009.04.001).

92 A. Anvari, Characterization of Implantation's Biomaterials Based on the Patient and Doctor Expectations, *Res. Med. Eng. Sci.*, 2018, **4**(2), 583, DOI: [10.31031/rmes.2018.04.000583](https://doi.org/10.31031/rmes.2018.04.000583).

93 *Handbook of Biomaterial Properties*, ed W. Murphy, J. Black, G. Hastings, 2nd edn, 2016, DOI: [10.1007/978-1-4615-5801-9](https://doi.org/10.1007/978-1-4615-5801-9).

94 N. Wegner, M. Klein, R. Scholz, D. Kotzem, M. Macias Barrientos and F. Walther, Mechanical *in Vitro* Fatigue Testing of Implant Materials and Components Using Advanced Characterization Techniques, *J. Biomed. Mater. Res. B*, 2022, **110**(4), 898–909, DOI: [10.1002/jbm.b.34970](https://doi.org/10.1002/jbm.b.34970).

95 C. Fleck and D. Eifler, Corrosion, Fatigue and Corrosion Fatigue Behaviour of Metal Implant Materials, Especially Titanium Alloys, *Int. J. Fatigue*, 2010, **32**(6), 929–935, DOI: [10.1016/j.ijfatigue.2009.09.009](https://doi.org/10.1016/j.ijfatigue.2009.09.009).

96 C. Garot, G. Bettega and C. Picart, Additive Manufacturing of Material Scaffolds for Bone Regeneration: Toward Application in the Clinics, *Adv. Funct. Mater.*, 2021, **31**(5), 2006967, DOI: [10.1002/adfm.202006967](https://doi.org/10.1002/adfm.202006967).

97 A. Mostafaei, A. M. Elliott, J. E. Barnes, F. Li, W. Tan, C. L. Cramer, P. Nandwana and M. Chmielus, Binder Jet 3D Printing—Process Parameters, Materials, Properties, Modeling, and Challenges, *Prog. Mater. Sci.*, 2021, **119**, 100707, DOI: [10.1016/j.pmatsci.2020.100707](https://doi.org/10.1016/j.pmatsci.2020.100707).

98 H. Hegab, N. Khanna, N. Monib and A. Salem, Design for Sustainable Additive Manufacturing: A Review, *Sustainable Mater. Technol.*, 2023, **35**, e00576, DOI: [10.1016/j.susmat.2023.e00576](https://doi.org/10.1016/j.susmat.2023.e00576).

99 ISO/ASTM 52900:2021 - Additive Manufacturing—General Principles—Fundamentals and Vocabulary; 2021. <https://www.iso.org/standard/74514.html> (accessed 2025-08-21).

100 K. S. Prakash, T. Nancharaih and V. V. S. Rao, Additive Manufacturing Techniques in Manufacturing -An Overview, *Mater. Today Proc.*, 2018, **5**(2), 3873–3882, DOI: [10.1016/j.matpr.2017.11.642](https://doi.org/10.1016/j.matpr.2017.11.642).

101 A. Jadhav and V. S. Jadhav, A Review on 3D Printing: An Additive Manufacturing Technology, *Mater. Today Proc.*, 2022, **62**, 2094–2099, DOI: [10.1016/j.matpr.2022.02.558](https://doi.org/10.1016/j.matpr.2022.02.558).

102 R. Alfattni, Comprehensive Study on Materials Used in Different Types of Additive Manufacturing and Their Applications, *Int. J. Math. Eng. Manage. Sci.*, 2022, **7**(1), 92–114, DOI: [10.33888/ijmems.2022.7.1.007](https://doi.org/10.33888/ijmems.2022.7.1.007).

103 A. Nazir, K. M. Abate, A. Kumar and J. Y. Jeng, A State-of-the-Art Review on Types, Design, Optimization, and Additive Manufacturing of Cellular Structures, *Int. J. Adv. Des. Manuf. Technol.*, 2019, **104**(9), 3489–3510, DOI: [10.1007/s00170-019-04085-3](https://doi.org/10.1007/s00170-019-04085-3).

104 P. K. S, A. K, H. C. S and K. M. S, Review on Surface Characteristics of Components Produced by Direct Metal Deposition Process, *J. Mech. Eng. Sci.*, 2022, **16**, 9197–9229, DOI: [10.15282/jmes.16.4.2022.05.0729](https://doi.org/10.15282/jmes.16.4.2022.05.0729).

105 R. Lakraimi, H. Abouchadi and M. T. Janan, Modeling the Physics of Selective Laser Sintering Using the Discrete



Element Method, *Int. J. Comput. Methods Exp. Meas.*, 2024, **12**(1), 21–33, DOI: [10.18280/IJCMEM.120103](https://doi.org/10.18280/IJCMEM.120103).

106 L. E. Murr and S. M. Gaytan, *Electron Beam Melting. Comprehensive Materials Processing: Thirteen Volume Set*, 2014, vol. 10, pp. V10-135–V10-161, DOI: [10.1016/B978-0-08-096532-1.01004-9](https://doi.org/10.1016/B978-0-08-096532-1.01004-9).

107 L. B. Said, B. Ayadi, S. Alharbi and F. Dammak, Recent Advances in Additive Manufacturing: A Review of Current Developments and Future Directions, *Machines*, 2025, **13**(9), 813, DOI: [10.3390/MACHINES13090813](https://doi.org/10.3390/MACHINES13090813).

108 S. C. Altiparmak, V. A. Yardley, Z. Shi and J. Lin, Extrusion-Based Additive Manufacturing Technologies: State of the Art and Future Perspectives, *J. Manuf. Process.*, 2022, **83**, 607–636, DOI: [10.1016/j.jmapro.2022.09.032](https://doi.org/10.1016/j.jmapro.2022.09.032).

109 J. P. Kruth, Material Ingress Manufacturing by Rapid Prototyping Techniques, *CIRP Ann.*, 1991, **40**(2), 603–614, DOI: [10.1016/s0007-8506\(07\)61136-6](https://doi.org/10.1016/s0007-8506(07)61136-6).

110 E. O. Olakanmi, R. F. Cochrane and K. W. Dalgarno, A Review on Selective Laser Sintering/Melting (SLS/SLM) of Aluminium Alloy Powders: Processing, Microstructure, and Properties, *Prog. Mater. Sci.*, 2015, **74**, 401–477, DOI: [10.1016/j.pmatsci.2015.03.002](https://doi.org/10.1016/j.pmatsci.2015.03.002).

111 N. Bastola, M. P. Jahan, N. Rangasamy and C. S. Rakurty, A Review of the Residual Stress Generation in Metal Additive Manufacturing: Analysis of Cause, Measurement, Effects, and Prevention, *Micromachines*, 2023, **14**, 1480, DOI: [10.3390/mi14071480](https://doi.org/10.3390/mi14071480).

112 S. L. Campanelli, N. Contuzzi, A. Angelastro and A. D. Ludovico, Capabilities and Performances of the Selective Laser Melting Process, in *New Trends in Technologies - Devices, Computer, Communication and Industrial Systems*, ed. Z. Lian, IntechOpen, 2010, DOI: [10.5772/10432](https://doi.org/10.5772/10432).

113 E. O. Olakanmi, Selective Laser Sintering/Melting (SLS/SLM) of Pure Al, Al-Mg, and Al-Si Powders: Effect of Processing Conditions and Powder Properties, *J. Mater. Process Technol.*, 2013, **213**(8), 1387–1405, DOI: [10.1016/j.jmatprotec.2013.03.009](https://doi.org/10.1016/j.jmatprotec.2013.03.009).

114 P. K. Gokuldoss, S. Kolla and J. Eckert, Additive Manufacturing Processes: Selective Laser Melting, Electron Beam Melting and Binder Jetting—Selection Guidelines, *Materials*, 2017, **10**, 672, DOI: [10.3390/ma10060672](https://doi.org/10.3390/ma10060672).

115 E. O. Olakanmi, R. F. Cochrane and K. W. Dalgarno, A Review on Selective Laser Sintering/Melting (SLS/SLM) of Aluminium Alloy Powders: Processing, Microstructure, and Properties, *Prog Mater Sci*, 2015, **74**, 401–477, DOI: [10.1016/j.pmatsci.2015.03.002](https://doi.org/10.1016/j.pmatsci.2015.03.002).

116 A. Popovich and V. Sufiarov, Metal Powder Additive Manufacturing, *New Trends in 3D Printing*, 2016, DOI: [10.5772/63337](https://doi.org/10.5772/63337).

117 P. Muthuswamy, Influence of Powder Characteristics on Properties of Parts Manufactured by Metal Additive Manufacturing, *Lasers Manuf. Mater. Process.*, 2022, **9**(3), 312–337, DOI: [10.1007/s40516-022-00177-3/figures/12](https://doi.org/10.1007/s40516-022-00177-3/figures/12).

118 P. Dixit and A. Suhane, A Comprehensive Review on Selective Laser Melting of Aluminium Matrix Composites Reinforced with Silicon Carbide Spark Plasma Sintering HIP Hot Isostatic Pressing CTE Coefficient of Thermal Expansion PM Powder Metallurgy, *Prog. Addit. Manuf.*, 2025, **10**, 4419–4445, DOI: [10.1007/s40964-024-00883-8](https://doi.org/10.1007/s40964-024-00883-8).

119 S. Dadbakhsh; R. Mertens; L. Hao; J. Van Humbeeck and J. P. Kruth, Selective Laser Melting to Manufacture “In Situ” Metal Matrix Composites: A Review, *Advanced Engineering Materials*, Wiley-VCH Verlag, 2019, DOI: [10.1002/adem.201801244](https://doi.org/10.1002/adem.201801244).

120 S. C. Tjong and Z. Y. Ma, Microstructural and Mechanical Characteristics of in Situ Metal Matrix Composites, *Mater. Sci. Eng. R. Rep.*, 2000, **29**(3–4), 49–113, DOI: [10.1016/S0927-796X\(00\)00024-3](https://doi.org/10.1016/S0927-796X(00)00024-3).

121 L. C. Zhang and H. Attar, Selective Laser Melting of Titanium Alloys and Titanium Matrix Composites for Biomedical Applications: A Review, *Adv. Eng. Mater.*, 2016, 463–475, DOI: [10.1002/adem.201500419](https://doi.org/10.1002/adem.201500419).

122 C. Han, R. Babicheva, J. D. Q. Chua, U. Ramamurty, S. B. Tor, C. N. Sun and K. Zhou, Microstructure and Mechanical Properties of (TiB + TiC)/Ti Composites Fabricated in Situ via Selective Laser Melting of Ti and B4C Powders, *Addit. Manuf.*, 2020, **36**, 101466, DOI: [10.1016/j.addma.2020.101466](https://doi.org/10.1016/j.addma.2020.101466).

123 Y. Yang, X. Guo, C. He, C. Gao and C. Shuai, Regulating Degradation Behavior by Incorporating Mesoporous Silica for Mg Bone Implants, *ACS Biomater. Sci. Eng.*, 2018, **4**(3), 1046–1054, DOI: [10.1021/acsbiomaterials.8b00020](https://doi.org/10.1021/acsbiomaterials.8b00020).

124 Y. Zhang, Y. Yu, L. Wang, Y. Li, F. Lin and W. Yan, Dispersion of Reinforcing Micro-Particles in the Powder Bed Fusion Additive Manufacturing of Metal Matrix Composites, *Acta Mater.*, 2022, **235**, DOI: [10.1016/j.actamat.2022.118086](https://doi.org/10.1016/j.actamat.2022.118086).

125 C. Körner, Additive Manufacturing of Metallic Components by Selective Electron Beam Melting—a Review, *Int. Mater. Rev.*, 2016, **61**(5), 361–377, DOI: [10.1080/09506608.2016.1176289](https://doi.org/10.1080/09506608.2016.1176289).

126 J. A. Tamayo, M. Riascos, C. A. Vargas and L. M. Baena, Additive Manufacturing of Ti6Al4V Alloy via Electron Beam Melting for the Development of Implants for the Biomedical Industry, *Heliyon*, 2021, **7**(5), e06892, DOI: [10.1016/j.heliyon.2021.e06892](https://doi.org/10.1016/j.heliyon.2021.e06892).

127 A. I. Mertens; J. Lecomte-Beckers; A. I. Mertens and J. Lecomte-Beckers, On the Role of Interfacial Reactions, Dissolution and Secondary Precipitation During the Laser Additive Manufacturing of Metal Matrix Composites: A Review, *New Trends in 3D Printing*, 2016, DOI: [10.5772/63045](https://doi.org/10.5772/63045).

128 D. D. Gu, W. Meiners, K. Wissenbach and R. Poprawe, Laser Additive Manufacturing of Metallic Components: Materials, Processes and Mechanisms, *Int. Mater. Rev.*, 2012, **57**(3), 133–164, DOI: [10.1179/1743280411Y.0000000014](https://doi.org/10.1179/1743280411Y.0000000014).

129 M. Ostolaza, J. I. Arrizubieta, A. Lamikiz, S. Plaza and N. Ortega, Latest Developments to Manufacture Metal Matrix Composites and Functionally Graded Materials through AM: A State-of-the-Art Review, *Materials*, 2023, **16**(4), 1746, DOI: [10.3390/MA16041746](https://doi.org/10.3390/MA16041746).

130 G. Muvvala, D. Patra Karmakar and A. K. Nath, Monitoring and Assessment of Tungsten Carbide Wettability in Laser



Cladded Metal Matrix Composite Coating Using an IR Pyrometer, *J. Alloys Compd.*, 2017, **714**, 514–521, DOI: [10.1016/j.jallcom.2017.04.254](https://doi.org/10.1016/j.jallcom.2017.04.254).

131 M. A. Mahmood, A. C. Popescu and I. N. Mihailescu, Metal Matrix Composites Synthesized by Laser-Melting Deposition: A Review, *Materials*, 2020, **13**(11), 2593, DOI: [10.3390/MA13112593](https://doi.org/10.3390/MA13112593).

132 S. Mihai, F. Baciu, R. Radu, D. Chioibasu and A. C. Popescu, In Situ Fabrication of TiC/Ti-Matrix Composites by Laser Directed Energy Deposition, *Materials*, 2024, **17**(17), 4284, DOI: [10.3390/MA17174284](https://doi.org/10.3390/MA17174284).

133 D. G. Ahn, Directed Energy Deposition (DED) Process: State of the Art, *Int. J. Pr. Eng. Manuf. Green Technol.*, 2021, **8**(2), 703–742, DOI: [10.1007/S40684-020-00302-7](https://doi.org/10.1007/S40684-020-00302-7).

134 B. Onuike, B. Heer and A. Bandyopadhyay, Additive Manufacturing of Inconel 718—Copper Alloy Bimetallic Structure Using Laser Engineered Net Shaping (LENS<sup>TM</sup>), *Addit. Manuf.*, 2018, **21**, 133–140, DOI: [10.1016/j.addma.2018.02.007](https://doi.org/10.1016/j.addma.2018.02.007).

135 K. Zhao, Z. Su, Z. Ye, W. Cao, J. Pang, X. Wang, Z. Wang, X. Xu and J. Zhu, Review of the Types, Formation Mechanisms, Effects, and Elimination Methods of Binder Jetting 3D-Printing Defects, *J. Mater. Res. Technol.*, 2023, **27**, 5449–5469, DOI: [10.1016/j.jmrt.2023.11.045](https://doi.org/10.1016/j.jmrt.2023.11.045).

136 E. Sachs, M. Cima and J. Cornie, Three-Dimensional Printing: Rapid Tooling and Prototypes Directly from a CAD Model, *CIRP Annals*, 1990, **39**(1), 201–204, DOI: [10.1016/S0007-8506\(07\)61035-X](https://doi.org/10.1016/S0007-8506(07)61035-X).

137 *Three-dimensional printing techniques*, Google Patents, US5204055A, <https://patents.google.com/patent/US5204055A/en> (accessed 2024-08-22).

138 D. A. Snelling, C. B. Williams, C. T. A. Suchit and A. P. Druschitz, Binder Jetting Advanced Ceramics for Metal-Ceramic Composite Structures, *Int. J. Adv. Manuf. Technol.*, 2017, **92**(1–4), 531–545, DOI: [10.1007/s00170-017-0139-y](https://doi.org/10.1007/s00170-017-0139-y)/metrics.

139 D. Gilmer, L. Han, E. Hong, D. Siddle, A. Kisliuk, S. Cheng, D. Brunermer, A. Elliott and T. Saito, An In-Situ Crosslinking Binder for Binder Jet Additive Manufacturing, *Addit. Manuf.*, 2020, **35**, 101341, DOI: [10.1016/j.addma.2020.101341](https://doi.org/10.1016/j.addma.2020.101341).

140 P. D. Enrique, Y. Mahmoodkhani, E. Marzbanrad, E. Toyserkani and N. Y. Zhou, In Situ Formation of Metal Matrix Composites Using Binder Jet Additive Manufacturing (3D Printing, *Mater. Lett.*, 2018, **232**, 179–182, DOI: [10.1016/j.matlet.2018.08.117](https://doi.org/10.1016/j.matlet.2018.08.117).

141 A. Borisov, A. Shamshurin, M. Kovalev, A. Popovich and V. Sufiilarov, Binder Jetting Additive Manufacturing of Inconel 718/TiC Metal Matrix Composites: Influence of TiC Content on Processing, Microstructure, Mechanical and Tribological Properties, *Materials*, 2024, **17**(20), 5050, DOI: [10.3390/ma17205050](https://doi.org/10.3390/ma17205050).

142 J. R. Poulin, A. Kreitberg, P. Terriault and V. Brailovski, Long Fatigue Crack Propagation Behavior of Laser Powder Bed-Fused Inconel 625 with Intentionally-Seeded Porosity, *Int. J. Fatigue*, 2019, **127**, 144–156, DOI: [10.1016/j.ijfatigue.2019.06.008](https://doi.org/10.1016/j.ijfatigue.2019.06.008).

143 M. Salarian, H. Asgari and M. Vlasea, Pore Space Characteristics and Corresponding Effect on Tensile Properties of Inconel 625 Fabricated via Laser Powder Bed Fusion, *Mater. Sci. Eng. A*, 2020, **769**, 138525, DOI: [10.1016/j.msea.2019.138525](https://doi.org/10.1016/j.msea.2019.138525).

144 A. Leicht, M. Rashidi, U. Klement and E. Hryha, Effect of Process Parameters on the Microstructure, Tensile Strength and Productivity of 316L Parts Produced by Laser Powder Bed Fusion, *Mater. Charact.*, 2020, **159**, 110016, DOI: [10.1016/j.matchar.2019.110016](https://doi.org/10.1016/j.matchar.2019.110016).

145 K. Rane, M. Strano, K. Rane and M. Strano, A Comprehensive Review of Extrusion-Based Additive Manufacturing Processes for Rapid Production of Metallic and Ceramic Parts A Comprehensive Review of Extrusion Based Additive Manufacturing Processes for Rapid Production of Metallic and Ceramic Parts, *Adv. Manuf.*, 2019, **7**, 155–173, DOI: [10.1007/s40436-019-00253-6](https://doi.org/10.1007/s40436-019-00253-6).

146 M. Strano, K. Rane, M. A. Farid, V. Mussi, V. Zaragoza and M. Monno, Extrusion-Based Additive Manufacturing of Forming and Molding Tools, *Int. J. Adv. Manuf. Technol.*, 2021, **117**(7–8), 2059–2071, DOI: [10.1007/s00170-021-07162-8](https://doi.org/10.1007/s00170-021-07162-8)/figures/18.

147 K. Rane and M. Strano, A Comprehensive Review of Extrusion-Based Additive Manufacturing Processes for Rapid Production of Metallic and Ceramic Parts, *Adv. Manuf.*, 2019, **7**(2), 155–173, DOI: [10.1007/s40436-019-00253-6](https://doi.org/10.1007/s40436-019-00253-6)/figures/12.

148 C. Suwanpreecha and A. Manonukul, A Review on Material Extrusion Additive Manufacturing of Metal and How It Compares with Metal Injection Moulding, *Metals*, 2022, **12**(3), 429, DOI: [10.3390/met12030429](https://doi.org/10.3390/met12030429).

149 A. Patel and M. Taufik, Extrusion-Based Technology in Additive Manufacturing: A Comprehensive Review, *Arabian J. Sci. Eng.*, 2022, **49**(2), 1309–1342, DOI: [10.1007/S13369-022-07539-1](https://doi.org/10.1007/S13369-022-07539-1).

150 J. Brackett, D. Cauthen, J. Condon, T. Smith, N. Gallego, V. Kunc and C. Duty, The Impact of Infill Percentage and Layer Height in Small-Scale Material Extrusion on Porosity and Tensile Properties, *Addit. Manuf.*, 2022, **58**, 103063, DOI: [10.1016/j.addma.2022.103063](https://doi.org/10.1016/j.addma.2022.103063).

151 D. Hong, D. T. Chou, O. I. Velikokhatnyi, A. Roy, B. Lee, I. Swink, I. Issaev, H. A. Kuhn and P. N. Kumta, Binder-Jetting 3D Printing and Alloy Development of New Biodegradable Fe-Mn-Ca/Mg Alloys, *Acta Biomater.*, 2016, **45**, 375–386, DOI: [10.1016/j.actbio.2016.08.032](https://doi.org/10.1016/j.actbio.2016.08.032).

152 M. P. Behera, T. Dougherty and S. Singarneni, Conventional and Additive Manufacturing with Metal Matrix Composites: A Perspective, *Proc. Manuf.*, 2019, **30**, 159–166, DOI: [10.1016/j.promfg.2019.02.023](https://doi.org/10.1016/j.promfg.2019.02.023).

153 L. Ceschini and R. Montanari, *Advances in Metal Matrix Composites*, 2011, p. 678, DOI: [10.4028/b-hs0j1s](https://doi.org/10.4028/b-hs0j1s).

154 S. K. Sharma, K. K. Saxena, K. H. Salem, K. A. Mohammed, R. Singh and C. Prakash, Effects of Various Fabrication Techniques on the Mechanical Characteristics of Metal Matrix Composites: A Review, *Adv. Mater. Process. Technol.*, 2024, **10**(2), 277–294, DOI: [10.1080/2374068x.2022.2144276](https://doi.org/10.1080/2374068x.2022.2144276).



155 W. C. Liu, H. W. Chang, S. I. Huang, K. Y. Yang, P. I. Tsai, C. H. Chen, Y. H. Wang, C. H. Ma, C. Y. Chen and Y. C. Fu, Biodegradable Porous Iron versus Titanium Interference Screws in Porcine ACL Reconstruction Model: A One-Year Observational Study, *Npj Mater. Degrad.*, 2025, **9**(1), 1–11, DOI: [10.1038/S41529-025-00602-W](https://doi.org/10.1038/S41529-025-00602-W) SUBJMETA = 54,61,631,990, 993; KWRD = BIOMEDICAL + MATERIALS, IMPLANTS.

156 K. Palka and R. Pokrowiecki, Porous Titanium Implants: A Review, *Adv. Eng. Mater.*, 2018, **20**(5), 1700648, DOI: [10.1002/adem.201700648](https://doi.org/10.1002/adem.201700648).

157 M. V. Kiselevskiy, N. Y. Anisimova, A. V. Kapustin, A. A. Ryzhkin, D. N. Kuznetsova, V. V. Polyakova and N. A. Enikeev, Development of Bioactive Scaffolds for Orthopedic Applications by Designing Additively Manufactured Titanium Porous Structures: A Critical Review, *Biomimetics*, 2023, **8**(7), 546, DOI: [10.3390/biomimetics8070546](https://doi.org/10.3390/biomimetics8070546).

158 Q. Han, C. Wang, H. Chen, X. Zhao and J. Wang, Porous Tantalum and Titanium in Orthopedics: A Review, *ACS Biomater. Sci. Eng.*, 2019, **5**(11), 5798–5824.

159 G. Kumar, E. Karakulak, M. Aikin, V. Shalomeev, V. Kukhar, A. Kostryzhev, I. Kuziev, V. Kulynych, O. Dykha, V. Dytyniuk, O. Shapoval, A. Zagorskis, V. Burko, O. Khliestova, V. Titov and O. Hrushko, Recent Advances in Biodegradable Magnesium Alloys for Medical Implants: Evolution, Innovations, and Clinical Translation, *Crystals*, 2025, **15**(8), 671, DOI: [10.3390/cryst15080671](https://doi.org/10.3390/cryst15080671).

160 X. N. Gu and Y. F. Zheng, A Review on Magnesium Alloys as Biodegradable Materials, *Front. Mater. Sci. China*, 2010, **4**(2), 111–115, DOI: [10.1007/S11706-010-0024-1](https://doi.org/10.1007/S11706-010-0024-1).

161 M. P. Staiger, A. M. Pietak, J. Huadmai and G. Dias, Magnesium and Its Alloys as Orthopedic Biomaterials: A Review, *Biomaterials*, 2006, **27**(9), 1728–1734, DOI: [10.1016/j.biomaterials.2005.10.003](https://doi.org/10.1016/j.biomaterials.2005.10.003).

162 N. Wang, Y. Ma, H. Shi, Y. Song, S. Guo and S. Yang, Mg-, Zn-, and Fe-Based Alloys With Antibacterial Properties as Orthopedic Implant Materials, *Front. Bioeng. Biotechnol.*, 2022, **10**, 888084, DOI: [10.3389/fbioe.2022.888084/xml](https://doi.org/10.3389/fbioe.2022.888084/xml).

163 M. Salama, M. F. Vaz, R. Colaço, C. Santos and M. Carmezim, Biodegradable Iron and Porous Iron: Mechanical Properties, Degradation Behaviour, Manufacturing Routes and Biomedical Applications, *J. Funct. Biomater.*, 2022, **13**(2), 72, DOI: [10.3390/jfb13020072](https://doi.org/10.3390/jfb13020072).

164 V. P. M. Rabeeh and T. Hanas, Progress in Manufacturing and Processing of Degradable Fe-Based Implants: A Review, *Prog. Biomater.*, 2022, **11**(2), 163, DOI: [10.1007/S40204-022-00189-4](https://doi.org/10.1007/S40204-022-00189-4).

165 J. Li, H. Yuan, A. Chandrakar, L. Moroni and P. Habibovic, 3D Porous Ti6Al4V-Beta-Tricalcium Phosphate Scaffolds Directly Fabricated by Additive Manufacturing, *Acta Biomater.*, 2021, **126**, 496–510, DOI: [10.1016/j.actbio.2021.03.021](https://doi.org/10.1016/j.actbio.2021.03.021).

166 F. H. Liu; R. T. Lee; W. H. Lin and Y. S. Liao, Selective Laser Sintering of Bio-Metal Scaffold. In *Procedia CIRP*, Elsevier B. V., 2013, Vol. 5, pp. 83–87, DOI: [10.1016/j.procir.2013.01.017](https://doi.org/10.1016/j.procir.2013.01.017).

167 T. Yi, C. Zhou, L. Ma, L. Wu, X. Xu, L. Gu, Y. Fan, G. Xian, H. Fan and X. Zhang, Direct 3-D Printing of Ti-6Al-4V/HA Composite Porous Scaffolds for Customized Mechanical Properties and Biological Functions, *J. Tissue Eng. Regen. Med.*, 2020, **14**(3), 486–496, DOI: [10.1002/term.3013](https://doi.org/10.1002/term.3013).

168 S. Park, J. Lee, J. J. Kim, M. Ji, E. Cho, H. B. Sim, Y. T. Chang, J. H. Chung, M. J. Paik, J. Kim and H. Seonwoo, Osseointegrative and Immunomodulative 3D-Printing Ti6Al4V-Based Implants Embedded with Biogenic Hydroxyapatite, *Mater. Des.*, 2024, **240**, DOI: [10.1016/j.matdes.2024.112822](https://doi.org/10.1016/j.matdes.2024.112822).

169 Y. Yin, Q. Huang, L. Liang, X. Hu, T. Liu, Y. Weng, T. Long, Y. Liu, Q. Li, S. Zhou and H. Wu, In Vitro Degradation Behavior and Cytocompatibility of ZK30/Bioactive Glass Composites Fabricated by Selective Laser Melting for Biomedical Applications, *J. Alloys Compd.*, 2019, **785**, 38–45, DOI: [10.1016/j.jallcom.2019.01.165](https://doi.org/10.1016/j.jallcom.2019.01.165).

170 Y. Yang, C. Lu, L. Shen, Z. Zhao, S. Peng and C. Shuai, In-Situ Deposition of Apatite Layer to Protect Mg-Based Composite Fabricated via Laser Additive Manufacturing, *J. Magn. Alloys*, 2023, **11**(2), 629–640, DOI: [10.1016/j.jma.2021.04.009](https://doi.org/10.1016/j.jma.2021.04.009).

171 J. Dong, P. Lin, N. E. Putra, N. Tümer, M. A. Leeflang, Z. Huan, L. E. Fratila-Apachitei, J. Chang, A. A. Zadpoor and J. Zhou, Extrusion-Based Additive Manufacturing of Mg-Zn/Bioceramic Composite Scaffolds, *Acta Biomater.*, 2022, **151**, 628–646, DOI: [10.1016/j.actbio.2022.08.002](https://doi.org/10.1016/j.actbio.2022.08.002).

172 H. Ma, T. Li, Z. Huan, M. Zhang, Z. Yang, J. Wang, J. Chang and C. Wu, 3D Printing of High-Strength Bioscaffolds for the Synergistic Treatment of Bone Cancer, *NPG Asia Mater.*, 2018, **10**(4), 31–44, DOI: [10.1038/s41427-018-0015-8](https://doi.org/10.1038/s41427-018-0015-8).

173 C. Shuai, Y. Li, Y. Yang, S. Peng, W. Yang, F. Qi, S. Xiong, H. Liang and L. Shen, Bioceramic Enhances the Degradation and Bioactivity of Iron Bone Implant, *Mater. Res. Express*, 2019, **6**(11), 115401, DOI: [10.1088/2053-1591/ab45b9](https://doi.org/10.1088/2053-1591/ab45b9).

174 C. Gao, M. Yao, S. Li, P. Feng, S. Peng and C. Shuai, Highly Biodegradable and Bioactive Fe-Pd-Bredigite Biocomposites Prepared by Selective Laser Melting, *J. Adv. Res.*, 2019, **20**, 91–104, DOI: [10.1016/j.jare.2019.06.001](https://doi.org/10.1016/j.jare.2019.06.001).

175 A. Markowska-Szczupak, M. Endo-Kimura, O. Paszkiewicz and E. Kowalska, Are Titania Photocatalysts and Titanium Implants Safe? Review on the Toxicity of Titanium Compounds, *Nanomaterials*, 2020, **10**(10), 2065, DOI: [10.3390/nano10102065](https://doi.org/10.3390/nano10102065).

176 K. T. Kim, M. Y. Eo, T. T. H. Nguyen and S. M. Kim, General Review of Titanium Toxicity, *Int. J. Implant Dent.*, 2019, **5**(1), 1–12, DOI: [10.1186/S40729-019-0162-X](https://doi.org/10.1186/S40729-019-0162-X).

177 D. M. Vasconcelos, S. G. Santos, M. Lamghari and M. A. Barbosa, The Two Faces of Metal Ions: From Implants Rejection to Tissue Repair/Regeneration, *Biomaterials*, 2016, **84**, 262–275, DOI: [10.1016/j.biomaterials.2016.01.046](https://doi.org/10.1016/j.biomaterials.2016.01.046).

178 D. G. Olmedo, D. Tasat, M. B. Guglielmotti and R. L. Cabrini, Titanium Transport through the Blood Stream. An Experimental Study on Rats, *J. Mater. Sci. Mater. Med.*, 2003, **14**(12), 1099–1103, DOI: [10.1023/b:bjmsm.0000004007.26938.67/metrics](https://doi.org/10.1023/b:bjmsm.0000004007.26938.67/metrics).

179 P. D. Bianco, P. Ducheyne and J. M. Cuckler, Systemic Titanium Levels in Rabbits with a Titanium Implant in the



Absence of Wear, *J. Mater. Sci. Mater. Med.*, 1997, **8**(9), 525–529, DOI: [10.1023/a:1018590513178/metrics](https://doi.org/10.1023/a:1018590513178).

180 C. Rehbock, J. Jakobi, L. Gamrad, S. van der Meer, D. Tiedemann, U. Taylor, W. Kues, D. Rath and S. Barcikowski, Current State of Laser Synthesis of Metal and Alloy Nanoparticles as Ligand-Free Reference Materials for Nano-Toxicological Assays, *Beilstein J. Nanotechnol.*, 2014, **5**(1), 1523–1541, DOI: [10.3762/bjnano.5.165](https://doi.org/10.3762/bjnano.5.165).

181 P. D. Bianco, J. P. Ducheyne and J. M. Cuckle, Local Accumulation of Titanium Released from a Titanium Implant in the Absence of Wear, 1996, **31**, 227–234, DOI: [10.1002/\(sici\)1097-4636\(199606\)31:2](https://doi.org/10.1002/(sici)1097-4636(199606)31:2).

182 P. D. Bianco, P. Ducheyne and J. M. Cuckle, Titanium Serum and Urine Levels in Rabbits with a Titanium Implant in the Absence of Wear, *Biomaterials*, 1996, **17**(20), 1937–1942, DOI: [10.1016/0142-9612\(96\)00023-3](https://doi.org/10.1016/0142-9612(96)00023-3).

183 C. B. Danoux, D. Barbieri, H. Yuan, J. D. Bruijn, C. A. de; Blitterswijk and P. van; Habibovic, *In Vitro* and *In Vivo* Bioactivity Assessment of a Polylactic Acid/Hydroxyapatite Composite for Bone Regeneration, *Biomater*, 2014, **4**, e27664, DOI: [10.4161/biom.27664](https://doi.org/10.4161/biom.27664).

184 H. Yuan, H. Fernandes, P. Habibovic, J. De Boer, A. M. C. Barradas, A. De Ruiter, W. R. Walsh, C. A. Van Blitterswijk and J. D. De Bruijn, Osteoinductive Ceramics as a Synthetic Alternative to Autologous Bone Grafting, *Proc. Natl. Acad. Sci. U. S. A.*, 2010, **107**(31), 13614–13619, DOI: [10.1073/pnas.1003600107/suppl\\_file/pnas.1003600107\\_si.pdf](https://doi.org/10.1073/pnas.1003600107/suppl_file/pnas.1003600107_si.pdf).

185 H. Lu, Y. Zhou, Y. Ma, L. Xiao, W. Ji, Y. Zhang and X. Wang, Current Application of Beta-Tricalcium Phosphate in Bone Repair and Its Mechanism to Regulate Osteogenesis, *Front. Mater.*, 2021, **8**, 698915, DOI: [10.3389/fmats.2021.698915/bibtext](https://doi.org/10.3389/fmats.2021.698915).

186 P. C. Banerjee, S. Al-Saadi, L. Choudhary, S. E. Harandi and R. Singh, Magnesium Implants: Prospects and Challenges, *Materials*, 2019, **12**, 136, DOI: [10.3390/ma12010136](https://doi.org/10.3390/ma12010136).

187 F. Witte, The History of Biodegradable Magnesium Implants: A Review, *Acta Biomater.*, 2010, **6**(5), 1680–1692, DOI: [10.1016/j.actbio.2010.02.028](https://doi.org/10.1016/j.actbio.2010.02.028).

188 X. Liu, S. Lu, T. Wang, X. Wang, K. Yang and H. Yang, Advances and Prospects of 3D Printed Antibacterial Bone Implants: A Systematic Review, *J. Mater. Sci. Technol.*, 2024, 227–242, DOI: [10.1016/j.jmst.2024.02.040](https://doi.org/10.1016/j.jmst.2024.02.040).

189 D. Noviana, D. Paramitha, M. F. Ulum and H. Hermawan, The Effect of Hydrogen Gas Evolution of Magnesium Implant on the Postimplantation Mortality of Rats, *J. Orthop. Translat.*, 2016, **5**, 9–15, DOI: [10.1016/j.jot.2015.08.003](https://doi.org/10.1016/j.jot.2015.08.003).

190 J. Kuhlmann, I. Bartsch, E. Willbold, S. Schuchardt, O. Holz, N. Hort, D. Höche, W. R. Heineman and F. Witte, Fast Escape of Hydrogen from Gas Cavities around Corroding Magnesium Implants, *Acta Biomater.*, 2013, **9**(10), 8714–8721, DOI: [10.1016/j.actbio.2012.10.008](https://doi.org/10.1016/j.actbio.2012.10.008).

191 Y. K. Kim, K. B. Lee, S. Y. Kim, K. Bode, Y. S. Jang, T. Y. Kwon, M. H. Jeon and M. H. Lee, Gas Formation and Biological Effects of Biodegradable Magnesium in a Preclinical and Clinical Observation, *Sci. Technol. Adv. Mater.*, 2018, **19**(1), 324, DOI: [10.1080/14686996.2018.1451717](https://doi.org/10.1080/14686996.2018.1451717).

192 R. K. Singh Raman and S. E. Harandi, Resistance of Magnesium Alloys to Corrosion Fatigue for Biodegradable Implant Applications: Current Status and Challenges, *Materials*, 2017, **10**(11), 1316, DOI: [10.3390/ma10111316](https://doi.org/10.3390/ma10111316).

193 M. Kappes, M. Iannuzzi and R. M. Carranza, Hydrogen Embrittlement of Magnesium and Magnesium Alloys: A Review, *J. Electrochem. Soc.*, 2013, **160**(4), C168–C178, DOI: [10.1149/2.023304jes/xml](https://doi.org/10.1149/2.023304jes/xml).

194 D. Noviana, D. Paramitha, M. F. Ulum and H. Hermawan, The Effect of Hydrogen Gas Evolution of Magnesium Implant on the Postimplantation Mortality of Rats, *J. Orthop. Translat.*, 2016, **5**, 9–15, DOI: [10.1016/j.jot.2015.08.003](https://doi.org/10.1016/j.jot.2015.08.003).

195 V. K. Bommala, M. G. Krishna and C. T. Rao, Magnesium Matrix Composites for Biomedical Applications: A Review, *J. Magn. Alloys*, 2019, **7**(1), 72–79, DOI: [10.1016/j.jma.2018.11.001](https://doi.org/10.1016/j.jma.2018.11.001).

196 Y. H. Ho, S. S. Joshi, T. C. Wu, C. M. Hung, N. J. Ho and N. B. Dahotre, In-Vitro Bio-Corrosion Behavior of Friction Stir Additively Manufactured AZ31B Magnesium Alloy-Hydroxyapatite Composites, *Mater. Sci. Eng. C*, 2020, **109**, DOI: [10.1016/j.msec.2020.110632](https://doi.org/10.1016/j.msec.2020.110632).

197 Y. H. Ho, K. Man, S. S. Joshi, M. V. Pantawane, T. C. Wu, Y. Yang and N. B. Dahotre, In-Vitro Biominerization and Biocompatibility of Friction Stir Additively Manufactured AZ31B Magnesium Alloy-Hydroxyapatite Composites, *Bioact. Mater.*, 2020, **5**(4), 891–901, DOI: [10.1016/j.bioactmat.2020.06.009](https://doi.org/10.1016/j.bioactmat.2020.06.009).

198 N. E. Putra, M. J. Mirzaali, I. Apachitei, J. Zhou and A. A. Zadpoor, Multi-Material Additive Manufacturing Technologies for Ti-, Mg-, and Fe-Based Biomaterials for Bone Substitution, *Acta Biomater.*, 2020, **109**, 1–20, DOI: [10.1016/j.actbio.2020.03.037](https://doi.org/10.1016/j.actbio.2020.03.037).

199 V. P. M. Rabeeh and T. Hanas, Progress in Manufacturing and Processing of Degradable Fe-Based Implants: A Review, *Prog. Biomater.*, 2022, **11**(2), 163–191, DOI: [10.1007/S40204-022-00189-4](https://doi.org/10.1007/S40204-022-00189-4).

200 J. F. Schenck, The Role of Magnetic Susceptibility in Magnetic Resonance Imaging: MRI Magnetic Compatibility of the First and Second Kinds, *Med Phys*, 1996, **23**(6), 815–850, DOI: [10.1118/1.597854](https://doi.org/10.1118/1.597854).

201 N. E. Putra, Extrusion-Based 3D Printing of Biodegradable, Osteogenic, Paramagnetic, and Porous FeMn-Akermanite Bone Substitutes, *Acta Biomater.*, 2023, **162**, 182–198, DOI: [10.1016/j.actbio.2023.03.033](https://doi.org/10.1016/j.actbio.2023.03.033).

202 N. E. Putra, Additive Manufacturing of Bioactive and Biodegradable Porous Iron-Akermanite Composites for Bone Regeneration, *Acta Biomater.*, 2022, **148**, 355–373, DOI: [10.1016/j.actbio.2022.06.009](https://doi.org/10.1016/j.actbio.2022.06.009).

203 T. Kihara, M. Hirose, A. Oshima and H. Ohgushi, Exogenous Type I Collagen Facilitates Osteogenic Differentiation and Acts as a Substrate for Mineralization of Rat Marrow Mesenchymal Stem Cells *In Vitro*, *Biochem. Biophys. Res. Commun.*, 2006, **341**(4), 1029–1035, DOI: [10.1016/j.bbrc.2006.01.059](https://doi.org/10.1016/j.bbrc.2006.01.059).

204 N. E. Putra, M. A. Leeflang, M. Minneboo, P. Taheri, L. E. Fratila-Apachitei, J. M. C. Mol, J. Zhou and



A. A. Zadpoor, Extrusion-Based 3D Printed Biodegradable Porous Iron, *Acta Biomater.*, 2021, **121**, 741–756, DOI: [10.1016/j.actbio.2020.11.022](https://doi.org/10.1016/j.actbio.2020.11.022).

205 N. E. Putra, M. A. Leeflang, P. Taheri, L. E. Fratila-Apachitei, J. M. C. Mol, J. Zhou and A. A. Zadpoor, Extrusion-Based 3D Printing of Ex Situ-Alloyed Highly Biodegradable MRI-Friendly Porous Iron-Manganese Scaffolds, *Acta Biomater.*, 2021, **134**, 774–790, DOI: [10.1016/j.actbio.2021.07.042](https://doi.org/10.1016/j.actbio.2021.07.042).

206 C. Öhman, M. Baleani, C. Pani, F. Taddei, M. Alberghini, M. Viceconti and M. Manfrini, Compressive Behaviour of Child and Adult Cortical Bone, *Bone*, 2011, **49**(4), 769–776, DOI: [10.1016/j.bone.2011.06.035](https://doi.org/10.1016/j.bone.2011.06.035).

207 K. Kovács, S. Váncsa, G. Agócs, A. Harnos, P. Hegyi, V. Weninger, K. Baross, B. Kovács, G. Soós and G. Kocsis, Anisotropy, Anatomical Region, and Additional Variables Influence Young's Modulus of Bone: A Systematic Review and Meta-Analysis, *JBMR Plus*, 2023, **7**(12), e10835, DOI: [10.1002/jbm4.10835](https://doi.org/10.1002/jbm4.10835).

208 F. Metzner, C. Neupetsch, J. P. Fischer, W. G. Drossel, C. E. Heyde and S. Schleifenbaum, Influence of Osteoporosis on the Compressive Properties of Femoral Cancellous Bone and Its Dependence on Various Density Parameters, *Sci. Rep.*, 2021, **11**(1), 1–13, DOI: [10.1038/S41598-021-92685-Z](https://doi.org/10.1038/S41598-021-92685-Z) SUBJMETA = 1023,166,301,54,639,985,994; KWRD = BIOMATERIALS, BIOMEDICAL + ENGINEERING, STRUCTURAL + MATERIALS, TISSUES.

209 K. Alvarez and H. Nakajima, Metallic Scaffolds for Bone Regeneration, *Materials*, 2009, **2**(3), 790–832, DOI: [10.3390/MA2030790](https://doi.org/10.3390/MA2030790).

210 *Technical Considerations for Additive Manufactured Medical Devices / FDA*. <https://www.fda.gov/regulatory-information/search-fda-guidance-documents/technical-considerations-additive-manufactured-medical-devices> (accessed 2025-08-20).

211 C. Wolf, D. Juchem, A. Koster and W. Pilloy, Generation of Customized Bone Implants from CT Scans Using FEA and AM, *Materials*, 2024, **17**(17), 4241, DOI: [10.3390/MA17174241](https://doi.org/10.3390/MA17174241).

212 R. J. Morrison, K. N. Kashlan, C. L. Flanagan, J. K. Wright, G. E. Green, S. J. Hollister and K. J. Weatherwax, Regulatory Considerations in the Design and Manufacturing of Implantable 3D-Printed Medical Devices, *Clin. Transl. Sci.*, 2015, **8**(5), 594–600, DOI: [10.1111/CTS.12315](https://doi.org/10.1111/CTS.12315).

213 Food, U. S. Biological Responses to Metal Implants. 2019.

214 A. Gilchrist, O. Omar, N. J. Hallab and J. J. Jacobs, Cytokines Associated with Pathologic Responses to Orthopedic Implant Debris, *Front. Endocrinol.*, 2017, **8**, 241218, DOI: [10.3389/FENDO.2017.00005](https://doi.org/10.3389/FENDO.2017.00005).

215 N. E. Vrana and N. Engin Vrana, Immune Responses to Implants: How Can They Be Anticipated and Managed?, *Expert. Rev. Med. Devices*, 2023, **20**(12), 991–993, DOI: [10.1080/17434440.2023.2260736](https://doi.org/10.1080/17434440.2023.2260736).

216 J. Kzhyshkowska, A. Gudima, V. Riabov, C. Dollinger, P. Lavalle and N. E. Vrana, Macrophage Responses to Implants: Prospects for Personalized Medicine, *J. Leukoc. Biol.*, 2015, **98**(6), 953–962, DOI: [10.1189/jlb.5vmr0415-166r](https://doi.org/10.1189/jlb.5vmr0415-166r).

217 W. Habraken, P. Habibovic, M. Epple and M. Bohner, Calcium Phosphates in Biomedical Applications: Materials for the Future?, *Mater. Today*, 2016, **19**(2), 69–87, DOI: [10.1016/j.mattod.2015.10.008](https://doi.org/10.1016/j.mattod.2015.10.008).

218 A. M. C. Barradas, H. Yuan, C. A. van Blitterswijk and P. Habibovic, Osteoinductive Biomaterials: Current Knowledge of Properties, Experimental Models and Biological Mechanisms, *Eur. Cell Mater.*, 2011, **21**, DOI: [10.22203/ecm.v021a31](https://doi.org/10.22203/ecm.v021a31).

219 X. Chen, J. Zhou, Y. Qian and L. Z. Zhao, Antibacterial Coatings on Orthopedic Implants, *Mater. Today Bio*, 2023, **19**, 100586, DOI: [10.1016/j.mtbi.2023.100586](https://doi.org/10.1016/j.mtbi.2023.100586).

220 S. Bose, N. Sarkar and Y. Jo, Natural Medicine Delivery from 3D Printed Bone Substitutes, *J. Controlled Release*, 2024, 848–875, DOI: [10.1016/j.jconrel.2023.09.025](https://doi.org/10.1016/j.jconrel.2023.09.025).

221 A. F. von Recum, *Handbook Of Biomaterials Evaluation: Scientific, Technical And Clinical*, ed Von Recum, A. F., CRC Press, 2nd edn, 1998.

222 N. E. Putra, V. Moosabeiki, M. A. Leeflang, J. Zhou and A. A. Zadpoor, Biodegradation-Affected Fatigue Behavior of Extrusion-Based Additively Manufactured Porous Iron-Manganese Scaffolds, *Acta Biomater.*, 2024, **178**, 340–351, DOI: [10.1016/j.actbio.2024.02.024](https://doi.org/10.1016/j.actbio.2024.02.024).

223 G. Parande, V. Manakari, S. D. Sharma Kopparthy and M. Gupta, A Study on the Effect of Low-Cost Eggshell Reinforcement on the Immersion, Damping and Mechanical Properties of Magnesium-Zinc Alloy, *Composites, Part B*, 2020, **182**, DOI: [10.1016/j.compositesb.2019.107650](https://doi.org/10.1016/j.compositesb.2019.107650).

224 A. B. Radwan, P. C. Okonkwo, S. Murugan, G. Parande, M. Taryba, M. F. Montemor, L. Al-Mansoori, M. A. Elrayess, N. Al-Qahtani, M. Gupta, K. M. Youssef, R. Case, R. A. Shakoor and A. M. Abdullah, Evaluation of the Influence of Eggshell (ES) Concentration on the Degradation Behavior of Mg-2.5Zn Biodegradable Alloy in Simulated Body Fluid, *ACS Biomater. Sci. Eng.*, 2023, **9**(5), 2376–2391, DOI: [10.1021/acsbiomaterials.2c01366](https://doi.org/10.1021/acsbiomaterials.2c01366).

225 J. Rao, S. Leong Sing, P. Liu, J. Wang and H. Sohn, Non-Destructive Testing of Metal-Based Additively Manufactured Parts and Processes: A Review, *Virtual Phys Prototyp*, 2023, **18**(1), e2266658, DOI: [10.1080/17452759.2023.2266658](https://doi.org/10.1080/17452759.2023.2266658).

226 K. Willemse, R. Nizak, H. J. Noordmans, R. M. Castelein, H. Weinans and M. C. Kruyt, Challenges in the Design and Regulatory Approval of 3D-Printed Surgical Implants: A Two-Case Series, *Lancet Digit Health*, 2019, **1**(4), e163–e171, DOI: [10.1016/S2589-7500\(19\)30067-6](https://doi.org/10.1016/S2589-7500(19)30067-6).

227 *Regulation - 2017/746 - EN - Medical Device Regulation - EUR-Lex*. <https://eur-lex.europa.eu/eli/reg/2017/746/oj/eng> (accessed 2025-08-20).

228 *Regulation - 2017/745 - EN - Medical Device Regulation - EUR-Lex*. <https://eur-lex.europa.eu/eli/reg/2017/745/oj/eng> (accessed 2025-08-20).

229 *America Makes, T. A. N. S. I. Standardization Roadmap for Additive Manufacturing*, 2023.



230 C. Huxman, FDA Regulatory Considerations for Innovative Orthopedic Devices: A Review, *Injury*, 2025, **56**(4), 112291, DOI: [10.1016/j.injury.2025.112291](https://doi.org/10.1016/j.injury.2025.112291).

231 H. S. Han, S. Loffredo, I. Jun, J. Edwards, Y. C. Kim, H. K. Seok, F. Witte, D. Mantovani and S. Glyn-Jones, Current Status and Outlook on the Clinical Translation of Biodegradable Metals, *Mater. Today*, 2019, **23**, 57–71, DOI: [10.1016/j.mattod.2018.05.018](https://doi.org/10.1016/j.mattod.2018.05.018).

232 *PMA Review Process* / FDA. U.S. Food and Drug Administration. <https://www.fda.gov/medical-devices/premarket-approval-pma/pma-review-process> (accessed 2025-09-03).

